Elucidation of a small regulatory RNA PsrR1 mediated photosynthetic gene regulatory mechanism during cold acclimation in Synechocystis sp. PCC 6803

Thesis submitted to the University of Hyderabad the award of

Doctor of Philosophy

By

Jahnabi Ramchiary

Reg. No. 14LTPH04



Department of Biotechnology & Bioinformatics
School of Life Sciences
University of Hyderabad
Hyderabad – 500 046
India
June, 2022





University of Hyderabad (A Central University established in 1974 by act of parliament) HYDERABAD- 500 046, INDIA

DECLARATION

I, Jahnabi Ramchiary hereby declare that the work embodied in this thesis entitled "Elucidation of the gene regulatory mechanism photosynthetic genes during cold acclimation in Synechocystis sp. PCC 6803" submitted by me under the guidance of Prof. J.S.S Prakash is an original and independent research work. I also declare that it has not been submitted previously in part or in full to this University or any other University or Institution for the award of any degree or diploma.

Date: 10-06-2022 Jahnabi Ramchiary

Jahnah Runchigry



University of Hyderabad (A Central University established in 1974 by act of parliament) HYDERABAD- 500 046, INDIA

CERTIFICATE

This is to certify that that this thesis entitled "Elucidation of the gene regulatory mechanism photosynthetic genes during cold acclimation in Synechocystis sp. PCC 6803" submitted by Mrs. Jahnabi Ramchiary bearing registration number 14LTPH04 in partial fulfilment of the requirements for award of Doctor of Philosophy in the School of Life Sciences is a bonafide work carried out by her under my supervision and guidance.

The thesis is free from plagiarism and has not been submitted previously in part or in full to this or any other University or Institution for award of any degree or diploma. The work was presented in the conferences.

Publication:

 Konduri Ranjith, Jahnabi Ramchiary, Jogadhenu S. S. Prakash, Kotakonda Arunasri, Savitri Sharma and Sisinthy Shivaji. Gene targets in ocular pathogenic *Escherichia coli* for mitigation of biofilm formation to overcome antibiotic resistance. Frontiers in Microbiology, Volume 10, 2019, p 1308.

Conferences:

1. International Symposium "Advances In Plant Biotechnology and Genome Editing"(APBGE 2021). Poster presented (Online), April 2021.

- 2. 59th Annual Conference of Association of Microbiologists of India (AMI-2018). Oral presentation (University of Hyderabad, India), November 2018.
- 3. 59th Annual Conference of Association of Microbiologists of India (AMI-2018). Poster presentation (University of Hyderabad, India), November 2018.

Further, the student has passed the following courses towards fulfilment of coursework requirement for Ph.D.

Co	ourse Code	Title of the Course	Credits	Pass / Fail
1.	AS 801	Analytical Techniques	4	PASS
2.	AS 802	Research Ethics, Data Analysis and Biostatistics	3	PASS
3.	AS 803	Lab Work and Seminar	5	PASS

Supervisor

Supervisor

Prof. J.S.S. PRAKASH
Dept. of Biotechnology & Bioinformatics
School of Life Sciences
University of Hyderabad
HYDERABAD-500 046. INDIA.

Buley

Head of the Department

HEAD

Dept. of Biotechantegy & Bioinformatics
University of Evperabad

myderabad.

Dean of the School

School of Life Sciences
University of Hyderabad
Hyderabad-500 046.

CONTENTS

	Page No.
Acknowledgement	i-ii
Abbreviation	1
List of figures	4
List of tables	6
Introduction	7-34
Objectives	35-37
Materials and Methods	38-70
Results	71-100
Discussion	101-107
Oligomers	109-112
References	113-123
List of publications and presentations	124-125

ACKNOWLEGDEMENT

This Report would not have been conceivable without the fundamental and thoughtful help of numerous individuals.

I would like to express my sincere gratitude to my supervisor Prof. Jogadhenu S. S. Prakash, for his consistent support, patience, motivation, enthusiasm, and immense knowledge. His guidance helped me in all the time of research and made an empowering environment to finish my research work.

Besides my supervisor, I would like to thank my thesis committee: Prof. P.B Kirti, Dr. N. Prakash Prabhu and Dr. M. Venkataramana for their encouragement and insightful comments.

I am thankful to the present and previous Deans, School of Life Sciences and the present and previous Heads, Department of Biotechnology and Bioinformatics for enabling me to utilize the offices and facilities of the School and the Department.

I genuinely recognize the infrastructural support given by UGC-SAP, DST-FIST, DBT-CREBB, to the Dept. of Biotechnology and Bioinformatics and the CSIR, Govt.of India for the fellowship.

I wish to express my gratitude to Dr. N. Prakash Prabhu, who thoughtfully broadened his research facility and guidance with his expertise towards completion of my work.

My sincere thanks goes to Prof. Sue Lin Chao and Prof. Iwane Suzuki for offering me scientific discussions and valuable suggestions that has immensely helped me towards the understanding and completion of my research.

Besides the sincere research work, this thesis is the result of a very lengthy and difficult experience throughout and I am thankful to many wonderful people who have added to the development of my scientific personality and helped towards the fulfilment of this work.

Here again I thank my supervisor Prof. Jogadhenu S. S. Prakash and his family for their good wishes and consistent support all throughout my Ph.D. duration.

I would like to mention the Project students who have helped me while being trained-

Neelima, Simanti, Azeem, Krishnapriya and Yasaswini.

I am thankful to all my labmates: Dr. Mahalaxmi, Dr. Arun, Dr. Deepak Singh, Dr.

Lingaswamy Bantu, Dr. Afshan Srikumar, Mr. Somasekhara, Pankaj, Suraj, Shubhangi,

Anamya, Ramana, Purna and Ranjana for their constant support, encouragement,

amusement too and for being my second family. I am also thankful to our lab helper-

Manohar and Lt. Sreedhar

I am very thankful to my two "yaar" -Dipti and Akash for always being by my side during

the difficult and pain-stacking Ph.D. days and filled the days with some of the best memories

of my lifetime, to be cherished forever. I am also grateful to Rakhi, Minu, Priyanka, Sangeeta

and Kavya for their constant encouragement and support.

I am thankful to all my batch mates and other researchers of the School of Life Sciences for

their appropriate support for their timely help.

I acknowledge the help and support of the Non-teaching staffs from the Department and

school.

Lastly and most importantly, I am very grateful to my Ma & Dauta - Mrs. Rebati Ramchiary

and Mr. B.K Ramchiary, my brother-Mr. Rupjit Ramchiary and my husband- Mr. Hemanga

Ojah for their trust, motivation, and constant support and for being the pillars of my life.

Thank You

Jahnabi Ramchiary

(ii)

ABBREVIATIONS

μg : microgram

μL : microliter

μM : micromolar

°C : degree centrigade/ degree celcius

crhR : cyanobacterial RNA helicase redox

apc : allophycocyanin

ATP : adenosine tri phosphate

bp : base pair

cDNA : complementary DNA

chl : chlorophyll

cpc : phycocyanin

Cyt C : cytochrome C

DEPC : diethylpyrocarbonate

DNA : deoxy ribonucleic acid

DTT : dithiothreitol

EDTA : ethylene diamine tetra acetic acid

ETC : electron transport chain

gm : gram

h : hour(s)

Hik33 : Histidine kinase 33

HEPES : 4-(-4-(2-hydroxyethyl)-1-piperazine ethane sulfonic acid

HL : high light

HLR1 : high light regulatory 1

IgG : immunoglobulin G

IPTG : isopropyl β-D-1-thiogalactopyranoside

kb : kilobase pair

kDa : kilodalton

L : litre

LB : Luria-Bertani

LL : low light

M : molar

Mb : megabase pair

mg : milligram

min : minute(s)

mL : millilitre

mM : millimolar

mRNA : messenger RNA

NADPH : nicotinamide adenine dinucleotide phosphate

NaOH : sodium hydroxide

ncRNA : non-coding RNA

Ni-NTA : nickel nitriloacetic acid

nm : nanometer

O.D : optical density

OEC : oxygen evolving complex

ORF : open reading frame

PAGE : polyacrylamide gel electrophoresis

PBS : phosphate buffer saline

PBS : phycobilisomes

PCR : polymerase chain reaction

PMSF : phenylmethylsulfonyl fluoride

PNPase : Polyribonucleotide Nucleotidyltransferase (*E. coli*)

PNP : Polyribonucleotide Nucleotidyltransferase (*Synechocystis sp*)

PS (I/II) : photosystem (I/II)

PsrR1 : photosynthesis stress responsive regulatory- 1

PVDF : polyvinylidine difluoride

qRT-PCR : quantitative real time polymerase chain reaction

RBS : ribosomal binding site

RNA : ribonucleic acid

RNase (E/II/R) : ribonuclease (E/II/R)

RpaB : regulator of phycobilisome associated B

rpm : revolutions per minute

RT-PCR : reverse transcriptase polymerase chain reaction

RuBisCO : Ribulose 1,5-bisphosphate Carboxylase/Oxidase

s : second(s)

SDS : sodium dodecyl sulphate

SPR : surface plasmone resonance

sRNA : small regulatory RNA

TE : tris-EDTA

Tris : tris-(Hydroxymethyl) aminoethane

V : photons

List of Figures

Figure	Title	Page No.
No		
1	Image of WT Synechocytis sp. PCC6803.	9
2	Schematic representation of the gene regulatory mechanism in	12
	response to stress.	
3	Diagrammatic representation of cyanobacterial photosystem-I	17
4	Diagrammatical representation of the cyanobacterial	19
	phycobilisomes associated with PSII.	
5	Absorption and transfer of photon energy by the phycobilisomes	20
6	Pictorial representation of the flow of electrons during photosynthesis.	21
7	Pictorial representation of the post-transcriptional regulation of the photosynthetic genes during high-light acclimation.	26
8	Schematic representation of the probable role of ribonucleases	28
	and RNA helicase involved in the decay of mRNA during post transcriptional regulation mediated by sRNA.	
9	Pictorial representation of RNA degradosome and bacterial	29
	Exosome-like complex.	
10	Pictorial representation of (A) bacterial PNPase, (B) Archeal	31
	RNA exosome complex and (C) Eukaryotic RNA exosome	
	complex.	
11	Maps of plasmid DNA constructs generated for ectopic	52
	expression of 3X-FLAG-PNP.	
12	Changes in the transcript level of PsrR1 in WT Synechocystis	72
	cells during low temperature stress.	
13	Generation of the mutant strain $\Delta psrR1$ and the overexpression	74
	strain psrR1 ⁺ .	

14	Comparative analysis of the expression level of photosystem I and phycobilisome genes by Next Generation Sequencing	
	analysis.	76
15	Transcript levels of photosystem I and phycobilisome genes in WT, $\Delta psrR1$ and PsrR1 ⁺ .	78
16	Phenotypes of the mutant strain <i>∆psrR1</i> compared to WT Synechocystis subjected to cold treatment at 20°C.	79
17	Pigment analysis in the WT cells and $\Delta psrR1$.	80
18	77K fluorescence emission spectra of the WT and <i>∆psrR1</i> .	82
19	Generation of the mutant strain $\Delta rpaB$.	83
20	Induction and expression of 3X FLAG-PNP in PNP ⁺ cells.	87
21	Bacterial two hybrid analysis of PNP, RNaseII and CrhR.	96
22	SDS–PAGE analysis of expressed and purified 6XHis-tagged RNaseII (A) in <i>E. coli</i> BL21 (DE3), 6X His-tagged PNP (B) and CrhR (C) recombinant proteins in <i>E. coli</i> Rosetta (DE3).	97
23	Kinetic analysis of the interaction between PNP – RNaseII and PNP- CrhR.	99
24	Schematic representation of the regulation of photosystem I and phycobilisomes genes at low temperature.	108

List of Tables

Table	Title	Page No.
No.		
1	List of some of the major ribonucleases found in the cyanobacterial species.	32
2	Composition of YBG-11 nutrient media.	41
3	Changes in the expression of photosynthesis related genes in $\Delta rpaB$.	84
4	List of the RNA targets co-eluted with the 3XFLAG tagged proteins and identified by RNA sequencing.	88
5	The calculated dissociation constant at equilibrium (K _D) from the kinetic analysis of the interaction between PNP –RNaseII and between PNP and CrhR.	100
6	List of oligomers and their sequences used for the study.	110

1.INTRODUCTION



1.1 Cyanobacteria

Cyanobacteria (blue-green algae) are Gram-negative prokaryotes which belong to the community of oxygenic photosynthetic organisms. The members of this phylum are found in various forms- single-celled (unicellular), multicellular, filamentous and can also into colonies which might appear in different forms like a thread-like filaments or a sphere hollow etc. Some cyanobacteria are capable of fixing nitrogen from the atmosphere, owe to their specialized cells known as heterocyst. Cyanobacteria are the oldest known fossils, believed to be beyond 3.5 billion years old. They are regarded as the main contributor in the remodelling the Earth's atmosphere into oxygenic during the Archaean and Proterozoic Eras and thus, facilitating the evolution of diverse aerobic life forms. These prokaryotic photosynthetic microorganisms are also presumed to have formed symbiosis with bacteria and credence as predecessor of the plastids of the cell organelle 'chloroplasts' in higher eukaryotic plants [1]. Cyanobacteria have diverse habitats in the nature. Cyanobacteria also have thermophilic members thriving in hot springs whereas some are found in the cold polar environments. They are used as model organisms in many research studies related to different biochemical processes and considered to be promising candidate for bio-industrial applications. Being photosynthetic, they are included in many studies related to photosynthesis. Besides a relatively faster growth rate, genetic manipulations are relatively easy in these organisms. Being prokaryotic in nature but owing to similar membrane structure and oxygen evolving apparatus, it is easy to use these cyanobacterial species as model organisms to study abiotic stress responses compared to higher eukaryotic plants. They are also used extensively in studies related to response mechanisms during abiotic stress conditions. Cyanobacteria produce many important secondary metabolites like enzymes, UV-absorbing pigments etc. and also some owe clinical properties like antibacterial, antiviral, antifungal and anti-proliferative. Currently, they are being studied for being a promising candidate in the production of biofuels, food supplements (superfoods), and bio-fertilizers for safe agriculture [2, 3].

One of the most common cyanobacterial model systems is *Synechocystis* sp. PCC6803 (here after *Synechocystis*). This unicellular cyanobacterium is used extensively for various studies including stress response and the regulatory mechanisms. The sequence of *Synechocystis* complete genome and naturally occurring seven plasmids is available in the database "cyanobase". One of the unique features of this organism is that it is naturally transformable. In the present study utilized *Synechocystis* to investigate and understand the regulation of photosynthesis during cold stress.

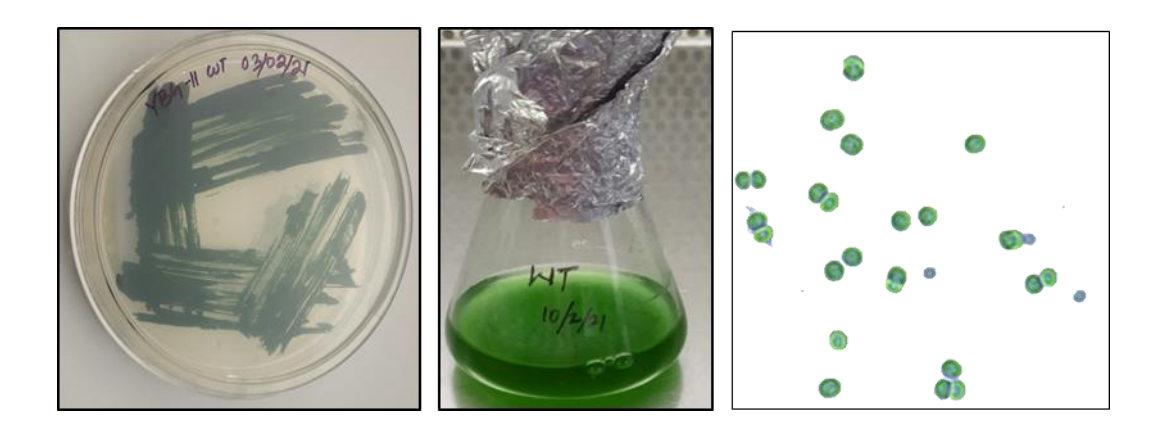


Figure 1. Image of wild-type (WT) *Synechocytis* **sp. PCC6803** (A) on solidified YBG-11 agar media, (B) on Y-BG11 broth media and (C) light microscopy image.

1.2 Abiotic stress

Any drastic change in the environmental factors is detrimental to the cellular homeostasis of organisms including the cyanobacteria. When they experience a certain magnitude of the environmental change for sufficient time period, such change is sensed as stress by the organisms. Moreover, cyanobacteria have a broad range of niche and thus, are often exposed to change in temperature, light intensity, nutrient deprivation, oxidative, osmotic stresses etc. [4]. Such stress causes various physio-chemical changes which affects their overall cellular functions. For example, at temperature below the optimum growth temperature, cyanobacteria lose their membrane fluidity. Alterations in the preferable range of pH (neutral to slightly alkaline) also evokes a wide spectrum of changes in their cellular behaviour. Being photosynthetic in nature, they are sensitive to changes in the light intensity. Irradiances beyond the threshold level of their photosynthetic machinery induces photoinhibition and photodestruction of the photosystems [4, 5]. Another consequence of high light (HL) stress is the built up of the deleterious reactive oxygen species. Cyanobacteria have existed and thrived in the environment owing to various survival strategies that they have adapted to evade the adverse conditions caused due to stress. One of these strategies is initiation of the transcription of various stress-responsive genes, thereby synthesizing proteins essential for acclimatization [6]. When exposed to stress, the following events occur; i) firstly, rapid sensing of the stress stimuli, ii) second, transduction of the signal to stress-responsive genes, thus modulating the expression of the genes. The proteins that are synthesized as a result of the stimuli helps in the process of in acclimation in response to the stress [4, 7, 8]. Cyanobacteria possesses wellstructured systems for transduction of stress signal to the organism which constitutes of two components; a sensory histidine kinase located on the membrane and a response regulator. The stress signalling system aids the organism to act swiftly during stress, and initiate the regulatory mechanism of stress-responsive genes [4, 8, 9]. Cyanobacterial alternative sigma factors replaces the primary σ factor during various stress conditions, to modulate the expression of the genes which are essential for acclimation [10]. For instance, during high salt stress the expression of salt stress inducible gene is modulated by SigF, an alternate sigma factor thus, facilitating cyanobacteria to resist and survive prolonged salt stress exposure [11]. During heat stress, upregulation of the heat shock genes like *groESL* and *groEL2* are assisted by two alternate sigma factors, SigB and SigE [12]. Besides the alternate sigma factors, stress condition also activates different transcriptional regulators that can either turn on or turn off the stress specific genes. The transcriptional regulator, HrcA is a repressor that works together with Sig B to regulate the transcript level of genes the heat shock genes such as *groES* and *groEL2* during heat stress [12]. *Synechocystis* acclimatize to the low carbon condition with the aid of the transcriptional regulator, CmpR which activates the genes encoding for bicarbonate transporter [4, 13]. Another extensively explored gene regulatory element are the small regulatory RNAs (sRNAs) which participates to mediate post-transcriptional gene regulation of the stress responsive genes required to acclimatize to unfavourable surrounding environment [4, 14] (Figure 2).

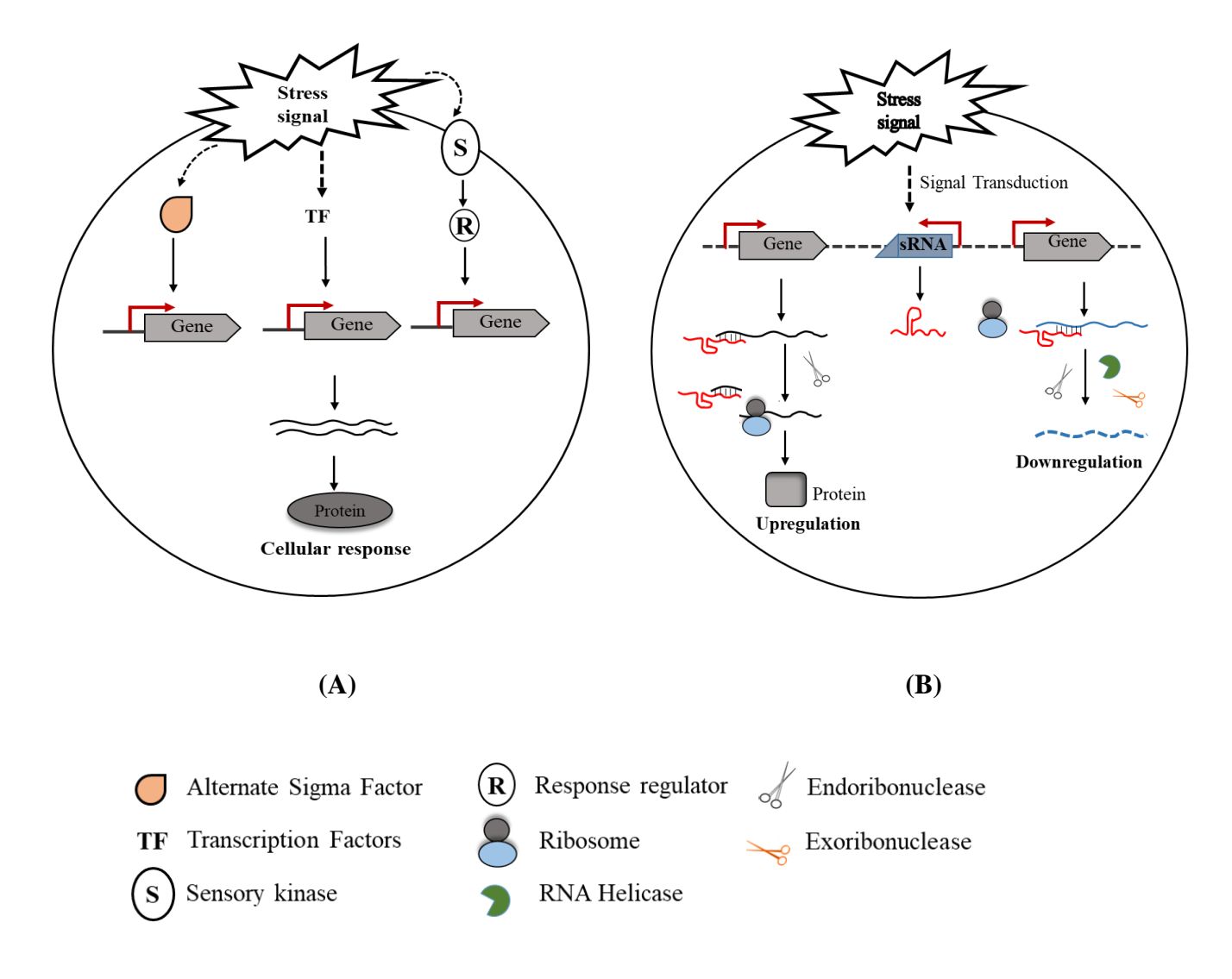


Figure 2. Schematic representation of the gene regulatory mechanism in response to stress. In cyanobacteria, majority of environmental stress signals are mediated by a 'two-component' signal transduction system. A membrane bound sensory histidine kinase perceives the stress signal and transduce the signal via its partner, a response regulator. (**A**) In cyanobacteria, different elements like the alternative sigma factors, transcription factors, and response regulators take part and plays a role in the transcriptional regulation of the set of genes that encodes for proteins that aid the organism to acclimatize to stress. (**B**) Stress also activates the post transcriptional regulation of stress-responsive genes mediated by small regulatory RNAs (sRNA), eventuating to altered expression level of the genes [adapted from Prakash *et al.*, 2013 [19]].

1.3 Cold stress

Low temperature affects various cellular components as well as the metabolism of an organism. Significant detrimental effect due to temperature fluctuations is observed in an organism depending on the temperature change rate as well as the magnitude and exposure duration. Low temperature beyond threshold tolerance level is cold stress for the organism. Cold stress leads to various physiological changes in cyanobacteria. Such changes in cyanobacteria is evident from the fact that on exposure to cold stress, they tend to lose their membrane fluidity, leading to rigidification of the plasma membrane. The resulting rigid membrane induces cyanobacteria to synthesize polyunsaturated fatty acids to restore the fluidity of their cell membrane [15]. Low temperature also brings changes to various metabolic processes. In the N₂-fixing unicellular cyanobacterium, Cyanothece sp. shift of temperature from the optimum range of growth temperature affects the growth and limits the fixation of nitrogen as well [16]. Different studies on micro-algal species also points out the role low temperature in the growth, composition of plasma membrane, enzyme efficiency, photosynthesis and photorespiration [17]. Moreover, the effect of cold stress is observed at the global gene expression profile in cyanobacteria. Microarray studies have identified the stress-signalling unit which consists of a sensor protein and a response regulator, functioning under various types of stress. The membrane fluidity is restored due to induction in the expression of the genes encoding fatty acid desaturase at low temperature. These desaturases; Des (A, B, C and D) introduces a double bond in the fatty acid chain in the membrane lipids and re-establishes the consistency of the membrane fluidity [6]. The induced expression of the desaturases genes is an example of the cold responsive alteration in gene expression. Low temperature leads to differential gene expression. There are set of genes; some are cold-inducible and some are cold-repressible.

1.3.1 Cold stress response signalling system

The two-component signal transduction unit of cyanobacteria enables it to sense the change in the surrounding temperature. The histidine kinase-Hik33 partners with a response regulator, RpaB/Rre26 and compose the cold stress signalling system of *Synechocystis* [9, 18, 19]. Whole transcriptome analysis by microarray pointed that cold stress signal perceived and transduced by Hik33 leads to the upregulation of about 50% of the total cold-inducible genes [9, 19]. The process of sensing the stress stimuli by Hik33 is not very clear. But it is widely accepted in the research community that Hik33 undergoes conformational change in the transmembrane domains due to the rigidification of the cyanobacterial plasma membrane, gets dimerized and undergo autophosphorylation [6, 7]. Interaction of a SipA like protein, Ssl3451 with Hik33 was demonstrated that enhances the autophosphorylation activity of Hik33 at low temperature [20]. However, the phosphorylated-Hik33 subsequently pass on the phosphoryl group to its partnerthe response regulator, RpaB. The activated RpaB acts as a transcription factor and binds to specific DNA sequence known as the HLR1 (high light regulatory-1) sequence. Based on the position of HLR1 sequence corresponding to the stress-responsive genes, RpaB can function as a positive or a negative regulatory element [21]. For example; binding of RpaB to its DNAbinding motif (HLR1), present in upstream region of the highlight-inducible genes was demonstrated to initiate transcription of the genes [22]. On contrary, the HLR1 sequence is located within the ribosomal binding site of a small regulatory RNA, PsrR1 and binding of RpaB to the DNA motif repressed expression of PsrR1[4, 21, 23]. Hik33 is recognized as a multi stress sensor and is functional under different stress like high-light, osmotic stress etc. It is to be noted that besides the sensor Hik33, Synechocystis employ the same response regulator, RpaB as the stress signal transduction system at cold and high-light stress [9, 24]. The protein, SipA was also reported as a participant in the stress signalling system during HL in the cyanobacterium Synechococcus sp. PCC 7942 [4].

1.3.2 Cold stress responsive genes

Modulation in the expression pattern of many genes is one of the major consequences of the effect of low temperature in Synechocystis. About 100 genes were identified as to be coldinducible which includes the genes encoding desaturases [9]. The cold inducibility of these group of genes leads to the synthesis of proteins necessary for cold acclimation. The coldinducible genes were grouped as; i) desaturases genes for retaining membrane fluidity, ii) genes encoding proteins involved in the nucleic acid metabolism, iii) genes of metabolic enzyme, iv) genes encoding GTP binding proteins, v) high light-inducible genes, vi) ABC-type transporter genes, vii) genes that encode proteins of translation and protein folding machinery; and viii) hypothetical genes encoding uncharacterized proteins [8, 19]. Some of these cold-inducible genes, such as hliA, crhR, ndhD2 etc. are transiently upregulated, whereas some are constantly upregulated at low temperature such as rbpA, desB, desD, nusG, pcnB etc. [9]. All the products of these cold-inducible genes have a role to play in the cold acclimation. The RNA helicase, CrhR encoded by the cold-inducible gene crhR, was reported to be very crucial for coldresponsive redistribution of energy and regulation of photosystem stoichiometry in Synechocystis [25, 26]. Besides the cold-inducible genes, there are set of genes that undergo downregulation in response to cold stress. Particularly, the genes encoding various subunits of photosystem I complex (psaD, psaF, psaJ, psaL etc), the phycobilisomes (apcA, apcB, apcC, apcE. apcF, cpcB, cpcC, cpcG etc) and the genes involved in the biosynthesis of the photosynthetic pigments (chlP, hemA, hemF and ho 1) are downregulated during cold stress [9, 25, 27]. Downregulation of many of the photosynthetic related genes during low temperature suggests that cold stress has an immense effect in the performance of photosynthesis in cyanobacteria. The cold-responsive altered expression of the genes prerequisite the cold stress signalling unit and a gene regulatory mechanism. The stimuli of cold stress in 50% of the genes were mediated by the pair, Hik33- RpaB; but identification of regulatory elements and the mechanism resulting into differential expression of the coldresponsive are still being studied. One of the proposed mechanism of regulation of altered
gene expression is temperature-dependent changes supercoiling of the genomic DNA [6, 28].

In *Synechocystis* during cold stress, an increase in the negative supercoiling in the promoter
region of the *desB* gene was found to be responsible for the induced expression of the DesB/ω3
desaturase during cold stress [6]. In case of cold repressible genes, one of the most significant
group of genes that are downregulated are the genes related to photosynthesis, namely the
photosystem I and phycobilisome genes were downregulated in *Synechocystis* during cold
acclimation [9, 25, 27]. Cyanobacteria are photosynthetic in nature, such down regulation of
many genes related to photosynthesis implies that they optimize photosynthesis by regulating
the gene expression at low temperature. But, the mechanism of the regulation of photosynthetic
genes at low temperature is unexplored.

1.4 Photosynthesis in cyanobacteria

The ancient cyanobacteria-like organisms are believed to be the pioneers of photosynthesis which have enabled in the evolution of complex life forms on the planet Earth. Oxygenic photosynthesis involves the transfer of electrons extracted from H₂O to fix CO₂ for the biosynthesis of energy-rich carbohydrates, thus releasing O₂ in the process. Cyanobacteria perform oxygenic photosynthesis and are responsible for 20 - 30% of global photosynthetic productivity. The mechanism of photosynthesis is very similar in cyanobacteria, algae, and the higher eukaryotic plants but with few exceptions. Thylakoids located in the chloroplast is the site of photosynthesis in eukaryotes. In cyanobacteria, the thylakoids are present as a stack of membranes in the cytoplasm. The units of the photosynthetic machinery are present on the thylakoid membrane which consists of the reaction centers- P680 of Photosystem II, P700 of

Photosystem I, phycobilisomes, $Ctyb_6f$ complex, and the cofactors required as the mediators for the transfer of the electrons. The photochemical reaction centers contain the most important light absorbing pigments-chlorophyll a (*Chl a*). There are also few other accessory pigments like the carotenoids. Other than the chlorophyll, cyanobacteria possess specialized light absorbing pigment associated proteins, the phycobilisomes which are unique to the phylum.

1.4.1 Photosystem I

One of the major component of photosynthetic machinery is the Photosystem I (PSI). It is a membrane bound multi-protein complex predominantly existing as a trimer. Its oligomeric form changes in response to different environmental conditions like high light stress. Generally, there are 12 protein subunits in each PSI monomer; the main core of the complex consists of the PsaA and PsaB protein subunits. Encircling the core complex are the other seven membrane integral subunits- Psa(F, I, J, K, L, M and X) and Psa(C, D and E) are three subunits present on the membrane towards the cytoplasmic side [29]. These protein subunits houses the different cofactors, the chlorophylls, phylloquinones, [4E-4S] clusters and lipids that are bound non-covalently. The photochemical reaction center of PSI is termed as P700.

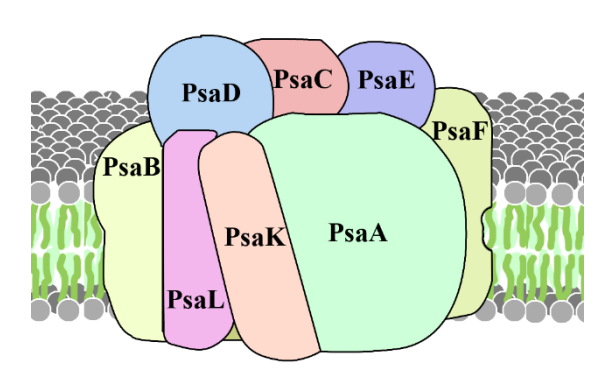


Figure 3: **Diagrammatic representation of cyanobacterial photosystem-I.** The different subunits of the multimeric protein complexes are presented in different colours. This multimeric complex is located in the thylakoids and is generally present as a timer on the membrane.

1.4.2 Photosystem II:

Photosystem II (PSII) is a large multimeric protein complex associated with photosynthetic pigment-*chl a* existing as a homodimer. The monomeric form constitutes of 20 different protein subunits (both transmembrane as well as peripheral proteins) and approximately 90 cofactors that are well-coordinated to transfer the excited electron in the electron transfer chain (ETC) of photosynthesis [29, 30]. The cofactors essential in the event of charge separation as well as splitting of water molecules are present on the heterodimer of D1 and D2 protein subunits.

1.4.3 Phycobilisomes

The light harvesting unit of cyanobacteria are the multiprotein-pigment complex, the phycobilisomes (PBS). The antennae harvest and delivers the photon energy to the reaction centres present in the photosystems- PSII and PSI in cyanobacteria. The protein components of the phycobilisome are the phycobiliproteins and the pigment present are the phycobilins. The phycobilins include the phycocyanin (cpc) and allophycocyanin (apc) and some cyanobacterial species also possess phycoerythrin. Phycobilins usually absorbs in the wavelength range of 495-655nm. Structurally, the phycobilin proteins are organised into 3 cylinders and 6 peripheral stack disk rods and the pigments are covalently bound to the proteins. PBS are larges compared to the photosystems and is usually associated to PSII. The size, the compositions, number and the placement of PBS varies during different environmental conditions as a response mechanism [29, 31].

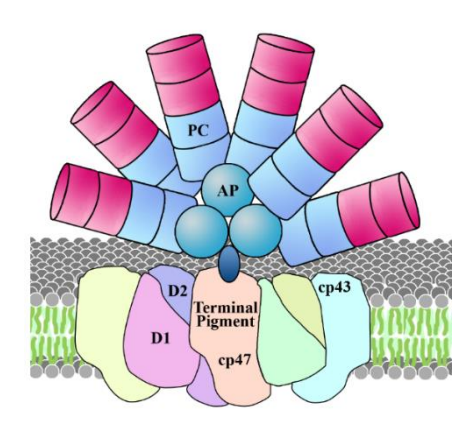


Figure 4: Diagrammatical representation of the cyanobacterial phycobilisomes associated with PSII. The phycobilisomes are the light harvesting multiprotein-pigment complex. It is associated with the PSII on the cytoplasmic side of the thylakoids.

1.4.4 Mechanism of photosynthesis

Photosynthesis involves the flow of electrons through a series of membrane bound carriers-the photosystems, the cytochromes, the quinones and iron-sulfur proteins [29]. The mechanism of the conversion of photon energy to chemical energy during photosynthesis in cyanobacteria is very similar to that of the algae and higher plants. During photosynthesis, transfer of electrons from H₂O to NADP⁺ leads to the synthesis of energy rich compounds, NADPH and ATP. The first event of photosynthesis starts with the absorption of photon energy with a wavelength of <680nm by the light harvesting antennae complex-PBS (Figure 5).

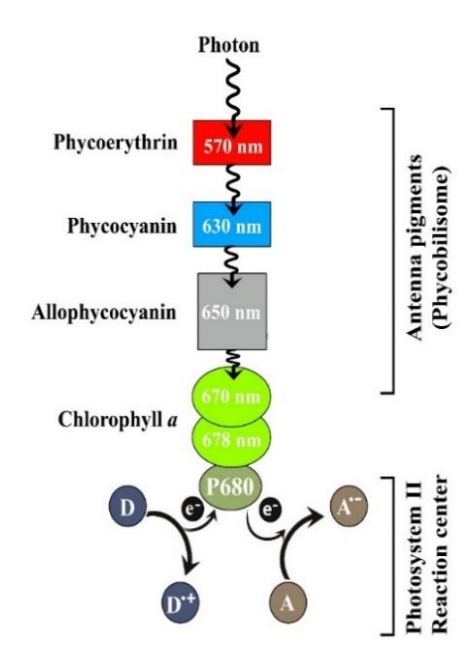


Figure 5. **Absorption and transfer of photon energy by the phycobilisomes.** The energy of the absorbed photons is sequentially passed on in the series; from phycocythrin (absent in most cyanobacteria) to phycocyanin and then to allophycocyanin. The photon energy is finally received by the reaction centre of PSII, the P680. On excitation, the excited P680 donates its electron to an electron acceptor **A**. The electron vacancy of the Chl a at P680 is filled by the electron donated by an electron donor **D**. The wavelength numbers (nm) inside the circles represent pigments the maxima the long wavelength absorbed by the corresponding to the pigments.

Absorption of photon leads to excitation of the antennae molecules and generates a chain reaction, that is, the transfer of the energy to the neighbouring molecules which is eventually delivered to the photochemical reaction center-P680 of PSII (Figure 6). The electrons in P680 gets excited and the energy in the form of electron is transferred to the electron carrier pheophytin which is then again quickly transferred to plastoquinone (PQ). PQ gets reduced to PQH₂ and transfer the electrons to the next component of the photosynthetic machinery-cytochrome b₆f complex. Finally, the electrons are transferred to PSI via plastocyanin from cytochrome b₆f complex to P700 of PSI. The excited P700 transfers the energy to ferrodoxin and thus reduces NADP⁺ to NADPH. The electron transferred from P680 is replaced with the

electrons extracted by oxidation of H₂O. NADPH is utilized in Calvin-Benson cycle in fixation of CO₂ and biosynthesis of carbohydrates [29].

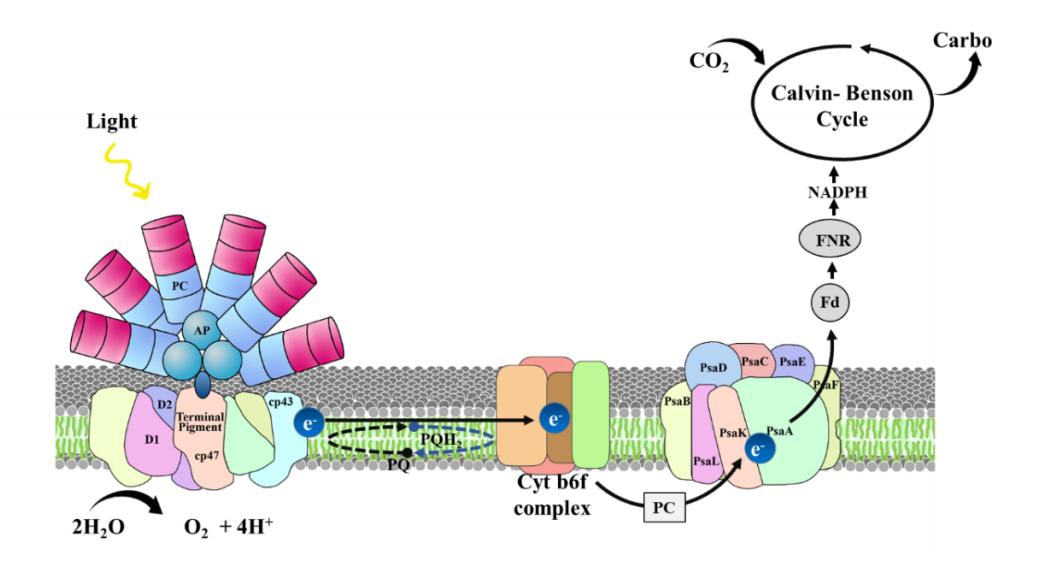


Figure 6. Pictorial representation of the flow of electrons during photosynthesis. The photosynthetic electron transport delivers electrons after light-induced water-splitting at the OEC. Abbreviations: PQ, plastoquinone; PC, plastocyanin; Fd, ferredoxin; FNR, ferredoxin–NADP reductase.

1.5 Cyanobacterial photosynthesis at low temperature

Photosynthesis is a complex biochemical process that is carried out by the photosynthetic machinery. Cyanobacteria performs photosynthesis efficiently owing to the well-co-ordinated functional balance between the units of the photosynthetic machinery. Changes in the parameters of the environmental factors creates interrupts the functional balance between PSII and PSI.

Temperature is an important factor that affects photosynthesis in cyanobacteria. When cyanobacteria experience cold stress, the activity of various enzymes involved in different biochemical reactions are compromised, leading to decreased metabolism [16, 32]. In

photosynthetic organisms, the decreased metabolic rates interferes the balance between the photochemistry and the cellular metabolism, which results into photodamage [33]. Cold stress leads to reduced efficiency of photosynthesis which results due to decreased activity of the Ribulose 1,5-bisphosphate Carboxylase/Oxidase (RuBisCO). The enzyme, RuBisCo is a key enzyme in the Calvin-Bensen Cycle (the light independent reaction of photosynthesis) wherein the NADPH and ATP produced during light dependent reaction of photosynthesis are utilized for the fixation of CO₂. The RuBisCo activity displays compromised activity in the cyanobacterium, Synechococcus elongatus at low temperature [32]. Thus, there will be less requirement of NADPH in the Calvin-Bensen cycle. In such scenario, the rate of movement of the excited electrons in the ETC of photosynthesis has to be re-adjusted to prevent build-up of NADPH in the cell. Therefore, re-adjustment of the functional co-ordination between the photosystems is necessary to optimize photosynthesis for better survival of cyanobacteria. Moreover, cold stress also affects the fluidity of the cyanobacterial membrane. The photosynthetic machinery resides in the thylakoid membrane. Any change in the membrane fluidity will affect the photosystems as well as the other components of photosynthesis. Thus, survival of the organism requires a regulatory mechanism to balance and maintain photosynthesis at cold stress. Cyanobacteria have adapted various mechanisms to regulate the effect of cold stress in photosynthesis. DNA microarray studies using Synechocystis have demonstrated that during cold acclimation, the genes related to photosystem I complex and phycobilisomes were strongly repressed [9, 25]. Cold stress also leads to decreased activity of PSII [9]. The regulatory mechanism of such differential expression of the photosynthetic genes during cold acclimation is not known. Such regulation usually takes place at transcriptional and post-transcriptional levels. Generally, acclimation to stress requires a quick response by the organism. Rapid response to a stress is possible due to post-transcriptional regulation which

results into stress-responsive altered gene expression profile. Post-transcriptional regulation involves different regulatory elements like the small regulatory RNAs and ribonucleases.

1.6 Small regulatory RNAs

Small regulatory RNAs (sRNA) are the non-coding RNA (ncRNA) transcripts. Studies have indicated its importance in the posttranscriptional gene regulation in both pro- and eukaryotes. sRNA mediated gene regulation results into a quick response and thus, is advantageous for adaptation against environmental changes for bacteria as fast responses is required for the survival of the organism [34, 35, 36]. Bacterial sRNA are usually 50-300 nucleotides long in length and regulates the expression of the target mRNA by various mechanisms. These regulatory RNAs regulate the expression by complementary base pairing to the target mRNA. Base-pairing of sRNA to its target may either inhibit or activate the translation of the target mRNA. Also, binding of sRNA can promote or block cleavage of the targets by ribonuclease (RNase) thus, alters the stability of the target mRNA [37]. sRNAs exhibits its negative regulation by base pairing in promoter region or in the vicinity of the ribosome binding site (RBS) and interferes in the ribosome binding. They can also base pairs at a distant locations in the genome and enhances the binding of ribosome to the promoter of the target genes by blocking formation of secondary structures [38, 39]. The sRNAs can be grouped into two types based on the location of their coding sequences; cis-encoded RNA when the coding sequence is located opposite DNA strand opposite to the target RNA, and trans-encoded sRNA which are encoded by sequences located distant away from the loci of the target genes in the genome. The cis-encoded RNA base-pairs by either complete or partial overlapping with their targets as they are transcribed from the complementary strand of the target gene. This group of antisense sRNA mostly are involved in the control mechanism of phage development as well as in the

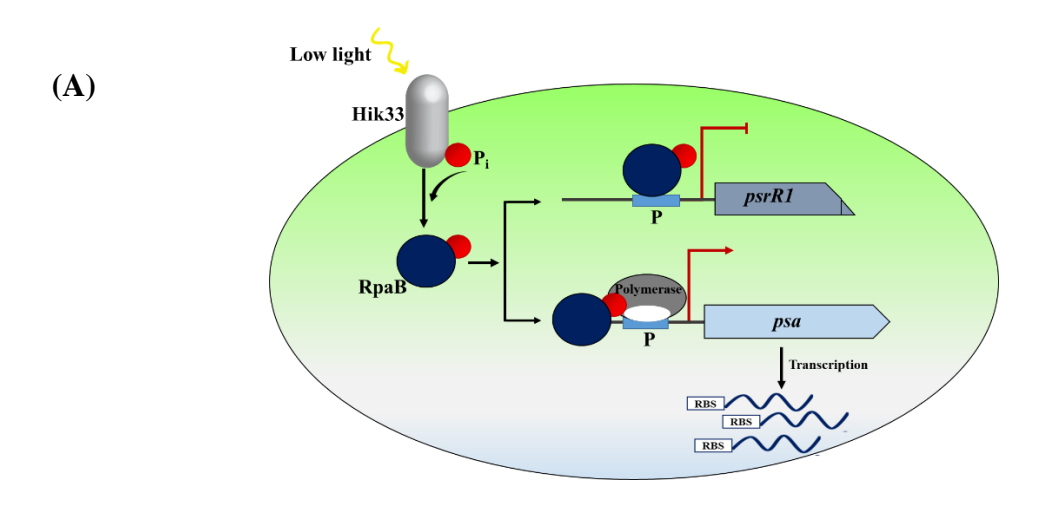
replication of plasmid in bacteria [40]. Contrary to cis-encoded sRNA, the trans-encoded RNA partially base pairs with their target mRNAs. The trans-encoded sRNAs mostly are negative regulators, and represses the expression of protein through different mechanism like inhibiting translation, degradation of the target mRNA or both [40, 41, 42].

1.6.1 Cyanobacterial sRNA

In cyanobacteria, most of the non-coding RNAs were identified to owe vital roles during acclimation responses to environment changes by regulating various cellular metabolic pathways including the photosynthesis, CO₂ fixation, and several other metabolisms. In Synechocystis, hundreds of promising regulatory RNA candidates were identified by comprehensive transcriptome analyses [43, 44]. In Synechocystis, 26% of all the genes are accounted to be sRNAs which control different cellular functions. Some of these sRNAs are conserved throughout the cyanobacterial phylum [35, 45]. Deep RNA-sequencing of the genome and its four mega-plasmids led to the identification of in 5261 putative sRNAs in Synechocystis [39, 44, 46, 47]. Several studies were conducted on some of these identified cyanobacterial sRNA and their functional role in the stress responsive gene regulation were elucidated in Synechocystis. The iron stress repressed RNA, IsrR is a sRNA that regulates the transcription of the iron stress inducible protein, IsiA (a component of photosystem) and thus, is an element in the gene regulatory mechanism during iron deficiency [48]. Some few more examples of sRNAs involved in the regulation of photosynthetic genes expression under different environmental conditions are PsbA2R, PsbA3R, PsrR1 and RblR [14, 47, 49]. Another sRNA, As1-Flv4 is a participant in the regulation of the set of genes that response to the changes in the supply of inorganic carbon [50]. The nitrogen stress-induced RNA 4, NsiR4 role as a sRNA involved in the nitrogen homeostasis was reported [51]. Another sRNA, Nc117 was discovered to be involved in the regulation of alcohol tolerance in *Synechocystis* [52].

1.6.2 PsrR1 mediated photosynthetic gene regulation during high-light stress

The sRNA, photosynthetic regulatory RNA1 (PsrR1) is a trans-encoded sRNA which is extensively conserved among the members of cyanobacteria. The transcript of PsrR1 (131bp in length) is encoded by the nucleotide region present between the two genes; fabF (slr1332) and hoxH (sll1226). Previously known as SyR1, it is conserved widely in the phylum cyanobacteria. Recent studies have reported that many of the photosynthesis-related genes are regulated post-transcriptionally by PsrR1 during high-light stress in Synechocystis. PsrR1 was reported to be strongly upregulated when exposed to HL [14]. Computational and experimental studies demonstrated that PsrR1 complementary base pairs in the promoter region of the mRNA of the genes-psaJ, psaL, cpcA and chlN) in Synechocystis [14, 23]. In a recent findings, PsrR1 was identified to form a feed forward loop with the RpaB, the response regulator to regulate the photosynthetic genes during high light acclimation [23] (Figure 7). The DNA binding motif of RpaB was found to be located in the upstream region of high light genes, photosystem related genes and also in the promoter region of the sRNA, PsrR1 [23, 53]. In Synechocystis, Hik33 and RpaB pair are also tasked to sense and transduce high-light stress [9, 19]. During low light (LL) condition, Hik33 undergoes autophosphorylation and in turn, phosphorylates RpaB. The active RpaB binds to HLR1 region and creates blockage in the binding of the ribosome inhibiting the expression of PsrR1. On the other hand, binding of RpaB facilitate the binding of RNA polymerase to initiate the events leading to upregulation in the expression of the PS I genes. But HL stress signal causes dephosphorylation of RpaB, leading to decrease binding affinity to the HLR1 region and as a consequence, de-repression of psrR1 expression as well as decrease in PSI promoter activity [23, 54].



(B)

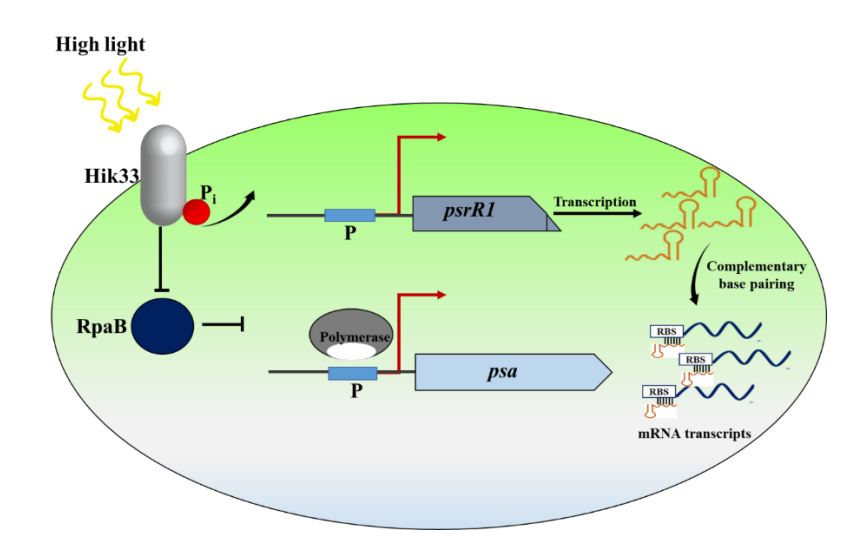


Figure 7: Pictorial representation of the post-transcriptional regulation of the photosynthetic genes during high-light acclimation. The signal of any change in the light intensity is transduced by the two component system Hik33-RpaB. (A)During low-light (LL) condition, binding of RpaB to promoter region leads to downregulation of PsrR1 but induces expression of the photosynthetic genes; (B) During high-light (HL) conditions, the binding affinity of non-phosphorylated RpaB to the promoter region declines, as a result de-repression of *psrR1* and repression of PSI genes occur. The PsrR1 expressed during HL conditions base pair in the ribosomal binding site in the transcripts of the PSI genes and blocks the translation, thus causes downregulation of the PSI genes (adapted from Kadowaki *et al.*, 2016 [23]).

The regulatory mechanism of the photosynthetic genes mediated by PsrR1 and RpaB during HL stress has been elucidated in *Synechocytis* [14, 23]. But the gene regulatory mechanism of the downregulated PS genes during cold acclimation is yet to be explored. It is to be noted that, the consequences of HL in photosynthesis observed in different studies is very similar to that observed during cold stress in cyanobacteria. Both cold stress and high light exposure leads to downregulation of the photosynthetic related genes [24, 25]. Also the same pair of sensor and response regulator i.e. Hik33-RpaB pair sense the temperature fluctuations (cold stress) and highlight stress [9, 54].

1.7 Ribonucleases: participant in the post transcriptional regulation

It is imperative that microorganisms respond rapidly to environmental stress for their survival. They alter the expression level of their stress responsive genes rapidly by regulating transcription, transcript degradation, and translation. Regulation of the stress responsive genes is mostly achieved by post-transcriptional regulation. During such mode of regulation, the increase rate of mRNA turnover mediates a swift adaptation to environmental changes. Besides mRNA turnover, post transcriptional regulation also might lead to the stability of those transcripts which are essential for the organism to acclimatize to the environmental stress. Various abiotic stress including low temperature modulates mRNA degradation [55]. During sRNA mediated posttranscriptional regulation, the sRNA base pairs with the mRNA targets and initiates the event of gene regulation in response to stress. Coupling of the sRNA to the genes that are ought to be downregulated are targeted by ribonucleases to undergo decay. Decaying of the mRNA-sRNA complex is the last event during post-transcriptional gene regulation [56, 57]. Thus, we can assume that the sRNA mediated post-transcriptional

regulation involves ribonucleases to decay the mRNA targets (Figure 7) and thus, regulates gene expression aiding the organism acclimatize to the unfavourable changing environment.

Ribonucleases (RNases) are the proteins that degrades RNA which were considered as just nonspecific degradative enzymes. Later on, different studies identified their role in maturation of various precursor RNA [58]. RNases are essential in almost all aspects of RNA metabolism which includes RNA degradation and turnover, maturation, quality control. They also plays as the mediator in stress responsive gene expression regulation [58]. RNases maintains the levels of cellular RNA by processing RNA transcripts thus, leading to either their stabilization or degradation. An insight to structural and functional role of RNase were studied extensively in *E. coli* and *Bacillus subtilis*.

In *E. coli*, even though many ribonucleases have been identified but only a few have been characterised. RNases are grouped according to their ability to cleave or degrade genes internally (endoribonucleases) or starting from the ends (exoribonucleases). These ribonucleases can associate with each other or other proteins and co-factors to for a RNA degrading machineries. These ribonucleases are known to associate with each other, RNA helicases and other co-factors to form a multimeric protein complexes [59, 60].

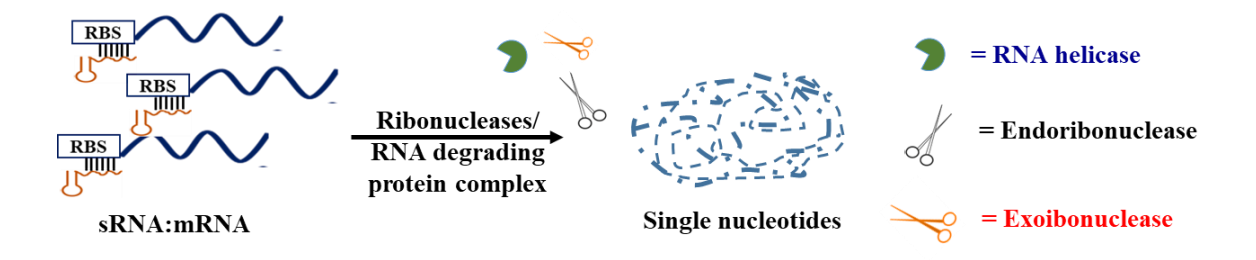


Figure 8: Schematic representation of the probable role of regulatory enzymes involved in the decay of mRNA during post transcriptional regulation mediated by sRNA. Binding of the regulatory sRNA to the targets can either lead to stabilization or destabilize the mRNA targets. During destabilization, the ribonucleases causes decay of the mRNA. The decay process is generally assisted by the RNA helicase.

1.7.1 RNA degradosome

The multiprotein complex, RNA degradosome is involved in bacterial mRNA degradation. RNA degradosome of *E. coli* comprises of the endoribonuclease RNaseE, 3'-5' exoribonuclease polynucleotide phosphorylase (PNPase), DEAD-box RNA helicase (RNA helicase B, RhlB) and the glycolytic enzyme, enolase (Figure 9) [61, 62]. Bacteria like the *Bacillus subtilis*, that lacks RNase E homologs in their genomes instead utilizes RNase Y, also a membrane-anchored endoribonuclease to construct the RNA degradosome [63].

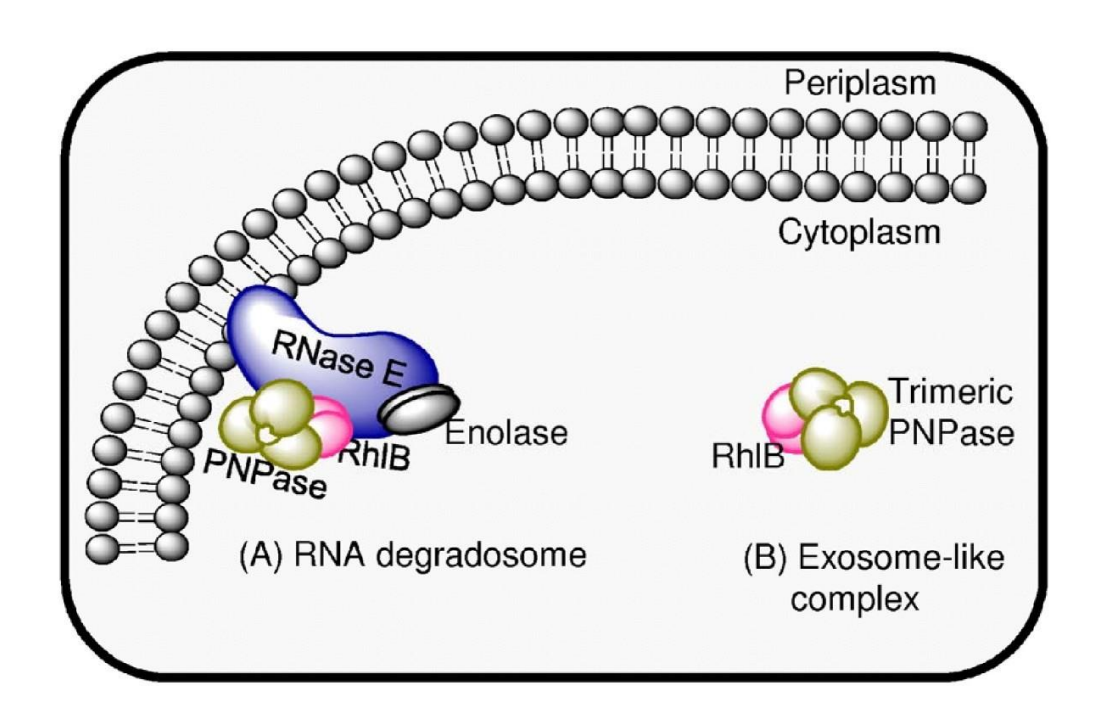


Figure 9. Pictorial representation of RNA degradosome and bacterial Exosome-like complex. (A) RNA degradosome, a multimeric protein complex consisting of an endoribonuclease (RNase E), a $3'\rightarrow 5'$ polynucleotide phosphorylase (PNPase) exoribonuclease, a DEAD-box RNA helicase (RhlB helicase), and the glycolytic enzyme enolase, and (B) In *E. coli*, PNPase is associated with the RhlB to form "bacterial exosome" which exhibits the $3'\rightarrow 5'$ exonucleolytic activity (adapted from Kaberdin *et al.*, 2011 [62]).

1.7.2 RNA Exosome

RNA exosome-complex is another example of RNA degrading machinery found in archaea, yeast and other higher eukaryotes. It is a large multiprotein complex formed by the association of different ribonucleases. Structurally, the RNA exosome complex is similar to that of the bacterial PNPase which contain the RNase PH-domain including two other domains-the RNA-binding S1 and KH domains. The bacterial PNPase exists as a trimer and thus, the structure of the trimer includes in total six of each of the RNase PH, S1 and KH domains which is similar to the number of domains contributed by different protein subunits in the RNA exosome complex. The archeal RNA exosome complex has 9 subunits consisting of a hexameric ring core of two proteins- Rrp41, Rrp42 (each containing one RNase PH-like domain) and a trimeric cap consisting of either Rrp4 or Csl4 or both (the S1 domain containing subunits). This ninth subunit of the archeal exosome is the homolog of the bacterial primase DnaG [64]. The archeal RNA exosme has 3'-5' phosphorolytic exoribonuclease activity. Compared to the archeal counterpart, the eukaryotic exosome complex is much more complex.

Besides the 9-subunit core complex, the complexity of the eukaryotic exosome is further increased by the incorporation of a tenth subunit, Rrp44 (Dis3). Homologous to bacterial RNase II, Rrp44 is a hydrolytic exonuclease and is responsible for the catalytic activity of the exosome complex (Figure 10C) [60]. A recent study suggests that in *E. coli*, an exosome-like complex formed by the association of PNPase and RhlB helicase is involved in cysteine biosynthesis [65]. Also the mitochondrial exosome complex consists of two members- Dss1 (3'-to-5' exoribonuclease) and Suv3 (RNA helicase) [66]. But such RNA degrading machineries have not been identified yet in cyanobacteria.

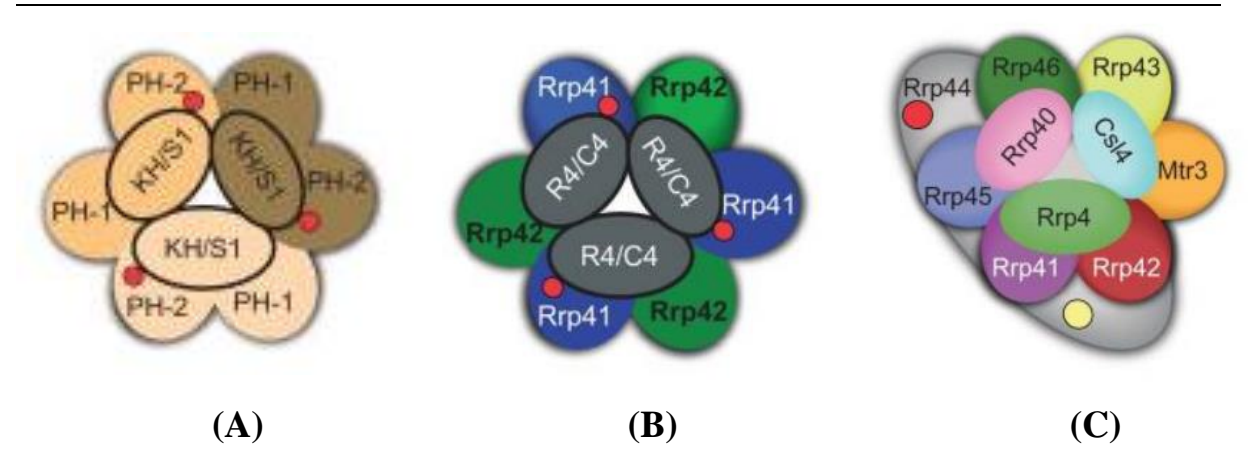


Figure 10. Pictorial representation of : (A) bacterial PNPase, (B) Archeal exosome complex (Rrp41, Rrp42, Csl4 or/and DnaG) and (C) Eukaryotic exosome complex (9 core subunit and Rrp44) (adapted from Januszyk *et al.*, 2010 [60]).

1.8 Cyanobacterial ribonucleases

Very little is known about the cyanobacterial ribonucleases. Homologs of the major ribonucleases studied in E. coli and found in cyanobacteria are yet to be explored to understand their role in the The 3'-5' organism. exoribonuclease, Polyribonucleotide Nucleotidyltransferase (PNP) of *Synechocystis* is encoded by the gene *slr1043*. PNP exhibits dual activity as it polyadenylates as well as also degrade RNA and thus, are considered to be very similar to the PNPase of the cell organelle, chloroplast of higher eukaryotic plants [67]. The essentiality of PNP for the survival of the cyanobacteria was indicated by the fact that a fully segregated mutant of PNP could not be generated [68]. Microarray studies indicates that PNP in Synechocystis is a cold-inducible protein [9, 19]. Homologs of another 3'-5' exoribonuclease, RNaseII/R- Sll1290 and Sll1910 was reported in Synechocystis. Sll1290 exhibiting RNaseII activity is reported to be an essential gene [69]. The other homolog, Sll1910 was similar to a protein that is responsible for conferring sensitivity to acetazolamide, which is a carbonic anhydrase inhibitor [68]. The ORF of some major ribonucleases found in Synechocystis and few other cyanobacterial species are listed in the Table 1.

Organism	Enzyme class				
	RNaseE/G	RNaseIII	RNaseJ1/J2	RNaseII/R	PNP
Synechocystis sp. PCC 6803	slr1129	slr1646	slr0551	sll1290	slr1984
		slr0346		sll1910	sll1043
Anabaena sp PCC 7120	alr4331	all4107	all3678	all4450	all0136
		alr0280		alr1240	all4396
		alr1158			
Gloeobacter violaceus PCC 7421	gvip208	gvip371 glr4180	glr1019	gll1616 gll1448	gvip129 glr4144 gll3149
Synechococcus elongatus PCC 7942	Synpcc7942_ 0878	Synpcc794 2_1645 Synpcc794 2_2120	Synpcc7942_1 846	Synpcc7942_1 911 Synpcc7942_1 124 Synpcc7942_1 546	Synpcc7942_2 440
Synechococcus sp. PCC 7002	SYNPCC700 2_A0788	SYNPCC70 02_A0061 SYNPCC70 02_A2542 SYNPCC70 02_A0384	SYNPCC7002 _A1273	SYNPCC7002 _A1543 SYNPCC7002 _A0574	SYNPCC7002 _A1066
Synechococcus elongatus PCC 7942	Synpcc7942_ 0878	Synpcc794 2_1645 Synpcc794 2_2120	Synpcc7942_1 846	Synpcc7942_1 911 Synpcc7942_1 124 Synpcc7942_1 546	Synpcc7942_2 440

Table 1: List of some of the major ribonucleases found in the cyanobacterial species.

1.9 Cyanobacterial ribonucleases: role at low temperature

As mentioned earlier, ribonucleases participate and act as the mediator of post-transcriptional gene regulation. For instance, in *Synechocystis*, RNaseE leads to the instability of the *psbA* mRNA transcripts, the gene that encodes D1 protein of PSII during dark induced post-transcriptional regulation [70]. The other active enzyme that plays role in the event of gene regulation are the RNA unwinding enzyme, RNA helicases. The formation of secondary structure of mRNA during cold stress needs to be stabilized by the unwinding enzymes and assists the ribonucleases in their activity in *E. coli* [71]. In *Synechocystis*, the RNA helicase, CrhR was observed to be highly upregulated at low temperature [9, 19]. Deletion of *crhR* increased the fold of cold-responsive downregulation of the photosynthetic genes- particularly the genes related to PSI and PBS at low temperature [25]. Studies also indicate that it is essential in stress inducible energy redistribution between the photosystems and maintains the stoichiometry of PSII: PSI during low temperatures [25].

The existence of cyanobacterial RNA degrading complex is still being investigated in cyanobacteria. The homologs of various protein subunits of the archaeal and eukaryotic RNA-exosome and the *E. coli* RNA degradosome complex are found in *Synechocystis*, however, no similar complexes have been identified to date in *Synechocystis*. The genes encoding the homologs of some of the components of archea, mitochondria as well as eukaryotic exosome are upregulated in *Synechocystis*. The gene *crhR* (*slr0083*) and *pnp* (*sll1043*) encoding RNA helicase and polynucleotide phosphorylase respectively are upregulated during low temperature [9, 19, 25]. Rrp44/Dis3 of the eukaryotic exosome is a bacterial RNaseII-like protein. Although the cold inducibility of *Synechocytsis* RNaseII is unknown, it is known that *E. coli* RNase II complements the cold shock function of PNPase [72]. Moreover, the 3'-5' exoribonuclease Dss1 of mitochondrial exosome, is an RNase II/RNB-type exonuclease. These

facts led us to an assumption of the possibility of formation of a cold-inducible cyanobacterial RNA degrading protein complex, and might be involved in the regulatory mechanism of the cold-responsive photosynthetic gene at low temperature. Interestingly, another candidate involved in the regulation of the PS genes might be the cold inducible sRNA PsrR1. Thus, it is likely that the rapid downregulation of the photosynthesis related genes might be regulated post-transcriptionally involving the sRNA PsrR1 together assisted by the ribonucleases; PNP, RNaseII and the RNA helicase, CrhR.

2. OBJECTIVES

The literature review indicated the possible involvement of the small regulatory RNA, PsrR1 together with the ribonucleases PNP, RNaseII and RNA helicase, CrhR in the optimization of cyanobacterial photosynthesis at low temperature. Hence, in the present study was an attempt to elucidate the gene regulatory mechanism involved in the regulation of photosynthetic genes during cold acclimation in the unicellular cyanobacterium, *Synechocystis* PCC6803. The following objectives were designed:

I. Elucidation of role of a sRNA, PsrR1 in the regulation of photosynthetic genes during cold acclimation.

- 1. To check if PsrR1 is a cold responsive small regulatory RNA by analyzing its expression in wild-type *Synechocystis* during cold stress.
- 2. Generation of $\Delta psrR1$ and $psrR1^+$ strains and compare them with the wild-type *Synechocystis* strain to analyze changes in the PSI and PBS gene expression during low temperature acclimation.
- 3. Comparison of growth and pigment composition in $\Delta psrR1$ and $psrR1^+$ strains with wild-type.
- 4. To check the effect of mutation of *psrR1* on relative content of PSI and PSII during cold stress.

II. Elucidation of role of the response regulator, RpaB in the regulation of photosynthetic genes at low temperature.

1. Generation of $\triangle rpaB$ to examine the effect of mutation on the expression level of photosynthetic genes.

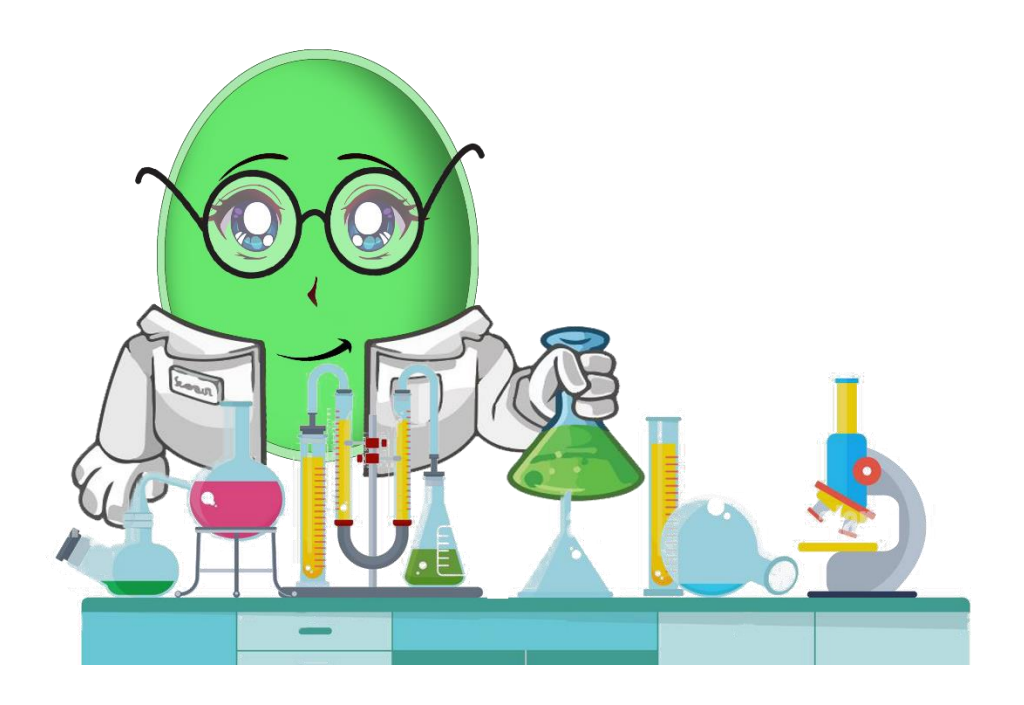
III. Elucidation of role of ribonucleases in the degradation of PSI and PBS transcripts during cold acclimation.

- 1. Generation of Synechocystis strain expressing PNP and CrhR with 3XFLAG tag.
- 2. To identify the RNA molecules associated with PNP and CrhR during cold stress.

IV. Investigation on existence of a cold inducible exosome complex.

- 1. Study of the interaction between PNP, CrhR, and RNaseII using the bacterial two hybrid system.
- 2. Study of the kinetics of the interaction of PNP, CrhR and RNaseII using Surface plasmon resonance (SPR).

3. MATERIALS AND METHODS



3.1 Escherichia coli

The bacterial strain, *Escherichia coli* (DH5α) was used as the host system to maintain the final plasmid DNA constructs. *E. coli* Rosetta (DE3) pLysS was used to induce and overexpress the 6XHis-tagged proteins. The bacterial cells were cultured / maintained with appropriate antibiotic(s) in Luria Bertani (LB) broth and / or on agar plates with LB at 37°C. For bacterial two-hybrid (BACTH; Bacterial Adenylate Cyclase-Based Two-Hybrid) assay, *E. coli* cya (DHP1) strain was used and the cultures were grown in the selective media, MacConkey agar plates supplemented with 1% maltose and appropriate antibiotics and incubated at 30°C in dark for screening the protein-protein interactions.

3.1.2 L.B. MEDIUM

The LB broth of 1 L was prepared by dissolving 10 g of Tryptone (Cat. No. CR014-500G, Himedia), 5 g of Yeast extract powder (Cat. No. RM027, Himedia) and 10 g of NaCl (Cat. No. MB023, Himedia) in 950 ml of double distilled water (DDW) and finally adjusted the volume to 1 litre with DDW. For the LB Agar, besides the three compositions of LB broth, additionally 1.5% of agar powder (w/v) (Cat. No. GRM026, Himedia) was added into LB broth solution. The LB broth/agar prepared were steam-sterilized for 20 minutes at 15 *psi* pressure in an autoclave. The sterilized LB agar media was cooled to 50°C followed by addition of appropriate antibiotics and mixed in the laminar hood. Approximately 25-30ml of the media was poured into 90 mm Petri-plate. The LB plates after solidification in the laminar hood were sealed and stored until use at 4°C.

3.1.3 Preparation of LB medium supplemented with Antibiotics

Screening of the positive clones after transformation was done by adding of the appropriate antibiotics to the growth media. Different antibiotics used in the study were kanamycin (Kan), ampicillin (Amp) and chloramphenicol (Cm). These antibiotics were sterilized using syringe

filters and were added to the LB medium. The final concentration of the antibiotics in the LB medium were 50µg/ml, 100µg/ml and 35µg/ml for Kan, Amp and Cm respectively.

3.2 Synechocystis sp. PCC 6803 GT-1

A glucose-tolerant strain, *Synechocystis* sp. PCC 6803 GT-1 obtained from Prof. Iwane Suzuki (Life and Environmental Sciences, University of Tsukuba, Tsukuba, Japan) served as the wild type (WT). The specialized cyanobacterial growth medium YBG-11 was used for culturing and maintenance of the WT, mutant and overexpression strains generated for the present study. For optimum growth, the WT cells were grown photoautotrophically with continuous illumination (75 μmol photons m⁻² s⁻¹) at 34°C [73].

Mutant strains $\Delta psrR1$ and $\Delta rpaB$, the overexpression strain $psrR1^+$, PNP^+ and $CrhR^+$ generated for the present work were cultured as the above mentioned growth conditions and the culture medium were supplemented with appropriate antibiotic(s) at recommended concentration in the medium. To overexpress PNP and CrhR under the copper repressible promoter, PpetJ; the strains were grown with the supply of illumination (75 μ mol photons m⁻² s⁻¹) to mid-exponential phase at 34°C. The cells were then washed twice with copper depleted YBG-11 medium followed by inoculation into copper depleted YBG-11 media.

3.2.1 Preparation of YBG-11 for Synechocystis culture

The chemical components required for YBG-11 were first prepared as stock solutions in autoclaved double distilled water, filter sterilized and stored at 4°C. These stock solutions were used for the final preparation of the YBG-11 media. The compositions of the each of the different ingredients in the stock solutions are given below:

A) Solution 1:

Components	Molecular formula	gram per litre	Concentration in stock
Sodium nitrate	NaNO ₃	148.73	1.75 M
Magnesium sulfate heptahydrate	MgSO ₄ .7H ₂ O	7.39	30mM
Citric acid	$C_6H_8O_7$	0.6	3mM
Boric acid	H ₃ BO ₃	0.28	4.5mM
Dipotassium hydrogen phosphate	K ₂ HPO ₄	3.05	17.5mM
Trace minerals		10ml	

B) Trace minerals:

Components	Molecular formula	gram per litre	Concentration in stock
Ethylenediaminetetraacetic acid disodium salt dihydrate	Na ₂ EDTA	5.5	14.7 mM
Zinc sulfate heptahydrate	ZnSO ₄ .7H ₂ O	2.22	7.7 mM
Sodium molybdate dihydrate	Na ₂ MoO ₄ .2H ₂ O	3.9	16.1 mM
Copper(II) sulfate pentahydrate	CuSO4.5H ₂ O	0.79	3.1 mM
Cobalt(II) nitrate hexahydrate	Co(NO ₃) ₂ .6H ₂ O	0.494	1.69 mM

C) Solution 2:

Components	Molecular formula	gram per litre	Concentration in stock
Ethylenediaminetetraacetic acid disodium salt dihydrate	Na ₂ EDTA	3.34	9 mM
Iron(III) chloride hexahydrate	FeCl ₃ . 6H2O	1.62	6 mM

D) EDTA solution:

Chemical Name	Molecular formula	g/L	Concentration in stock
Ethylenediaminetetraacetic acid disodium salt dihydrate	Na ₂ EDTA	3.72	10mM

E) Solution 3:

Chemical Name	Molecular formula	g/L	Concentration in stock
Sodium carbonate	Na ₂ CO ₃	20	188mM

F) Solution 4:

Chemical Name	Molecular formula	g/L	Concentration in stock
HEPES		119.4	500mM

G) Solution 5:

Chemical Name	Molecular formula	g/L	Concentration in stock
Calcium chloride dihydrate	CaCl ₂ .2H ₂ O	36	244.8 mM

H) Solution 6:

Chemical Name	Molecular formula	g/L	Concentration in stock
Manganese(II) chloride tetrahydrate	MnCl ₂ .4H ₂ O	119.4	500mM

The final YBG-11 media of 1L was prepared using the stock solutions

I) Components of the YBG-11 medium.

Solution	Volume of the solution		
Solution 1	10 mL		
Solution 2	1.66 mL		
EDTA solution	111 μL		
Solution 3	1 mL		
Solution 4	20 mL		
Solution 5	1 mL		
Solution 6	1 mL		

Table 2: Compososition of YBG-11 medium. (A-H) The compositions of the different stock solutions required for the preparation of YBG11. (I) Volume of the stock solutions used for YBG-11 nutrient media preparation

3.2.2 Preparation of YBG-11 Antibiotic medium

Appropriate antibiotics were added to the YBG-11 medium to give a selection pressure during the generation and maintenance of the mutant cyanobacterial strains. Antibiotic stock solutions were prepared and sterilized by syringe filters. Three different antibiotics used were Kanamycin, Spectinomycin and Chloramphenicol. The final concentration of these three antibiotics in the YBG-11 media were $25\mu g$ / ml, $25\mu g$ / ml and $35\mu g$ / ml respectively.

3.2.3 Preparation of YBG-11 Agar plates

To prepare YBG-11 agar plates, 2X YBG-11 supplemented with sodium thiosulfate (Na₂S₂O₃.5H₂O) (6g for 1 L) was prepared by addition of the stock solutions under the laminar hood into autoclaved double distilled water. Separately in a conical flask, 2X agar (3% agar, Cat. No. RC1011, G Biosciences) was prepared and autoclaved. For the final preparation, two autoclaved solutions were mixed in equal ratio (1:1 ratio). Filter sterilized antibiotics as per requirement were added into the mixture and poured in sterile 90mm Petri plate in the laminar hood and cooled down to solidify. The prepared YBG-11 agar plates were stored at 4°C till use.

3.2.4 Preparation of nutrient limited YBG-11 medium

For cyanobacterial over expression strains, copper depleted YBG-11 media was prepared. To prepare the copper depleted YBG-11 media, the component CuSO₄. 5H₂O of the trace minerals in Solution 1 was eliminated.

3.2.5 Low temperature treatment

WT, $\Delta psrR1$, psrR1⁺ cultures were grown at 34°C with illumination of 75 μ mol photon m⁻² s⁻¹, until the value of O.D₇₃₀ was 0.4. The cultures were then shifted to water-bath which was set at 20°C with continuous illumination (75 μ mol photon m⁻²s⁻¹) and filter-sterilized air was

continuously bubbled into the cultures. For RNA immunoprecipitation (RIP) analysis, PNP⁺ and CrhR⁺ cells were used to overexpress 3X-FLAG-PNP and 3X-FLAG-CrhR in the copper depleted YBG11 media for 45 h, the cells were shifted to from 34°C to 15°C for 30 mins immediately after copper depletion.

3.3 Molecular biology kits, enzymes, and chemicals

Different kits of molecular biology tools and enzymes were acquired from Qiagen (Germany), Takara bio (Japan), Thermo Fischer Scientific (USA), and Sigma-Aldrich (USA). These enzymes and kits were stored as per the instructions mentioned in the kits. Analytical graded reagents and chemicals were procured from Thermo Fischer Scientific (USA), Takara (Japan), Sigma-Aldrich (USA), GE Health Care (USA), , , Himedia (India), G Biosciences (India) and SRL (India).

3.4 Molecular biology protocols

The protocols for various molecular biology techniques like isolation of plasmid and genomic DNA, enzymatic reactions like restriction digestion, ligation, polymerase chain reaction, transformation, competent cell preparation, and agarose gel electrophoresis were executed as per the manual provided protocols in the kits or was referred from the book on laboratory manual authored by Sambrook J [74].

3.5 Plasmid DNA vectors

To generate mutants by targeted inactivation of selected genes, a blunt cloning vector pJET1.2 (CloneJET PCR Cloning Kit, Cat No: K1231-Thermo Fischer Scientific) was used. For ectopic expression of selected proteins tagged with 3X-FLAG tag in *Synechocytis*, we had modified the plasmid pVZ321. The pVZ321 plasmid which was originally designed for functional complementation studies [75], modified to express proteins of interest with 3X-FLAG tag

under the control of copper repressible promoter PpetJ. For heterologous expression of PNP and CrhR in *E. coli*, a pCold-1 bacterial expression vector and for RNaseII, pET28a(+) were used. For the purpose of cloning and overexpression of PsrR1 in the genome of *Synechocystis*, the plasmid vector pSyn-slr2030-2031 with the copper repressible promoter, petJ promoter was generated and used. The plasmid vectors, pT25 and pT18 were used for BATCH assay to investigate interaction of PNP, CrhR and RNaseII in the *E. coli* cya- (DHP1) strain [76].

3.6 Quantification of nucleic acids

3.7 Cell culture collection for qRT-PCR, NGS and microarray analysis:

The WT, $\Delta psrR1$, $psrR1^+$ and $\Delta rpaB$ cells were allowed to grow to an O.D₇₃₀ of 0.4. A volume of 50 ml of the cultures of each strain (in triplicates) were instantaneously killed by mixing the cultures with equal volume of ice cold 5% phenol (in ethanol). The remaining cultures were exposed to cold treatment and were harvested at the following time points- 0.5, 3, 6 and 12h for RNA isolation. The instantaneously killed cells were stored at -80°C till use.

3.8 Generation of the mutants and overexpression strains:

3.8.1 Targeted inactivation of psrR1

A deletion mutant strain of PsrR1, \(\Delta psrR1 \) was generated by replacing the DNA region which is transcribed into the non-coding RNA, PsrR1 with a chloramphenical antibiotic resistance cassette. The 131 DNA region encoding PsrR1 along with 472 upstream and 492 downstream flanking DNA region was amplified from the genomic DNA of Synechocystis by PCR with the primer set-psrR1-FP: 5'ATC GAG CTC CCA CAG TGC CCA GCA AGC CG 3' and psrR1-RP: 5'ATA CCC GGG GCT GGA GGT GTG GCC ACG TCC 3'. To clone the amplified DNA fragment, it was ligated into the blunt site of the pJET1.2 / blunt cloning vector (Cat No. K1231, Thermo Fisher Scientific, USA). Then, a 79 DNA region of psrR1 was replaced with a chloramphenicol antibiotic resistance cassette. Firstly phosphorylation of the primer pair, psrR1-INV-FP: 5'ATG CCC TCG GTG ATG CCG 3' and psrR1-INV-RP: 5'CTG TCG GGT TTC CAT AGC C 3' were done using T4 PNK (Cat No. EK0031, Thermo Fisher Scientific, USA). These primer set were designed such that during an inverse PCR reaction, they amplified the pJET1.2 vector along with the cloned psrR1-flanking DNA regions but excluded 79 DNA fragment corresponding to psrR1. The nucleotide sequence of the chloramphenicol resistance cassette was amplified by PCR using the plasmid pRL1075 with the phosphorylated primer set, Cm-FP: 5'AAT GAG ACG TTG ATC GGC ACG TAA G 3' and Cm-RP: 5' GTC CAA AGG TTG TCT TTA CGC CCC GCC CTG CCA C 3'. The PCR amplified products were blunt ligated with the inverse PCR amplified product to generate pJET-ΔpsrR1::Cm^R. The $\Delta psrR1$ plasmid vector was transformed into the mid-exponential growing WT Synechocystis cells. The complete inactivation of mutant colonies were checked by segregation analysis.

3.8.2 Generation of overexpression strain *psrR1*⁺:

A psrR1⁺ strain was generated to overexpress PsrR1 in the WT cells. A 131 bp corresponding to PsrR1 DNA region together with the PpetJ promoter was cloned into the region of the neutral site slr2030 and slr2031 in the genome of Synechocytis. The plasmid, pSyn-slr2030-2031-Cm^R was used to generate the vector backbone by an inverse PCR reaction using the primer set. PpetJ-PsrR1-INV-FP: 5' TGC CTG GCG GCA GTA GCG C 3' and PpetJ-PsrR1-INV-RP: 5'AAT GAG ACG TTG ATC GGC ACG TAA GAG GTT CCA ACT TTC ACC 3'. Two separate PCR reactions were set to amplify the copper repressible promoter, PpetJ and the DNA fragment, psrR1 with its downstream 52 bp region. In the first reaction (PCR-1), the primers-PpetJ-pSyn-INF-FP: 5' GAT CAA CGT CTC ATT GGA ATT GCT CTG GCA ACT GAT TAA TCC A 3' and PpetJ-PsrR1-INF-R1: 5'CCA TAG CCT TAT GAA GGT ATT ATG GGA GG 3' were used to amplify the DNA fragment of PpetJ. In the second reaction (PCR 2), psrR1 was PCR amplified along with 52 bp from the downstream region using Synechocystis genomic DNA as a template. The primers used in the second reaction were - PpetJ-psrR1-INF-FP: 5'CAT AAT ACC TTC ATA AGG CTA TGG AAA CCC GAC 3' and PpetJ-psrR1-INF-RP: 5' TAC TGC CGC CAG GCA GGA ACT AAT TAA GTC CAT CCA GCG 3'. We designed the primers in such a way that PCR-1 reaction resulted into amplified DNA product with 15 bp on the 5' end which was homologues to the 3' end of the nucleotide sequence of the inverse-PCR amplified vector backbone. Also, the 3' end had 15 bp homologous to the 5' end of the PCR amplified product of PCR-2. The 3' end of PCR amplified product of PCR-2 had 15 bp homologous to the 5'end of the vector backbone. The inverse PCR amplified vector backbone, the PpetJ promoter and the PsrR1 was used to set up infusion reaction (Infusion HD cloning kit, Clonetech, Takara). Thus generated pSyn-Slr2030-PpetJ-PsrR1-31-Cm^R plasmid DNA construct was transformed into WT Synechocystis cells by natural transformation [77].

3.8.3 Inactivation of RpaB:

A partially segregated $\triangle rpaB$ was generated by replacing the ORF slr0947 that codes for RpaB, with spectinomycin resistance cassette. The gene slr0947 together with its flanking upstream region of 491 bp and 474 bp from upstream and downstream region was amplified in a PCR from the Synechocystis genomic DNA using the primer set-slr0947-FP: 5' CTT TGC CAA AAC TTT AGG GGC CGG C 3' and slr0947-RP: 5' GTT TGC ATT ACC CGT TCT ACA ATC GG 3'. The PCR amplified product was ligated by blunt ligation into the pJET1.2 vector. The recombinant plasmid construct generated was named as pJET-slr0947. A 530 bp DNA coding region corresponding to slr0947 was deleted and replaced with spectinomycin cassette by infusion cloning technique (Cat no. 638910, Takara). For the deletional inactivation of slr0947, the vector backbone was first amplified using the primer set, mut-inv-947 FP: 5'CTA GAG GAA GAC CCC AGC AAT CCC G 3' and mut-inv- 947 RP: 5' CAG CGG TCA CCA CTT CAT AGC CAA TC 3'. The spectinomycin cassette (1147 bp) was amplified from the vector-pSyn_6 (Cat no. A24230, Invitrogen) using the primer set Spec-FP: 5' AAG TGG TGA CCG CTG TTA TTT GCC GAC TAC CTT GGT GAT CTC G 3' and Spec-RP: 5'GGG GTC TTC CTC TAG AGC CAG CCA GGA CAG AAA TGC CTC G 3'. The PCR amplified products were used to generate the plasmid DNA construct, pJET-\(\triangle rpaB::Sp^R\) by infusion cloning reaction. The final plasmid DNA construct was transformed into WT Synechocystis cells. The positive $\Delta rpaB$ mutant colonies were screened on spectinomycin antibiotic supplemented YBG-11 agar plates.

3.8.4 Generation of the *Synechocystis* strains overexpressing 3X-FLAG tagged CrhR and PNP.

The plasmid vector, pVZ321 was used to clone PNP and CrhR with 3X-FLAG tag with the PpetJ promoter and rrnB terminator to overexpress these proteins in *Synechocystis*. Since

pVZ321 is a low copy number and a large (~9 kb) plasmid, the cloning was done in two major steps:

 Cloning of the promoter PpetJ, 3X-FLAG-PNP / 3X-FLAG-CrhR and the terminator into the blunt cloning vector- pJET1.2:

The DNA fragment covering the promoter of petJ gene (496 bp upstream of petJ) was amplified from the genomic DNA of Synechocystis in a PCR using the primers- PpetJprom-F: 5'GGG AAT TCA GGT TGA CCA CAT CGG-3' and PpetJ prom-R: 5' AAC ATA TGT TCT CCT TTC AAG G 3'. The amplified PCR product was ligated into the linear pJET 1.2 vector. Then, 3XFLAG-PNP was cloned downstream to the PpetJ promoter. Three forward primers 3X-FL-PNP-2015-F1: 5' GAT TAC AAG GAT GAC GAT GAC AAG CAA GAG TTT GAC AAG TCC ATA TCC 3', 3XFL-PNP-2015-F2: 5' GAT TAT AAA GAT CAT GAT ATC GAT TAC AAG GAT GAC GAT GAC AAG C 3' and 3XFL-PNP-2015-F3: 5' GCC ATA TGG ACT ACA AAG ACC ATG ACG GTG ATT ATA AAG ATC ATG ATA TC 3' with a single reverse primer-3XFLAG-PNP-R: 5' CCG TCT AGA CC A GAG CTC ATT AAC CCC GGC TAG CGT TAC GAC GGG - 3' were designed to generate 3X-FLAG-PNP. 3XFL-PNP-2015- forward primers were designed to introduce 3X-FLAG to the upstream of pnp open reading frame in a three sequential PCR reactions. In the first reaction 3XFL-PNP-2015-F1 and 3XFLAG-PNP-R was used to amplify the ORF sll1043 that encodes PNP from the genomic DNA of Synechocystis. The purified PCR amplified product (F1) was used as the template for the second PCR reaction. 3XFL-PNP-2015-F2 forward primer and 3XFLAG-PNP-R reverse primer were used as in the second round of PCR to generate F2 PCR product. The PCR amplified product from the second round of PCR (F2) was used as the template to generate F3 PCR product using the primers 3XFL-

PNP-2015-F3 and 3XFLAG-PNP-R in the third round of PCR reaction. The 3X-FL-PNP-2015-F3 and 3X-FL-PNP-2015-R primers were designed with *NdeI* and *SacI* sites respectively for cloning the final 3X-FLAG-PNP PCR product into petJ-pJET1.2 vector. Next the terminator *rrnBT* was PCR amplified from the plasmid vector *p*BAD and was cloned downstream of 3X-FLAG-PNP into *SacI* and *XbaI* site. The recombinant plasmid, pJET1.2-petJ-3X-FLAG-PNP-rrnBT was successfully generated and confirmed by DNA sequencing analysis.

ii. Cloning of the PpetJ-3XFLAG-PNP/3XFLAG-CrhR-rrnBT DNA fragment from pJET1.2 vector into a cyanobacterial self-replicating plasmid vector pVZ321:

The plasmid DNA construct pJET1.2-petJ-3X-FLAG-PNP-rrnBT was digested with *EcoRI*. Digestion with *EcoRI* released the DNA fragment PpetJ-3X-FLAG-PNP-rrnBT and the resulted DNA fragment of 3kbwas cloned into the *EcoRI* site located within the chloramphenicol cassette in *pVZ321*. Cloning of PpetJ-3X-FLAG-PNP-rrnBT disrupted the cassette and generated pVZ321-PpetJ-3X-FLAG-PNP-rrnBT (Figure 11). Similarly, pVZ321-PpetJ-3X-FLAG-CrhR-rrnBT and pVZ321-PpetJ-3X-FLAG-rrnBT (negative control) were also generated. The plasmid DNA constructs generated were also confirmed by DNA sequencing analysis. The confirmed plasmids; pVZ321-PpetJ-3X-FLAG-PNP-rrnBT and pVZ321-PpetJ-3X-FLAG-rrnBT were mobilized into WT Synechocystis cells and pVZ321-PpetJ-3X-FLAG-CrhR-rrnBT was mobilized into ΔcrhR mutant [25] via tri-parental mating respectively [75]. The strains generated were named as PNP+, CrhR+ and FLAG^{neg}.

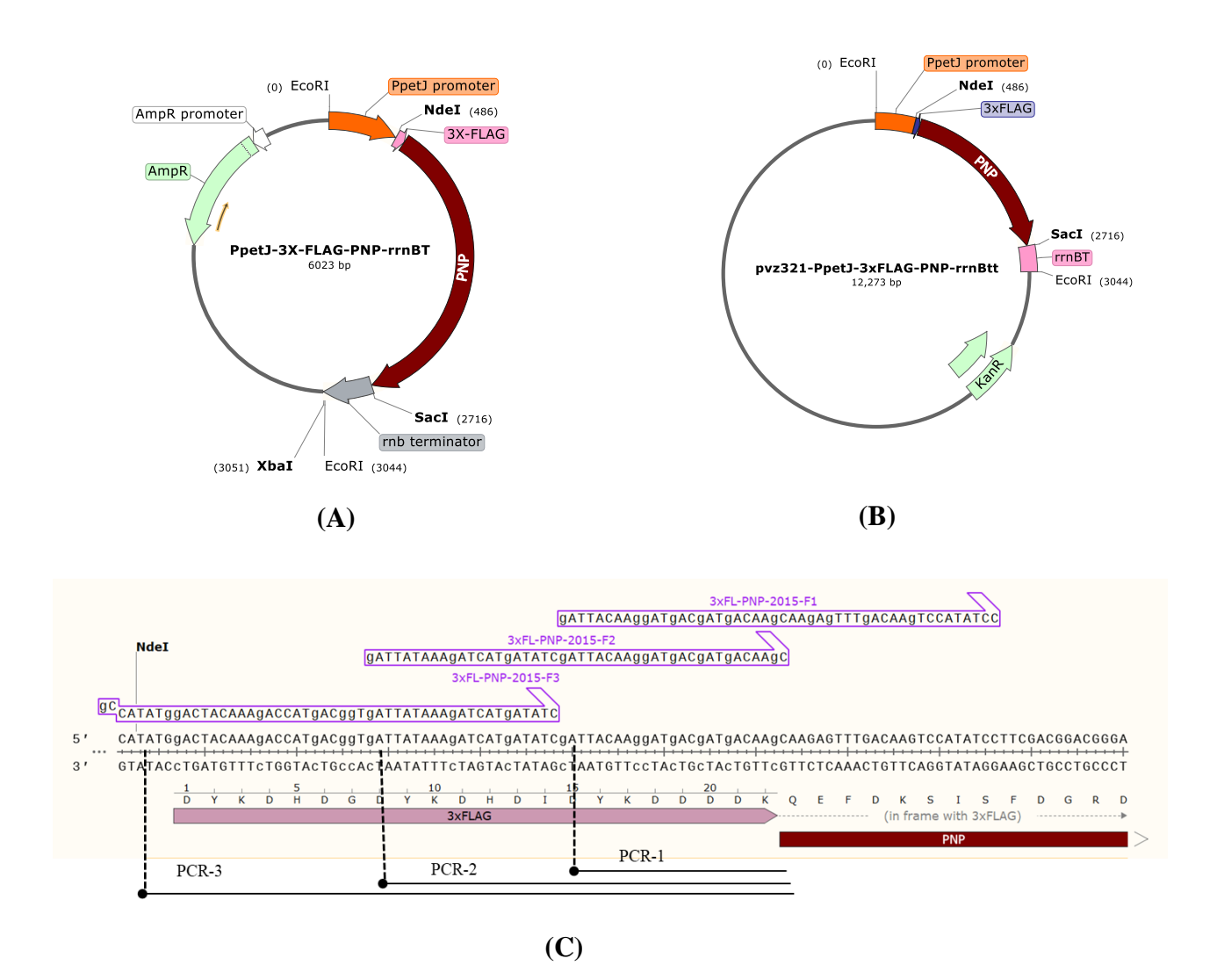


Figure 11. Maps of plasmid DNA constructs generated for ectopic expression of 3X-FLAG-PNP in *Synechocystis*. (A) pJET1.2-petJ-3X-FLAG-PNP-rrnBT and (B) pVZ-petJ-3X FLAG-PNP-rrnBT. The plasmid constructs were generated and confirmed by sequence analysis; (C) Schematic presentation of the three forward primers designed to introduce the nucleotide sequence of 3X-FLAG upstream of the ORF of *pnp* by PCR.

3.9 Overexpression of 3X FLAG-PNP and 3X FLAG-CrhR in Synechocytis cells:

PNP⁺ and CrhR⁺ Synechocystis cells were used to overexpress 3X FLAG-PNP and 3X-FLAG-CrhR proteins. The strains were cultured in YBG-11 medium to an O.D₇₃₀ of 0.8 and then washed thrice with copper depleted YBG-11 medium. It was re-inoculated into YBG-11

medium without copper and allowed to grow for 48 h. The cells were collected and stored in -80°C until use. FLAG Immunoprecipitation kit (Cat No. FLAGIPT1- Sigma Aldrich, USA) was used for purification of 3X-FLAG-PNP. The purification was done as per the instructions given in the user manual provided with the kit. The pelleted cells were resuspended in the lysis buffer. Equal volume of glass beads (Cat No. G9143, Sigma Aldrich, USA) were added to the resuspended cell pellet. Lysing of the cells with the glass beads were done by vortex mixing for 30 sec followed by incubation period of 1 min on ice. The cycle of vortex mixing followed by 1 min ice incubation was repeated for 14 times. The microfuge tubes were left undisturbed in ice to settle down the glass beads. The supernatant was collected in a fresh centrifuge tube without disturbing the glass beads. The cell debris were removed (2000 rpm for 2 min. at 4 °C). The soluble protein fraction was collected and resolved and separated in 10% SDS-PAGE. Using the TE77-PWR semi dry transfer unit (GE health care), the proteins resolved on the SDS-PAGE were transferred and immobilized onto a PVDF [polyvinylidene fluoride (Immobilon-P; Millipore)] membrane. For immune-detection, the proteins on the membrane were treated with primary antibody, Anti-FLAG antibody (Cat No. F7425, Sigma-Aldrich, USA) followed by a secondary antibody, Anti –Rabbit IgG Peroxidase antibody raised (Cat. No. A6154, Sigma-Aldrich). The presence of the induced 3X-FLAG tagged PNP on the membrane was detected using the chemiluminescent detection system (Pierce ECL western blotting substrate, Cat No. 32106, Thermo Fisher Scientific, USA) by following instructions as per the user manual. The chemiluminescent signal from the protein bands were captured using the ChemiDoc XRS+ (BioRad).

3.10 RNA extraction:

The WT, ΔpsrR1 and ΔpsrR1⁺ Synechocystis cultures (both untreated and cold-treated) were collected as mentioned in Section 3.7. The cells harvested were freezed in liquid nitrogen and stored at -80°C till extraction. The cells were allowed to thaw and resuspended in Solution I [50 mM Tris-HCl (pH 8.0), 5 mM EDTA and 0.5 % SDS]. The resuspended cells were lyzed following the hot-phenol method using acid phenol (Cat. No. P4682, Sigma-Aldrich) at 70°C. The contaminating DNA and proteins in the solution were removed by DNaseI and ProteinaseK treatment followed by phase separation by phenol / chloroform / isoamylalcohol (PCI). The RNA extracted from the phase separation was transferred into a fresh microfuge tube followed by its precipitation using 3 M NaOAc (pH 5.2) and 2.5 volume of chilled absolute alcohol. The precipitated RNA pellet rinsed with 70% ethanol was air dried and finally resuspended in 20 μL of DEPC treated milliQ water.

3.11 Preparation of cDNA library and template preparation for whole transcriptome analysis by NGS:

- I. Preparation of barcoded whole transcriptome library: The total RNA extracted from the WT and ∠lpsrR1 (non-treated and cold-treated for different time durations) were used for the preparation of cDNA library.
 - a. The first step was to get rid of the ribosomal RNA from the RNA samples. Ribodepletion was performed using the kit Ribominus Bacteria Module, Invitrogen Life Technologies). For the purpose, 2 μg of the isolated total RNA from the respective samples was added to a reaction mixture containing 50 μL of 2X Hybridization Buffer, 4 μL of RiboMinus Probe Mix and the volume of the reaction mixture was made to 100 μL with addition of nuclease free water. The reaction mixture was incubated at 70°C for 10 mins to denature the RNA.

After the incubation period, the reaction mixture was immediately transferred to 37°C and allowed the reaction mixture to cool down to 37°C during a period of 20 mins. Meanwhile RiboMinus Magnetic Beads (250 µL) were prepared for each sample as per the instruction manual provided with the kit. The beads were washed as per the instruction and finally resuspended in 200 µL of Hybridization Buffer (B10). To these resuspended beads, the incubated 100 μL of the RNA/probe mix was added and mixed well by gentle pipetting. The reaction mixture was next incubated at 37°C for 15 minutes with occasional mixing during the duration of incubation. After the incubation period, the solution was allowed to clear out on a magnetic stand. The collected supernatant that contains the ribosomal (rRNA) depleted RNA was further concentrated using the Magnetic Bead Cleanup Module (Cat No. 4475936, Part No. 44754861, Ion torrent- Thermo Fisher Scientific, USA). In a fresh 2 mL microfuge tube, nucleic acid binding beads (10 µL) and Binding solution concentrate (400 µL) was mixed. The rRNA-depleted RNA was added to the prepared reaction mixture followed by 1 mL of 100% ethanol and was mixed well. The beads were separated and the supernatant was discarded by placing the tubes on magnetic stand. The beads with the rRNA-depleted RNA was washed with 300 µL of Wash Solution. Finally the rRNA-depleted RNA was eluted in 8µL of pre-heated (37°C) nuclease free water. The concentration of the rRNA-depleted RNA was quantified using Qubit RNA assay kit (Cat. No. Q32852, Invitrogen) and the Qubit 4.0 Fluorometer (Cat No. Q33221, Invitrogen).

b. The rRNA-depleted RNAs were then used for the preparation of cDNA library following the instruction manual of the kit Ion Total RNA-Seq Kit v2 (Cat No.

(Cat. No. 4479789, Ion torrent- Thermo Fisher Scientific). The kit has two parts; i) Ion RNA-Seq Core Kit v2 (Part No. 4475482) which contains all the buffers and enzymes, ii) Ion RNA-Seq Primer Set v2 (Part No. 4475481) which contains the adaptor and the primers and iii) Magnetic Bead Cleanup Module (Part No. 4475486). The preparation of the cDNA library was done in 3 steps; i) fragmentation of the rRNA-depleted RNA, ii) hybridization and ligation of adaptor, iii) reverse transcription and iv) amplification of the cDNA with the barcodes. The fragmentation of the rRNA-depleted RNA was performed in a reaction mixture containing RNase III Reaction Buffer and the enzyme RNaseIII. The digestion was carried out at 37°C for 1.5 mins. The fragmented rRNA-depleted RNA samples were purified using the kit-Magnetic Bead Cleanup module and was finally eluted in 10 µL of nuclease free water. The Magnetic Bead Cleanup module was used for the purification of the RNA/cDNA samples at the end of each reactions involved during the preparation of barcoded whole transcriptome library. The fragmented and purified RNA samples were concentrated using centrifuge concentrator (Concentrator plus, Eppendorf, Germany) to reduce the volume from 10 µL to 3.5 µL. Next, the purified rRNA-depleted RNA samples were used to proceed for hybridization followed by ligation. Hybridization master mixture was prepared on ice by adding 2 µL of Ion Adaptor Mix v2 and 3 µL of Hybridization solution. The master mix prepared was added to the 3.5 µL of the fragmented RNA samples and mixed with gentle pipetting the solution in and out for 2-3 times. The hybridization reaction was carried out in a thermal cycler for 65°C for 10 mins followed by 5 mins incubation at 30°C. Next, on ice 10 μL of 2X Ligation buffer and 2 µL of Ligation enzyme mix were added to the

hybridization solution and incubated at 30°C in a thermal cycler with open lid for 1 h. The ligated RNA samples were then used to prepare reaction mixture to perform reverse transcription (RT). Firstly, 16 µL of RT reaction master mix was prepared (in a micro centrifuge tube placed on ice) by mixing 4 µL of 10X RT buffer, 2 µL of 2.5 mM dNTP Mix, 8µL of Ion RT Primer v2 and 2 µL of nuclease free water. The RT master mix was added to the ligated RNA samples and incubated at 70°C for 10 minutes in a thermal cycler followed by snap cooling on ice. Next, 4 µL of 10X SuperScriptTM III Enzyme Mix was added to the RT reaction mixture followed by incubation at 42°C for 30 minutes in a thermal cycler. The RNA were reverse transcribed to their respective cDNA during the reverse transcription reaction. The reverse transcribed cDNA in the reaction mixture was purified and eluted in 12 µL of nuclease free water. Next, amplification of the cDNA was carried out. A barcoded library PCR Mix was prepared by mixing 45 μL of PlatinumTM PCR SuperMix High Fidelity and 1 μL of Ion Xpress RNA3' Barcode Primer and added to 6 μL of the purified cDNA samples. To this mixture, 1 µL of the selected Ion Xpress RNA-Seq Barcode BC primer (Cat. No. 4475485, Ion Torrent, Thermo Scientific) was added and mixed gently by pipetting the solution up and down five times. The reaction was allowed to run in a thermal cycler. The reaction mixture was initially was incubated at 94°C for 2 mins followed by 2 cycles of the following condition; 94°C for 30s, 50°C for 30s and 68°C for 30s. The amplified cDNA with the barcodes were purified from the reaction mixture and thus, the barcoded whole transcriptome library prepared. A total of 100 pM of each of the prepared barcoded library prepared from the RNA isolated from the samples were pooled into a single centrifuge tube. These pooled barcoded library mix were used for the preparation of template for sequencing.

- II. Template preparation and sequencing: The pooled barcoded library mix prepared in the above steps was then employed to make template-positive ion sphere particles using the components provided in the Ion 540 Kit-OT2 (Cat. No. A27753, Ion Torrent, Thermo Fisher Scientific).
 - Firstly, the Ion OneTouch 2 instrument was set up by following the guidelines in the user manual using the materials from the Ion S5 OT2 Supplies (Part No. A27748) and Ion S5 OT2 Solutions (Part No. A27747). As per the user guide, two Recovery tubes containing 150 µL Ion OneTouch™ Breaking solution and the Ion OneTouch Recovery Router was placed in the slots of the centrifuge in the instrument. Then the Ion OneTouch 2 Amplification plate with the disposable injector was installed. After setting up the instrument, amplification solution was prepared. The 12 µL of the pooled barcoded library was diluted with nuclease free water to a volume of 100 µL. The tube which contained 2 mL of Ion S5 Reagent Mix provided in the kit was allowed to reach the room temperature. To the tube, the following components- nuclease free water (80 μL), Ion S5 Enzyme Mix (120 μL), Ion Sphere Particles (100 μL) followed by the diluted 100 µL of barcoded cDNA library were added. The mixture was then mixed and carefully pipetted into the Ion Onetouch Reaction Filter assembly's sample port (Ion S5 OT2 supplies-Part No. A27748). Next, 200 uL of Ion Onetouch Reaction oil (Ion S5 OT2 solutions- Part No. A27747) was pipetted into the same sample port. The filter assembly was then placed onto the designated holes on the top stage of the Ion One Touch instrument and the reaction was initiated by following the screen prompts displayed on the

instrument display. At the end of the run, the sample was pelleted down by a final spin. After the run was over, the supernatant from the two Recovery tubes was removed without disturbing the pellet by leaving behind ~100 μL of the Recovery Solution. The template-positive ISPs was resuspended in the remaining Recovery Solution in each and pooled together in a 1.5 mL microcentrifuge tube. The residual beads in the Recovery Tubes were recovered by addition of volume 100 μL of nuclease-free water and transferred to the tube containing the resuspended template-positive ISPs and the volume was made to 1 mL. The template-positive ISP suspension were pelleted down by centrifugation for 8 minutes at 15,500 \times g. The supernatant was removed very carefully leaving behind 20 μL of supernatant. To it, 80 μL of Resuspension Solution was added to resuspend the template positive ISPs.

b. Enriching of the template positive ISPs recovered was done using the reagents and materials from the kit; Ion S5 OT2 Supplies (Part No. A27748) and Ion S5 OT2 Solutions (Part no. A27747) and the Ion Onetouch ES instrument. Besides the reagents in the kit, Dynabeads MyOne Streptavidin C1 beads (Cat No. 65001, Thermo Fisher Scientific, USA) were used for the enrichment of the template positive ISPs as per the user guide. For the enrichment of the template positive ISPs, firstly, combining 280 μL of Tween solution with 40 μL of 1 M NaOH, a Melt-Off solution was prepared. Secondly, 100 μL of Dynabeads MyOne Streptavidin C1 Beads were prepared by washes with 1 mL of Ion OneTouch Wash Solution and were finally resuspended in 130 μL of MyOne Beads Capture Solution. Next an 8-well strip was filled up with the prepared solutions and beads. The template positive ISPs was filled into Well-1, the prepared Dynabeads MyOne Streptavidin C1 Beads into Well-2 and the Melt-

Off solution in Well-7. The Well -3, 4 and 5 was filled with 300 μ L of Ion OneTouch ES Wash Solution. Well-6 and 8 was left empty. The filled 8-well strip was placed on the slot of the tray of Ion OneTouch ES instrument. Next, a fresh tip was loaded in the Tip Arm and an open 0.2 mL PCR tube was placed into the hole in the base of the Tip Loader of the instrument and the run was performed. At the end of the run, the solution containing the enriched ISPs was collected in the 0.2 mL PCR tube. The enriched ISPs was pelleted down and washed twice with nuclease free water by centrifugation (15,500 × g for 5 mins). The supernatant was removed leaving ~10 μ L to resuspend the enriched ISPs.

The enriched ISPs were used to proceed for sequencing using the sequencer-Ion S5 System. The reagents, the solutions and the enzymes required for the initialization and to perform the run was provided in the kit- Ion 540 Loading Reagents OT2 (Part No. A27897), Ion S5 Sequencing Solutions (Part No. A27767) and Ion S5TM Sequencing Reagents (Part No. A27768). The Ion S5 Sequencing Reagents cartridge, Ion S5 Cleaning Solution bottle and the waste reservoir were properly installed into the instrument. Also a used chip was properly loaded into the chip clamp system and the instrument was initialized by following the on-screen recommendations. The initialization was over in 40 mins. Meanwhile, was prepared to be loaded into the Ion 540 Chip (Cat No. A27765, Ion Torrent, Thermo Fisher Scientific, USA) placed on a flat surface. To the enriched template positive ISPs, Ion S5 Annealing Buffer (15 µL) and Ion S5 Sequencing Primer (20 µL) were added, mixed and incubated in a thermal cycler programmed at 95°C for 2 mins and 37°C for 2 mins. After the run, Ion S5 Loading Buffer (10 µL) was added and vortexed and the contents were collected at the bottom of the tube by brief centrifugation. The entire prepared sample was pipetted into the chip loading well of the chip and centrifuged for 5 mins in the Ion Chip Minifuge. In a fresh microfuge tube, 50% Annealing Buffer (49 μ L) was combined with Foaming Solution (1 μ L) to create foam by pipetting the mixture up and down. Then, 100 µL of the prepared foam was injected into the chip loading port. The excess liquid expelled from the opposite port was removed. Next, 55 µL of 50% Annealing buffer was injected into the chip loading well followed by centrifugation in the Ion Chip Minifuge for 30 s. The above steps involving injection 100 µL of foam, removal of excess liquid, injection of 55 µL of 50% Annealing buffer followed by centrifugation was repeated again. After the centrifugation, the liquid collected on the well of the chip was removed. Next, 100 µL of the Flushing solution was pipetted into the chip loading port two times followed by injecting 100 μL of 50% Annealing Buffer into the chip loading port three times. In a fresh micro centrifuge tube, 6 µL of Ion S5TM Sequencing Polymerase was combined with 60 µL of 50% Annealing buffer and the mixture was injected into the chip loading port. The excess liquid was removed and the chip was incubated at room temperature for 5 mins. The chip was finally loaded into the Ion S5 sequencer and the sequencing run was performed.

3.12 Quantitative real-time PCR assays

Firstly, the total RNA extracted from the WT, Δ*psrR1* and *psrR1*⁺ cells were reverse transcribed using the kit- PrimeScript 1st strand cDNA synthesis Kit (Cat No: 6110A, Takara) to synthesize cDNA of the selective target genes. Next, the cDNA synthesized was used to perform the qRT-PCR assay using the KAPA SYBR Fast Biorad (Cat No. KK4608). The total volume of the reaction mixture was 20 μL containing 2X KAPA SYBR Fast qPCR master mix

(10 μ L) and gene specific primer pairs (0.2 μ M each) and diluted cDNA (21 ng / μ L). The reaction was run in triplicates using the thermal cycler (CFX96 Real-Time System, BioRad). The instrument was programmed as per the guidelines of the KAPA SYBR Fast BioRad and the thermal cycler: 95°C for 3 mins, 95°C for 3 sec, 60°C for 20 sec and 72°C for 60 sec. The reaction was allowed to run for 39 cycles and the amplification of the targets were examined by looking into the melting curve. The *gap1* gene was used as an internal reference to normalize the expression level of the targets. The primers used for qRT-PCR to amplify the target genes are listed in **Table 6.**

3.13 Growth analysis and pigment estimation:

The growth of the WT, $\Delta psrR1$, $psrR1^+$ and $\Delta rpaB$ were monitored. All the strains were inoculated to 0.1 O.D at 730 nm and was cultured for 20 h at 34°C. For the cold treatment, the cultures were shifted to 20°C without altering the other conditions of the growth parameters. Absorbance of the cultures at 730nm (O.D₇₃₀) was measured for each culture using spectrophotometer (Nanodrop2000C, Thermo Fisher Scientific, USA) at regular intervals.

3.14 Pigment estimation

The content of the photosynthetic pigments, phycocyanin, allophycocyanin and chlorophyll in the WT and $\Delta psrR1$ were estimated with the protocol mentioned in De Marsac *et al.*, 1988 [78]. Four millilitres of the culture was pelleted down and was lyzed in 4 ml of 20 mM sodium acetate buffer (pH 5.5) by sonication (30 sec pulse followed by 1 min incubation on ice) for 12 cycles. The crude extract was incubated in presence of 1% (w/v) streptomycin sulfate for 30 min at 4 °C. The chlorophyll containing membrane fragments was removed by centrifugation at 10,000g for 10 min at 4°C. Absorbance at 620 nm and 650 nm was measured using

spectrophotometer. The amount of the phycocyanin and allopycocyanin in the supernatant was calculated from the following equation;

PC (mg m1⁻¹) =
$$(O.D_{620 \text{ nm}} - 0.7 \text{ x } O.D_{650 \text{ nm}})/7.38$$

AP (mg ml⁻¹) =
$$(O.D_{650 \text{ nm}} - 0.19 \text{ x } O.D_{620 \text{ nm}})/5.65$$

The chlorophyll content was extracted from 500 µL cultures twice with 90% (v/v) methanol for 1 hr at 4°C in dark/dim light. The cell debris were removed by centrifugation at 10,000 g for l0min at 4°C. the chlorophyll a (*chl a*) content in the supernatant was estimated using the absorbance of the methanolic extract at 665 nm in the following equation:

$$C (\mu g/m1) = O.D_{665 \text{ nm}} \times 13.9$$

The total protein content in 500 µL of *Synechocystis* cultures was precipitated with 10% (w/v) trichloroacetic acid. The cell debris were removed by centrifugation at 10,000 g for l0min at 4° C. The pellet was resuspended in 1 N NaOH, boiled for 30 min, cooled and then recentrifuged. The protein content in the supernatant was estimated by Bradford assay (VWR, Amresco Life Sciences), using bovine serum albumin as standard.

3.15 77 K Fluorescence Spectroscopy

77 K fluorescence emission spectrum of WT and $\Delta psrR1$ (untreated and cold treated) were measured using the FP-8500 spectrofluorometer from Jasco. The cells were allowed to grow to an O.D₇₃₀ of 0.5 and 500 μ L cells from the culture was used for the measurement of 77K fluorescence emission spectra. For the cold treated samples, cells at the following time points 0.5, 6 and 16 h after shift to 20°C were used for the measurement. The cell samples were excited at 443 nm and the emission spectrum was measured in the range of 650 – 750 nm. Fluorescence emission spectra were recorded with excitation and emission band widths of 10 nm and 5 nm

respectively. The fluorescent spectra obtained were normalized to the peak at the wavelength of 695 nm which corresponds to the emission spectra of chlorophyll content present in PSII.

3.16 Microarray analysis of *∆rpaB* mutant *Synechocystis* strain:

Genome-wide analysis of transcript levels in the $\Delta rpaB$ relative to WT was analysed using a custom made DNA microarray chip (Synechocystis microarray chip with 8 x 15 K format, Agilent, La Jolla, CA) that covered 3611 genes including the genes of all native plasmids of Synechocystis. The protocol to carry out the microarray assay was followed from Srikumar et al., 2017 [77]. The custom made chips were prepared using noncontact inkjet technology from Agilent. Probes of 60-mer oligomers selected from the 3' end of the genes were printed in the preparation of the arrays. cDNA synthesized from the RNA extracted from the samples with the fair playIII microarray labelling kit (Cat.No.252009, Agilent, La Jolla, CA) was labelled with Cy3 and Cy5 dyes (Cat.No. PA23001 and PA25001, GE Healthcare). Dye coupled cDNA after purification using microspin columns was hybridized to the custom made DNA microarray chip (Gene expression hybridization kit, Cat No. 5188-5281). The hybridization was carried out in a hybridization chamber which was set at 65°C for 16 h. Following hybridization, the chip was rinsed and then washed with 2 X SSC (1X SSC is 150 mM NaCl and 15 mM Sodium citrate) at 60°C for 10 min and 0.2 X SSC, 0.1 % SDS at 60°C for 10 min, followed by rinsing with DDW at room temperature for 2 min. Prior scanning, moisture was removed from the chip with an air spray and was scanned using Agilent microarray chip scanner (G2505B, Microarray scanner, Agilent Technologies). Scanning was performed using green and red PMT at 100% (XDR Hi 100%) and at 70%. Feature extraction was done using Agilent feature extraction (FE) software version 9.5.1 as per protocol available in the web site (www.agilent.com/chem/feprotocols). The signal from each gene on the microarray was normalized by reference to the total intensity of signals from all genes. The change in the level of the transcript of each gene relative to the total amount of mRNA was calculated.

3.17 RNA co-immunoprecipitation:

The PNP+ and CrhR+ cells were collected as mentioned in Section 3.2.5. We have used the Magna RIP RNA Binding Protein Immunoprecipitation kit (Cat No. 17-700, Millipore, USA) to perform the RNA immunoprecipitation (RIP) analysis. The cell pellet collected were resuspended in 12 mL of PBS buffer (prepared in nuclease free water) and crosslinked using UV Stratalinker (900mJ for 3 times). The crosslinked cells were pelleted and resuspended in RIP lysis buffer (800 µL) which contained protease inhibitor cock tail and RNase inhibitor. An equal volume of glass beads (Cat No. G9143, Sigma Aldrich, USA) were pre-treated with DEPC water was added to the tube containing the resuspended cells. Lysing of the cells were done by vortex mixing repeatedly at full speed for 30 sec followed with 1 min incubation on ice for 12 times. After removal of the cell debris, the cell free extract was filtered with 0.45 micron syringe filter and centrifuged at 14500 rpm for 30 mins. The filtrate collected served as the RIP lysate. The magnetic beads for performing the immunoprecipitation were prepared by following the user manual provided with the kit. The magnetic beads (50 µL) were washed twice followed by resuspension in 100µL of the RIP wash buffer. The washing step was carried out by placing the tubes on a Magna GrIP Rack (Cat. No. 20-400, Millipore, Sigma Aldrich, USA). To the resuspended beads, 5 µg of Anti-FLAG antibody (Cat No. F7425, Sigma Aldrich, USA) were added and incubated for 30 mins in a rotator at room temperature. After the incubation period, the magnetic beads were again washed twice and resuspended in RIP wash buffer. RIP immunoprecipitation buffer comprising of 0.5 M EDTA (35 μL), RNase inhibitor (5 μL) and RIP Wash Buffer (860 μL) was added to the resuspended magnetic beads. To it, 100 µL of the RIP lysate was added and incubated overnight at 4 °C for by mixing the contents in a rotator. The beads were separated from the supernatant and washed 5 times with RIP wash buffer. The washed beads were then treated with Proteinase K buffer [prepared by mixing RIP Wash Buffer (117 μ L), 10% SDS (15 μ L) and 10 mg/mL proteinase K (18 μ L)] by incubation at 55 °C for 30 mins to digest the protein. The magnetic beads were separated and the supernatant was in a microfuge tube and the volume was made to 400 μ L with RIP wash buffer. The RNA in the supernatant was extracted by phase separation with phenol: chloroform: isoamyl alcohol followed by chloroform extraction. To the aqueous solution, Salt Solution I (50 μ L), Salt Solution II (15 μ L), Precipitate Enhancer (5 μ L) (provided in the kit) and 2.5 volume of absolute ethanol were added and incubated overnight at -80°C. The RNA was pelleted down by centrifugation at a high speed of 14,000 rpm for 30 mins at 4°C was washed with 80% ethanol. The RNA pellet was air dried and finally resuspended in 20 μ L of nuclease-free water. The RNA suspension was the RNA that co-eluted with the 3XFLAG tagged proteins and was further identified by facilitating the sequence analysis with Ion torrent next generation sequencing platform.

3.18 Bacterial two hybrid assay

The open reading frames *sll1043* and *sll1290* encoding for PNP and RNaseII were amplified by PCR from the *Synechocystis* genomic DNA using primer sets specific for the genes, PNPase-T25-F: 5' GGG CTG CAG GGA TGC AAG AGT TTG ACA AGT CC-3' and PNPase-T25-R: 5' GGA CCC GGG CTT AAC CCC GGC TAG CGT TAC 3' and, RNaseII-t25-F: 5' GGG CTG CAG GGA TGG AAA AAG GAC AAC TAA TTG AAT TCC 3' and RNaseII-t25-R: 5' GGA CCC GGG CTT AGG CTT CAT TGG CCA ACA ATT CC 3' respectively. The amplified PCR amplified DNA fragment were cloned into the plasmid vector, pT25 at the *PstI* and *XmaI* restriction enzyme sites. The ORFs (*pnp* and *crhR*) were also amplified from the genome of *Synechocytis* using different primer sets PNPase-T18-F: 5'

CCC TCG AGG ATG CAA GAG TTT GAC AAG TCC 3', PNPase-T18-R: 5' CGG AAG CTT AT A CCC CGG CTA GCG TTA CG 3' and CrhR-T18-F: 5' CCC TCG AGG ATG ACT AAT ACT TTG ACT AG 3', CrhR-T-18-R: 5' CGG AAG CTT ATC TGT TGG CGA TCA CTA TAG G 3' respectively and cloned into pT18 plasmid in the *XhoI* and *HindIII* restriction enzyme sites. The plasmid in combination were transformed to *E. coli*, DHP1 competent cells. The combination of pT25 and pT18 vectors without any insert was transformed and served as negative control. pT25-*sll1130* & pssl2245-T18 were co-transformed to *E. coli* DHP1, served as positive control. The combination of plasmid constructs to investigate the protein-protein interactions among RNaseII, PNP and CrhR were pT25-*RNaseII* & p*PNP*-T18, pT25-*RNaseII* & p*CrhR*-T18, pT25-*PNP* & p*CrhR*-T18. The cells were plated onto MacConkey agar plates [76]. The plates were examined for any change in the colour of the MacConkey agar as a result of protein interactions.

3.19 Over expression of PNP, RNaseII and CrhR in the *E.coli* bacterial expression system:

Three plasmid DNA constructs *pCold-PNP*, *pCold-CrhR* and *pET28-RNaseII* were generated. The ORFs *sll1043*, *slr0083* and *sll1290* encoding PNP, CrhR and RNaseII respectively, were PCR amplified using the genome of *Synechocystis* and the following gene specific primer setspet-RNaseII-INF-FP: 5' CCG CGC GGC AGC CAT ATG GAA AAA GGA CAA CTA ATT GAA TTC C-3', pet-RNaseII-INF-RP: 5'ACG GAG CTC GAA TTC TTA GGC TTC ATT GGC CAA CAA TTC CC-3'; pet28-synPNP FP: 5'-CCG CGC GGC AGC CAT ATG CAA GAG TTT GAC AAG TCC-3', pet28-synPNP-RP: 5'-ACG GAG CTC GAA TTC TTA ACC CCG GCT AGC GTT ACG-3' and crhR-pet28a-FP: 5' CGG CAT ATG ACT AAT ACT TTG ACT AGT ACC TTC GCT GAC C-3', crhR-pet28a-RP: 5'- GGC AAG CTT TTA CTG TTG GGA TCA CTA TAG GCA GG -3'. The PCR amplified fragment corresponding to *sll1043* (2157 bp) and *sll1290* (2001bp) were digested with *NdeI* and *SacI*. The *slr0083* (1482 bp)

PCR amplified product was digested with *NdeI* and *HindIII*. The digested product of *sll1043* and *slr0083* were ligated to pCold-1 vector separately (Cat No. 3361, Takara) and *sll1290* was ligated to pET28a(+) vector (Cat No. 69864-3, Novagen). These plasmid constructs generated were transformed into *E. coli* Rosetta (DE3) pLysS host strain and used to overexpress and purify the His-tagged proteins using the Nickel affinity gel (His60 Ni Superflow resin, Cat No. 635660, Clontech laboratories Inc., Takara, Japan).

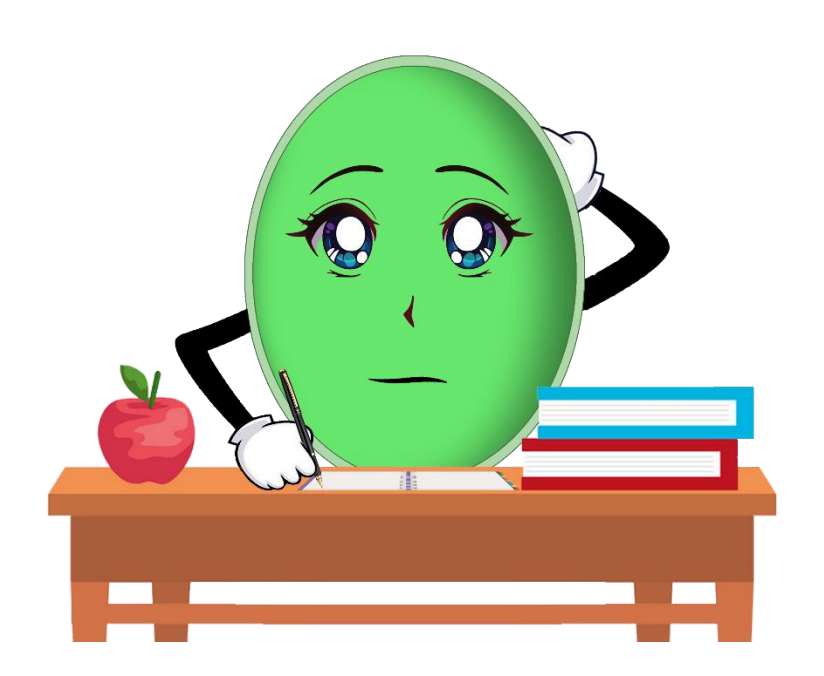
The overexpression of the protein, 6X Histidine tagged RNaseII (6XHis-RNaseII) was induced by the addition of 1 mM final concentration of IPTG. The induction was carried out for 3 hours after which the cells were collected by centrifugation at 10,000 rpm for 10 min at 4 °C. For expression of 6X Histidine tagged PNP (6X His-PNP) and 6X Histidine tagged CrhR (6X His-CrhR), the cells were induced by addition of 1 mM final concentration of IPTG followed by incubation at 15°C for 24 h. The cells were collected by centrifugation at 10,000 rpm for 10 min at 4°C. The cell pellets were resuspended in lysis buffer (20 mM Tris-HCl, pH 7.5 / 500 mM NaCl / 1 mM PMSF), lysed the cells by sonication at an amplitude of 40 %, each cycle consisted of a pulse run for 45 seconds with 1 min incubation on ice. The process was repeated for 20 more cycles. In case of 6X His- CrhR, the pH of the lysis buffer was 6.4. The unbroken cells from the cell lysate were removed by centrifugation at 10,000 rpm for 10 min at 4°C to remove the unlysed cells. The supernatant was filtered through a 0.45 µm filter and then loaded into the Nickel affinity column. The column was flushed twice with 20 mM Tris-HCl / 500 mM NaCl / 40 mM imidazole and sequentially the 6X His-tagged proteins were eluted with 20 mM Tris-HCl / 500 mM NaCl / 100 mM, 200 mM and 300 mM imidazole respectively. These elutes containing same protein were pooled together and were dialyzed against 20 mM Tris-HCl / 150 mM NaCl. The proteins were then concentrated using Amicon ultra centrifugal filters (Cat. No. UFC800324, Merck Millipore, Germany) with a 3 kDa cutoff. The purity of the proteins was checked by SDS-gel electrophoresis and were used for surface plasmon resonance (SPR).

3.20 Surface Plasmon Resonance (SPR) analysis:

The equilibrium constant of interaction (K_D value) between the interacting protein-pairs was calculated using SPR (Surface plasmon resonance system Biacore T200) and the analysis was done using the BiacoreT200 Evaluation software version 2.0. The mode of kinetic calculation was 1: 1. We had immobilized 6X His-PNP on the Series S sensor chip CM5 (Cat No. BR100530, GE Healthcare Bio-Sciences Limited) which served as the ligand. On the other hand, 6X His-RNaseII and 6X His-CrhR were used as the analyte. Firstly, the purified 6X His-PNP was diluted in the buffer, HBS-EP (HEPES Buffer saline-NaCl with 3 mM EDTA, Cat. No. BR-1001-88, Biacore) to obtain the concentration of 150 µg / mL and used for the immobilization. The immobilization was done in the Flow cell-2 of the Series S sensor chip CM5. Next, serial dilution of 6X His-RNaseII in HBS-EP buffer was done obtaining the following concentrations of 2.5, 1.25, 0.625, 0.3125, 0.156, 0.078, 0.039 µM in two sets (for replicates). The prepared samples (300 µL) of each concentration were pipetted into the vials with caps (used for Biacore systems) and were placed in the sample and reagent and loaded into the rack tray port of the Biacore T200 system. Next, the experimental conditions were set up in the BiacoreT200 Evaluation software as per the Biacore T200 Software Handbook. The contact time of the analyte with the ligand was set for 120 s with a flow rate of 30 µL / min, and a dissociation time of 300 s. The analysis of the interaction between the proteins was performed at two different temperatures- 25°C and 34°C. Similarly, under the same experimental conditions, the analysis of the interaction study between PNP and CrhR was also performed. Serial dilution of 6X His-CrhR was done with HBS-EP buffer to obtain the following concentrations- 2.5, 1.25, 0.625, 0.3125, 0.156, 0.078, 0.039 µM. The analysis of the

interaction	between	PNP	and	CrhR	was	performed	l at	25°C	and	34°C	using	BiacoreT200
Evaluation	software	versio	on 2.0).								

4.RESULTS



4.1 Expression level of PsrR1 during cold stress.

The sRNA, PsrR1 is upregulated during HL acclimation and leads to downregulation of PSI genes post-transcriptionally [14, 23, 35]. Literature review indicated that the effect of low temperature stress on the genes related to photosynthesis is similar to that of HL stress. Low temperature leads to downregulation of the photosynthetic genes [25]. Therefore, it is possible that PsrR1 has a role to play during post-transcriptional regulation of photosynthetic genes during cold acclimation. Hence, in order to establish the regulatory mechanism of photosystem related genes by PsrR1 during cold acclimation, we examined changes in expression levels of PsrR1 during low temperature. Transcript levels of PsrR1 was analysed by qRT-PCR of the WT cells growing at optimal growth temperature (34°C) and then shifted to low temperature (20°C). We observed a transient upregulation of PsrR1 transcript levels in the WT cells when shifted from 34°C to 20°C (Figure 12).

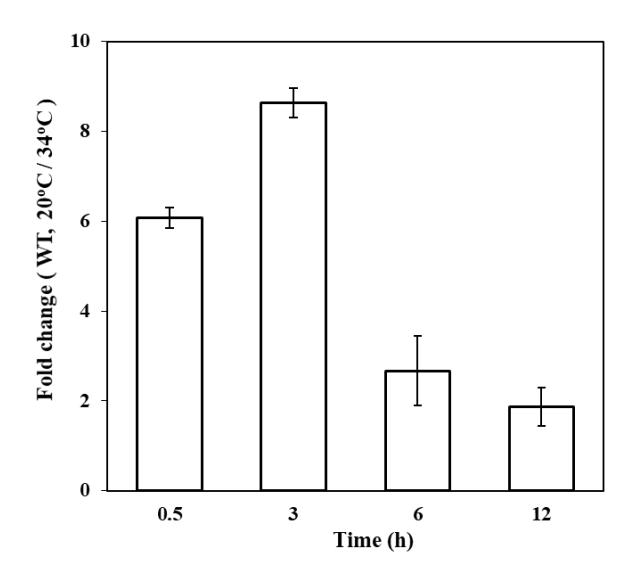


Figure 12. Changes in the transcript level of PsrR1 in WT *Synechocystis* cells during low temperature stress. Cells actively growing at 34° C (0.4-0.5 O.D₇₃₀) were incubated at 20° C and cells were harvested at various points during cell incubation. The abundance of PsrR1 transcripts was quantified by qRT-PCR analysis using *gap1* as an internal control. The amount of PsrR1 in cold-treated WT is expressed as a fold change with respect to the level in WT cells grown at 34° C.

The expression level of PsrR1 increased to more than 6-fold when the cells were incubated at 20°C for a duration of 30 minutes (0.5 h), which further increased approximately to 9 fold at 3 h time point. Prolonged incubation of WT cells after 3 h at low temperature led to a gradual decline in the expression level of PsrR1. This data indicates that PsrR1 is also a cold-responsive non-coding RNA that gets transiently upregulated during cold acclimation.

4.2 Targeted inactivation and overexpression of PsrR1

Further, we have generated $\triangle psrR1$ and $psrR1^+$, an over-expression strain (Figure 13). In the $\triangle psrR1$, the nucleotide sequence of psrR1 was replaced with the chloramphenicol antibiotic-resistant cassette (Figure 13A & B). The chloramphenicol resistant gene cassette replaced majority of the nucleotide sequence of psrR1 in reverse orientation (Figure 13A); the strain thus generated does not express psrR1. As Synechocystis possess multiple copies of identical genomes, we checked the percentage of replacement of WT copy of psrR1 with the disrupted copy of the psrR1. The mutated copy of psrR1 was PCR amplified using a specific set of primers as detailed in the section of materials and methods. From the Figure 13B it was observed that all the copies of psrR1 were replaced with the disrupted copies, suggesting that the $\triangle psrR1$ strain is a completely segregated mutant (Figure 13B). The overexpression strain was generated by cloning the psrR1 gene with a copper repressible promoter PpetJ into the neutral site of the genome i.e., the DNA region covering ORFs slr2030-slr2031 (Figure 13C & D). The intergenic region between slr2030 and slr2031 is frequently used as neutral loci [79]. PCR analysis indicated successful integration of the extra copy of psrR1 along with the promoter, PpetJ, in the neutral site of the genome of psrR1 (Figure 13D).

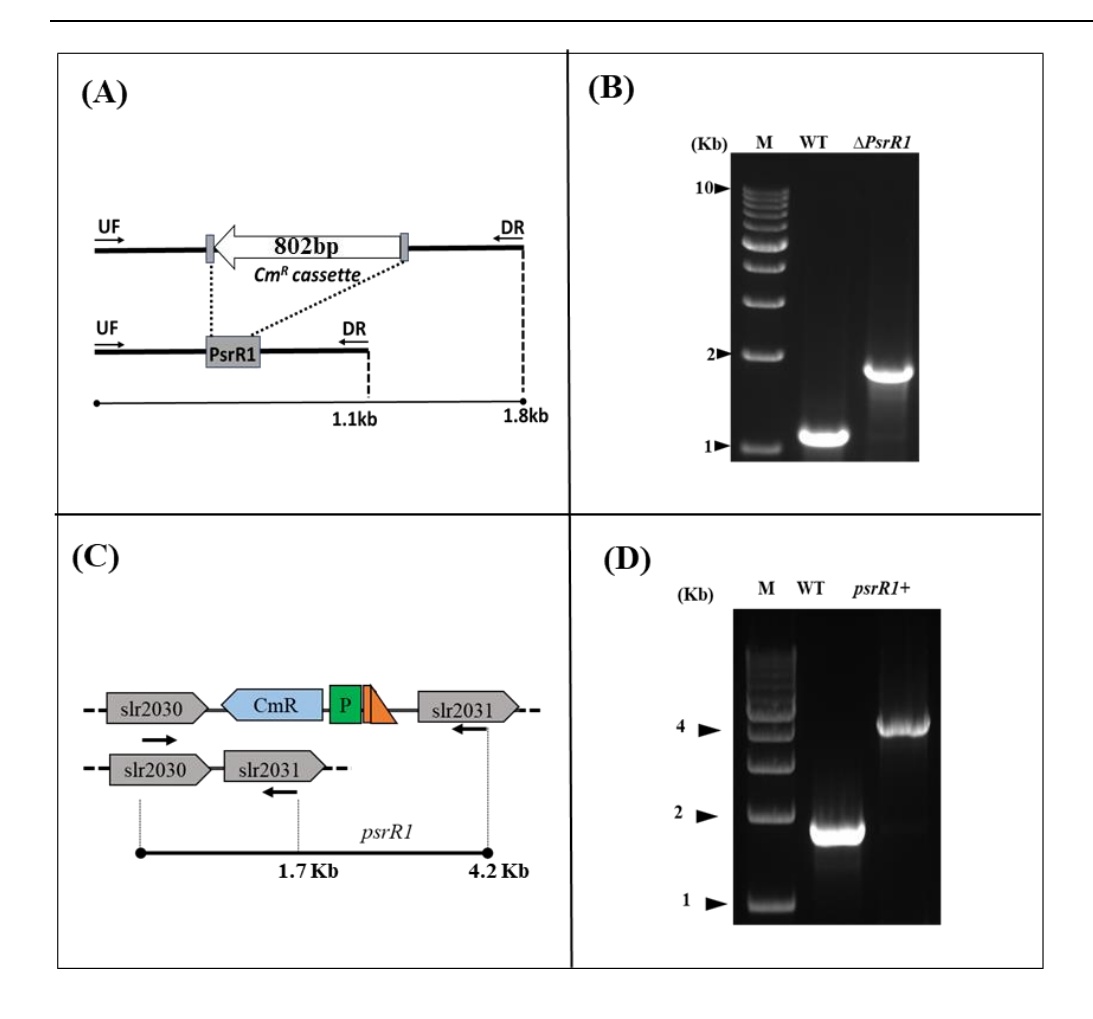


Figure 13: Generation of the mutant strain $\Delta psrR1$ and the overexpression strain $psrR1^+$. psrR1 in the WT cells was replaced with disrupted copy of PsrR1 to generate $\triangle psrR1$ mutant strain. The mutant construct of psrR1 was generated by replacing 79 bp region corresponding to 131 bp full length non-coding RNA, with chloramphenicol antibiotic resistant cassette (803bp). (A) Schematic representation of the ΔpsrR1 genotype. The primer set psrR1–FP and psrR1-RP amplified 131 bp psrR1 along with 472 nucleotides upstream and 492 downstream flanking DNA regions. The chloramphenicol cassette (803bp) replaced the 79 bp region within the psrR1 non-coding gene in $\triangle psrR1$ mutant. (B) PCR analysis with the genomic DNA as a template with the primer set mentioned in (A). M, DNA ladder 1-kb (Cat No. 3412A, Takara); WT, PCR product using genomic DNA of WT as the template and $\Delta psrR1$, PCR product with $\Delta psrR1$ DNA as the template. (C) Schematic diagram of the $psrR1^+$ overexpression strain genotype. psrR1 was cloned with the promoter PpetJ into the neutral site slr2030 and slr2031 in the genome of psrR1⁺ cell. (D) PCR analysis with the genomic DNA as template with the primers mentioned in (A). M, DNA ladder 1-kb (Cat No. 3412A, Takara); WT, PCR product with genomic DNA of WT as the template and psrR1+, PCR product with psrR1+ genomic DNA.

4.3 Effect of inactivation of PsrR1 on the gene expression profile during cold acclimation

The regulatory RNAs including sRNA are involved in various stress responsive gene regulatory mechanisms. Understanding the role of PsrR1 will give information on the gene regulatory mechanism during cold acclimation. Importantly, PsrR1 was already reported to regulate post transcriptionally photosystem genes during highlight-acclimation [14]. Since, the same genes coding for photosystem I and phycobilisome protein components were known to be down regulated during cold acclimation, it is likely that the PsrR1 is involved in cold The WT and $\Delta psrR1$ were incubated at low temperature (20°C). Whole acclimation. transcriptome analysis with the RNA isolated from the cold-treated cells at different time points was done by Next Generation Sequencing (NGS) analysis. The RNA isolated from the cells growing at the optimum growth temperature (34°C) were used as the control. From the NGS data, the change in the transcript levels of photosynthetic genes were observed (Figure 14). The fold change in the expression level of the few genes representing both PSI and phycobilisomes were calculated by using the RPKM values of cold-treated versus the non-treated samples. The observations indicated that the genes that code for PSI and phycobilisome protein components were down-regulated in the WT during low temperature stress. However, in the cold treated-\(\triangle psrR1 \) mutant, the genes were relatively high compared to the cold treated WT cells (Figure 14).

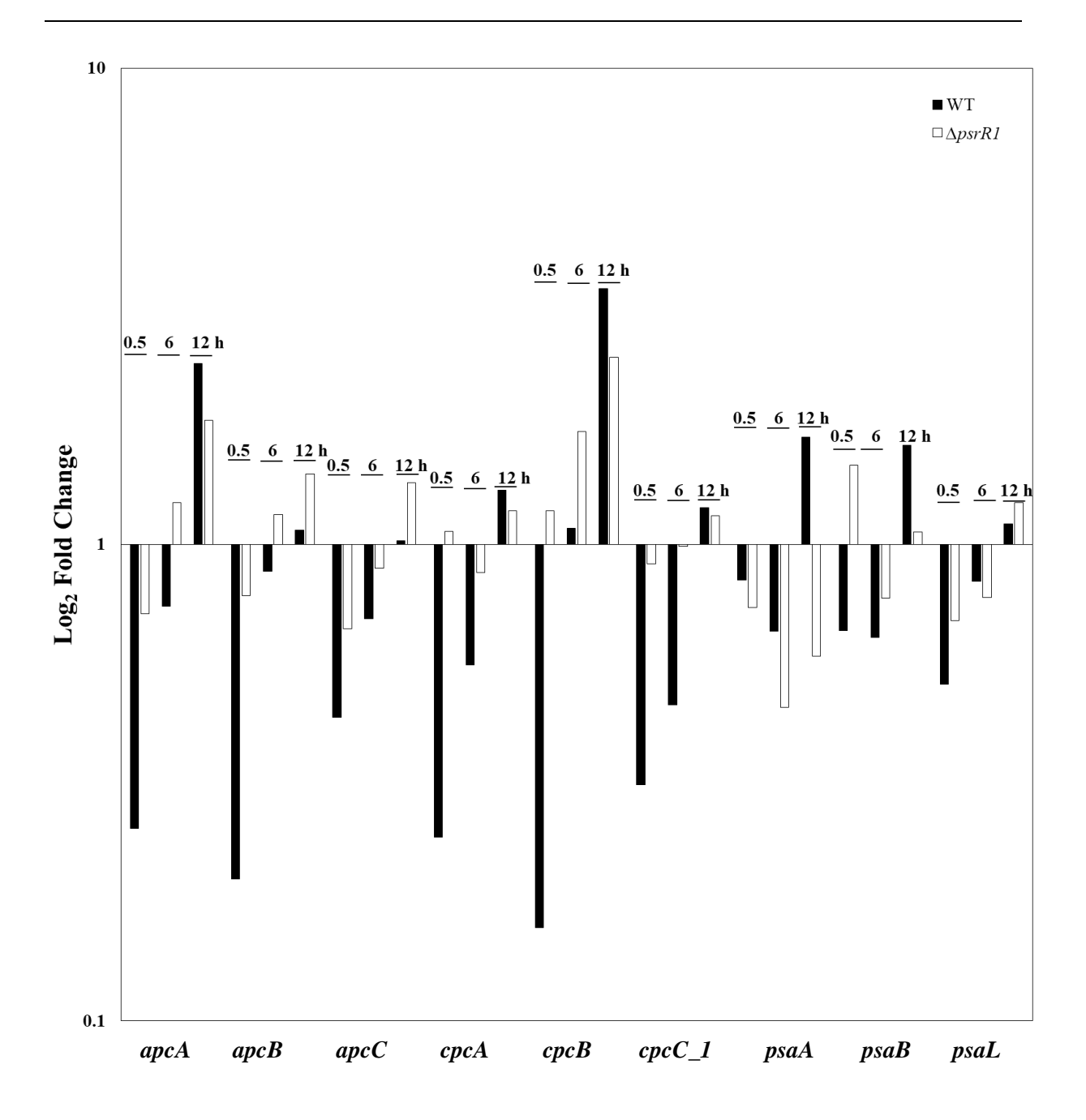


Figure 14. Comparative analysis of the expression level of photosystem I and phycobilisome genes by Next Generation Sequencing analysis. The genes encoding the different components of PSI and PBS were analyzed by qRT-PCR analyses during cold treatment of the WT, $\Delta psrRI$, and $psrRI^+$ strains. The \log_{10} expression values were plotted, the closed bars represent the fold change in the WT cell, open bars represent the fold change in the $\Delta psrRI$ mutant cell and the stripped bars represent the fold change in $psrRI^+$ cells. In $\Delta psrRI$ when compared to the WT cells, the fold of downregulation of the genes were reduced and was maintained to be higher throughout the treatment. Whereas in $psrRI^+$, the expression of those genes was further downregulated compared to the WT cells.

4.4 Real-time PCR analysis of PSI and phycobilisome genes during low temperature stress.

The NGS analysis indicated the effect of mutation of psrR1 on the expression level of the PSI and PBS genes during cold acclimation. Four genes related to PSI and PBS were selected for qRT-PCR analysis for further confirmation. The two phycobilisomes related genes- Cphycocyanin beta subunit, cpcB; allophycocyanin alpha chain, apcA and two genes encoding PSI P700 chlorophyll a apoprotein A1, psaA and PSI reaction centre protein subunit XI, psaL were selected for the analysis. The level of expression of the selected genes in the $\Delta psrR1$ grown at 20°C for the time points 0.5, 6 and 12h were compared with the WT and the overexpression strain, psrR1⁺ (Figure 15). The graph plotted showed the gene expression pattern of the four selected genes in the three strains. In the WT, all the four genes; cpcB, apcA, psaA and psaL were observed to undergo transient downregulation when shifted from 34°C to 20°C. Such low temperature responsive downregulation of the cpcB gene was not observed in $\Delta psrR1$. On the contrary, the data suggested increased accumulation of cpcB transcript within $\Delta psrR1$ cells with the increase in the duration of cold treatment (Figure 15). The other two genes apcA and psaL had undergone downregulation but the fold change in the repression level of these two genes in $\Delta psrR1$ was less when compared to WT. In the overexpression strain $psrR1^+$, the fold of downregulation of all the four genes were comparatively more compared to both WT and $\Delta psrR1$. The expression level of psaA remained almost similar in all three strains during the cold treatment. The results observed in qRT-PCR analysis corroborates the pattern of change in the expression of the photosynthesis-related genes observed in whole transcriptome analysis (Figure 14).

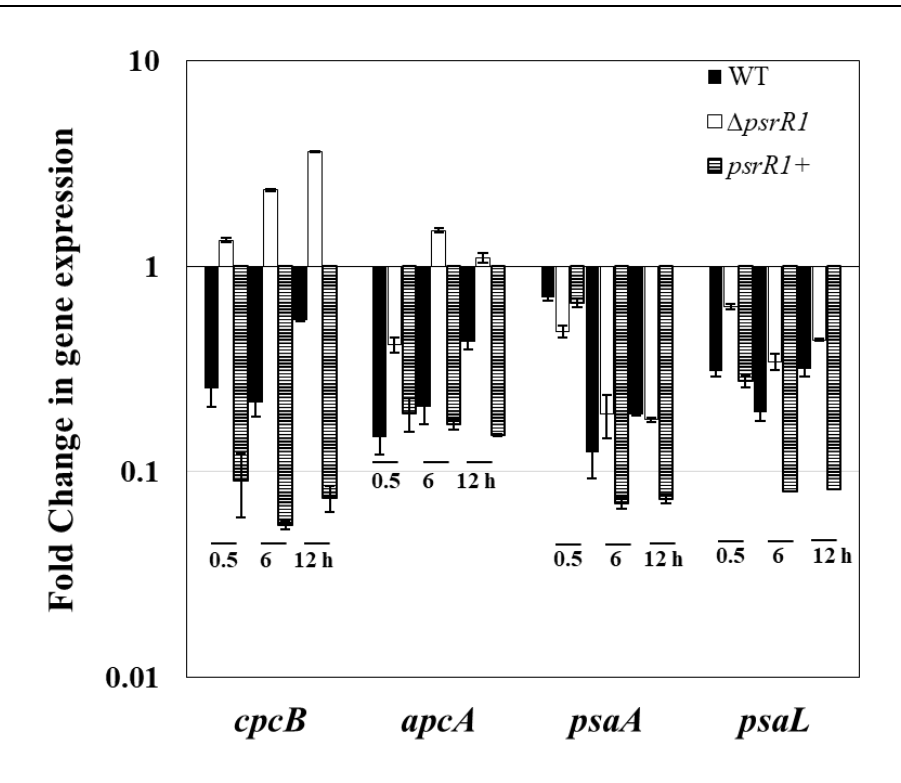


Figure 15. Transcript levels of photosystem I and phycobilisome genes. The genes coding for components of PS I and PBS were analyzed by qRT-PCR analyses during cold treatment in the WT, $\Delta psrRI$, and $psrRI^+$ strains. The \log_{10} expression values were plotted, the closed bars represent fold change in the WT cell, open bars represent the fold change in the $\Delta psrRI$ mutant cell and the stripped bars represent the fold change in $psrRI^+$ cells. In $\Delta psrRI$ when compared to the WT cells, the fold of downregulation of the genes were reduced and was maintained to be higher throughout the treatment. Whereas in $psrRI^+$, the expression of those genes was further downregulated compared to the WT cells. The results obtained in three independent set of experiments are presented as mean ratios $\pm S.D$ (error bars).

4.5 Growth analysis of WT, ∆psrR1 and psrR1+

We monitored the growth of the strains WT, $\Delta psrR1$ and $psrR1^+$ to probe the effect of mutation and overexpression of PsrR1 in the growth at low temperature. The three strains grown at 34°C for 20 h were shifted to 20°C (Figure 16A). The O.D₇₃₀ measured did not exhibit significant differences in the pattern of growth among the cultures grown at 34°C for 20h. When shifted to low temperature (20°C) after 20h (~0.7 O.D₇₃₀), the O.D₇₃₀ of the cultures were recorded at

regular intervals till 72 h of cold treatment. The O.D₇₃₀ of the cultures at different time points were plotted on a graph. The peak in the graph indicated decline in the growth of WT and $psrR1^+$ whereas, the $\Delta psrR1$ growth surpassed the other two strains (Figure 16A). $\Delta psrR1$ relatively exhibited fast growth throughout the cold treatment. The growth of WT and $psrR1^+$ was similar till 24 h at low temperature; but at the later time-points, comparatively slow growth of $psrR1^+$ was observed compared to WT (Figure 16A). On visual inspection of the cultures grown till 60 h at low temperature, $\Delta psrR1$ mutant appeared to be relatively dark green compared to WT and $psrR1^+$ (Figure 15B). These observations suggest that PsrR1 impacts the overall growth of cells at low temperature.

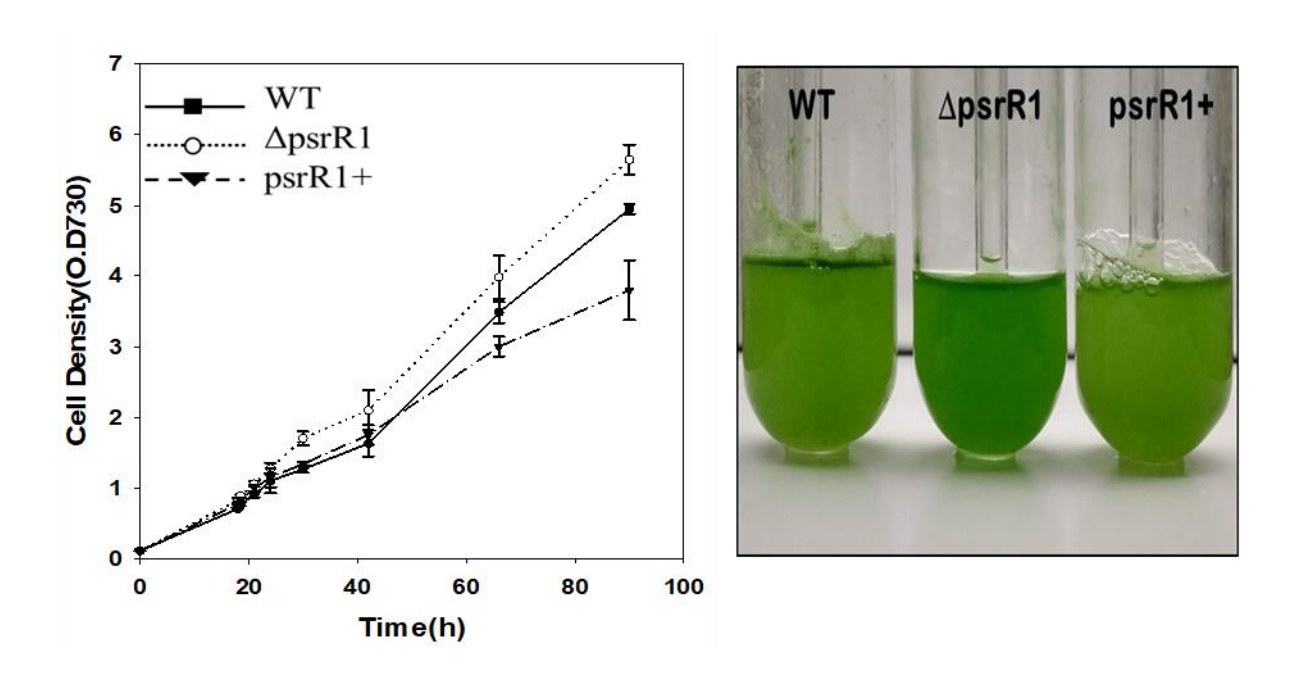


Figure 16. Phenotypes of the mutant strain ΔpsrR1 compared to WT *Synechocystis* subjected to cold treatment at 20°C. The cells were grown in YBG11 medium photoautotrophically (75 μE / m2/s) at the optimum growth temperature of 34°C to an O.D₇₃₀ of 0.6 and then shifted to 20°C. The cells were supplied with continuous air bubbling with illumiation (75 μmol photons m− 2 s− 1). (A) Growth curves for WT (■), $\Delta psrR1$ (○) and $psrR1^+$ (▼). (B) The image of photoautotrophically grown cells for 20 hrs at 34°C when shifted and cultured for 60 hrs at 20°C.

4.6 Pigment analysis in WT and *∆psrR1*

The inactivation of PsrR1 led to relatively better growth. The photosynthetic pigment contents of phycocyanin, allophycocyanin and chlorophyll were estimated in WT and $\Delta psrR1$ (Figure 17). Pigment estimation of the cells incubated at the time points; 0 h (cultures at 34°C), 6 h and 48 h (at 20°C) were measured and normalized to the total protein content in the cells. Allophycocyanin and phycocyanin were higher in $\Delta psrR1$ at optimal conditions (34°C). When shifted to 20°C for 6 and 48h, decrease in the content of allophycocyanin and phycocyanin was observed. However, the pigment content were always high in $\Delta psrR1$ compared to WT. The chlorophyll content was observed to be similar in both WT and $\Delta psrR1$ at optimal growth temperature (34°C). There was decrease in the chlorophyll content in WT when shifted to low temperature for 6 and 48 h. In $\Delta psrR1$, no change in the chlorophyll content was observed at initially but decrease in the chlorophyll content was observed at 48h (Figure 17).

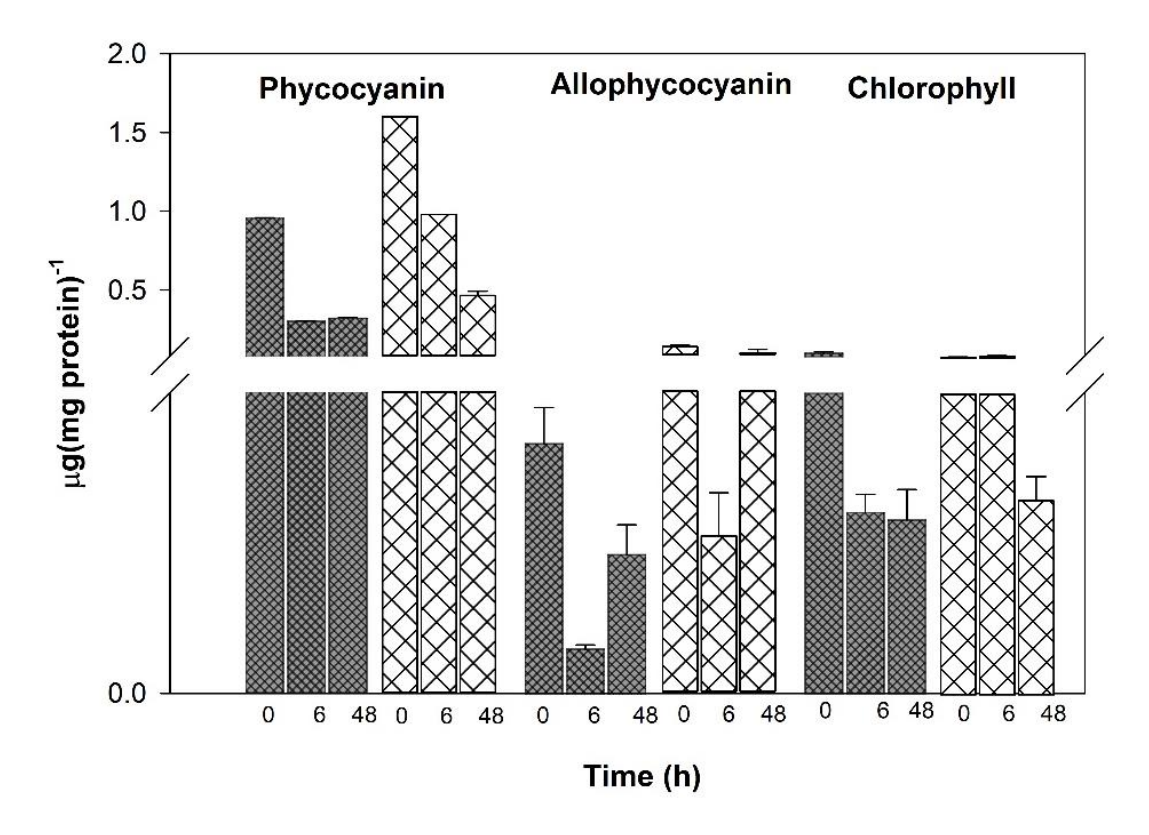


Figure 17. Pigment analysis in the WT cells and $\Delta psrR1$. The cells WT (a) and $\Delta psrR1$ (b) were grown in YBG-11 medium at the optimum growth temperature of 34°C to an O.D₇₃₀ of

0.6 and then shifted to 20°C. The cells were supplied with continuous air bubbling with illumination (75 μ mol photons m⁻² s⁻¹). The phycocyanin, allophycocyanin and chlorophyll content in the cells were estimated and normalized to the whole protein content of the cell.

4.7 77K Fluorescence emission spectra of the WT and △psrR1

When exposed to low temperature, the photosynthetic organisms require to optimize photosynthesis as essential for better survival of the organism. Such optimization results from changes in the ratio of PSI to PSII. 77K (-196.15°C) fluorescence emission spectra record the chlorophyll fluorescence emission from the photosystems PSI and PSII. The spectra can give us an insight into the state of the photosystems. The 77K fluorescence emission spectra of both the WT and *∆psrR1* cells cultured at 34°C and 20°C were recorded (Figure 18). The cells were excited at 430 nm, the excitation wavelength of chlorophyll. The spectra generated were normalized to the peak at 695nm corresponding to the maximum absorption of PSII. In the WT at 34°C, the fluorescence spectra displayed a characteristic pattern where PSII peaks at around 680 nm and PSI at 720 nm. When shifted from 34°C to low temperature (20°C), we observed a drastic decrease in the PSI/PSII ratio in the WT. This data is in consistent with the observation of rapid down regulation PSI and phycobilisome genes in the WT cells during low temperature acclimation (Figures 14). The ratio of PSI / PSII in \(\Delta psrR1 \) was seen to remain unaltered even when the cells were shifted to low temperature. Compared to WT, the PSI / PSII ratio observed to be higher in ∆psrR1 at both 34°C and 20°C. When shifted to low temperature, decrease in PSI / PSII ratio was seen in the WT. But in $\Delta psrR1$, the low temperature did not alter the PSI / PSII ratio. Since change in the stoichiometry is proposed as one of the important mechanism to evade the consequences of cold stress, no change in PSI/PSII ratio in $\Delta psrR1$ clearly implies

its important role in the optimization of photosynthesis during cold acclimation. This observations is also evident from gene expression studies.

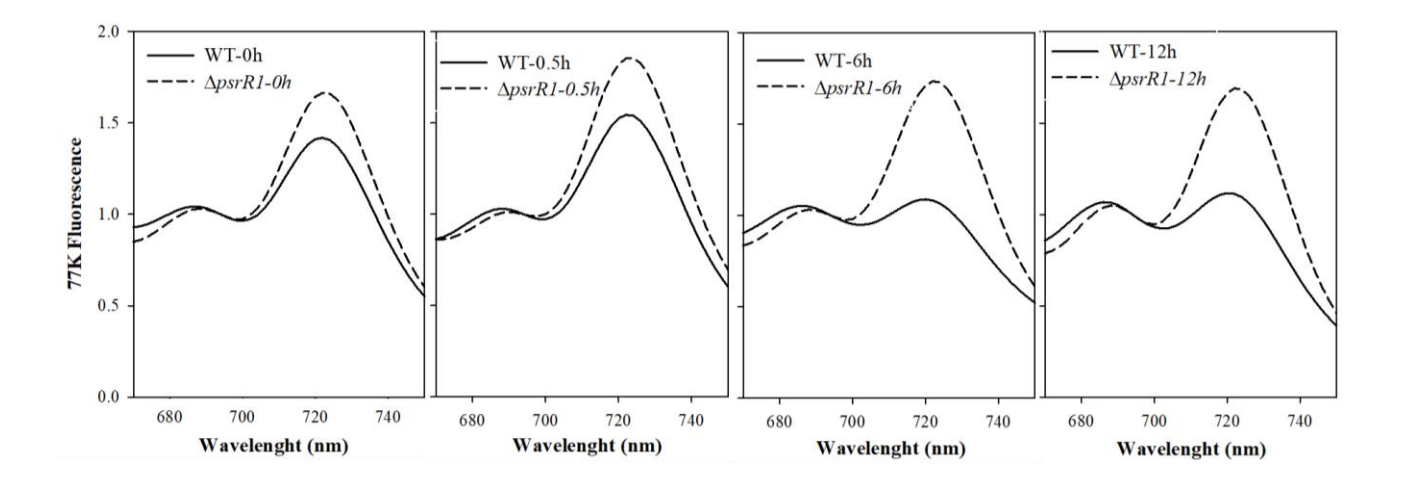


Figure 18. 77K fluorescence emission spectra of the WT and $\Delta psrR1$. The WT *Synechocystis* and $\Delta psrR1$ grown in YBG11 medium at the optimum growth temperature of 34°C to an O.D₇₃₀ of 0.6 with continuous air bubbling and illumination (75µmol photons m⁻² s⁻¹) were shifted to 20°C. The cells were excited with the chlorophyll excitation wavelength of 430nm. The emission spectra were normalized to 1 at the peak 695 nm corresponding to PSII fluorescence.

4.8 Generation of mutant strain-∆rpaB

RpaB is the response regulator functions during both cold and high light stress conditions. During high light stress, dephosphorylated RpaB, no longer induces the expression of the PSI and phycobilisome proteins. But there is no report that states if RpaB is a positive or negative regulator during cold stress. We have generated a partial mutant of Slr0947; $\triangle rpaB$, it being an essential gene a complete mutation is lethal (Figure 19A & B). Further mutation of *slr0947*, leads to slower growth rate compared to the WT cells grown at the optimum growth temperature (Figure 19C & D). Microarray analysis with $\triangle rpaB$ indicates that decrease in the

copy number of *slr0947* leads to upregulation of genes associated to photosystem I, phycobilisomes and ATP synthase complexes (Figure 19 & Table 2).

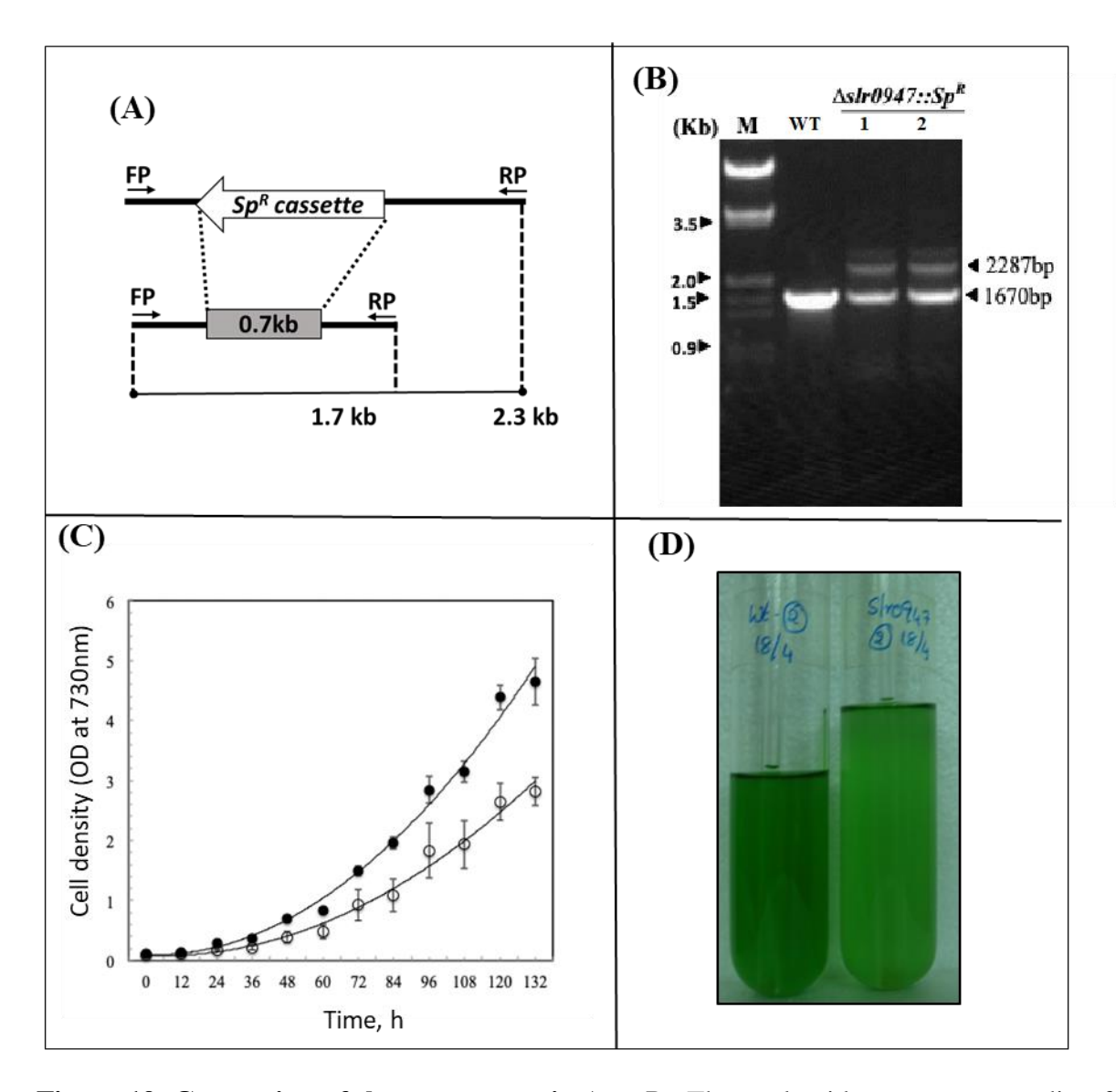


Figure 19. Generation of the mutant strain $\Delta rpaB$. The nucleotide sequence encoding for RpaB was replaced in the WT cell with the mutated copy in the $\Delta rpaB$ mutant cell. The mutant construct of $\Delta rpaB$ was generated by replacing 530 bp DNA fragment of the total 705 bp with spectinomycin antibiotic cassette (1147 bp). (A) Diagrammatic presentation of the $\Delta rpaB$ mutant genotype. The primer set slr0947–FP and slr0947-RP amplifies 705 base pair of slr0947 along with 491 nucleotide upstream and 474 downstream flanking DNA region. The spectinomycin antibiotic resistance cassette replaces 175bp of slr0947 in the mutant $\Delta rpaB$. (B) PCR analysis using the genomic DNA as template with the primers mentioned in (A). M, DNA ladder 1-kb (Cat No. 3412A, Takara); WT, PCR product with WT genomic DNA as the template; and $\Delta rpaB$, PCR product with the genomic DNA of $\Delta rpaB$. (C) The growth curve of the WT and the $\Delta rpaB$ mutant cells. The WT (•) and the $\Delta rpaB$ strain (\circ) were grown photoautotrophically (75 μmol photons m⁻² s⁻¹) at 34°C. The growth was monitored by

measuring the OD₇₃₀. Similar results were obtained in three independently; (D) The WT and the $\Delta rpaB$ ($\Delta slr0947$) strain grown at 34°C.

4.9 Microarray

The RNA extracted from the WT and $\Delta rpaB$ grown at 34°C were used for microarray analysis. The mutant, $\Delta rpaB$ was partially segregated indicating that slr0947 is an essential gene and is required for the survival of Synechocystis. The effect of decreased copy number of slr0947 in the expression profile of many phycobilisomes and photosynthesis-related genes were observed to be very evident in the microarray analysis (Table 3). Most of the genes coding for different subunits of the phycobilisomes complex were highly upregulated.

ORF No	Function	∆rpaB	/WT
sll1322	ATP synthase A chain of CF(0)	8.1±	2.100
ssl3093	phycobilisome small rod linker polypeptide	7.2±	0.191
sll1579	phycobilisome rod linker polypeptide	6.7±	0.189
sll1580	phycobilisome rod linker polypeptide	6.4±	1.075
sll1577	phycocyanin beta subunit	5.0±	0.169
sll1578	phycocyanin alpha subunit	4.7±	0.428
sll1326	ATP synthase alpha chain	4.3±	1.599
sll1451	nitrate/nitrite transport system permease protein	4.2±	0.447
sll1325	ATP synthase delta chain of CF(1)	4.2±	0.233
slr0898	ferredoxinnitrite reductase	4.1±	0.196
sll1453	nitrate/nitrite transport system ATP-binding protein	4.0±	0.185
slr1330	ATP synthase epsilon chain of CF(1)	3.9±	0.215
sll1327	ATP synthase gamma chain	3.7±	0.088
sll1324	ATP synthase B chain (subunit I) of CF(0)	3.6±	0.136

slr1986	allophycocyanin beta subunit	3.5±	0.134
sll1452	nitrate/nitrite transport system ATP-binding protein	3.4±	0.378
ssr3383	phycobilisome small core linker polypeptide	3.3±	0.097
sll1323	ATP synthase subunit b' of CF(0)	3.2±	0.114
slr2067	allophycocyanin alpha subunit	3.2±	0.054
slr0506	light-dependent oxidoreductase NADPH-protochlorophyllide	3.1±	0.068
sll0427	photosystem II manganese-stabilizing polypeptide	3.0±	0.136
ssl2615	ATP synthase C chain of CF(0)	2.9±	0.064
slr1329	ATP synthase beta subunit	2.9±	0.066
slr0758	circadian clock protein KaiC homolog	2.7±	0.426
slr1459	phycobilisome core component	2.6±	1.475
sll0038	positive phototaxis protein, two-component response regulator PatA subfamily	2.6±	3.755
sll1734	protein involved in low CO2-inducible, high affinity CO2 uptake	2.6±	0.230
smr0008	photosystem II PsbJ protein	2.4±	0.068
ssr3451	cytochrome b559 alpha subunit	2.4±	0.039
slr1643	ferredoxin-NADP oxidoreductase	2.4±	0.025
smr0007	photosystem II PsbL protein	2.3±	0.092
ssr0390	photosystem I reaction center subunit X	2.2±	0.043
slr0228	cell division protein FtsH	2.0±	0.067
slr0474	two-component response regulator CheY subfamily, regulator for phytochrome 1 (Cph1)	0.2±	0.019
slr0473	cyanobacterial phytochrome 1, two-component sensor histidine kinase	0.1±	0.003

Table 3: Effect in the photosynthetic gene expression profile in $\Delta rpaB$. The total RNA extracted from the WT and $\Delta rpaB$ cells grown at 34°C were used to examine the fold changes in the gene expression with Agilent custom-made DNA microarray chips.

4.10 Expression of PNP and CrhR with 3X-FLAG tag:

A rapid downregulation of PSI and phycobilisome-related genes occurs during cold acclimation. Such a rapid downregulation is probably involved in balancing the PSI to PSII stoichiometry and functional coordination during cold acclimation. Our data suggest that the inactivation of psrR1 leads to an imbalance in PSI to PSII ratio. PsrR1 being a non-coding RNA it is likely that complementary base pairing with the target mRNA (PSI and phycobilisomes), triggers its rapid degradation. Various exo- and endo-ribonucleases are known to degrade RNA in bacteria. However, the ribonucleases involved in such rapid degradation during post-transcriptional regulation is not yet been studied well. However, the endoribonuclease RNaseE had been earlier shown to be involved in light to dark regulation of psbA genes [70]. The cold-inducible RNA helicase, CrhR was reported to be essential for the regulation of photosystem stoichiometry at low temperature in Synechocystis. [25, 26]. In E. coli, RNA helicase, RhlB interacts with the exoribonuclease, PNPase to form an exosome-like complex to regulate cysteine biosynthesis [65]. In Synechocystis, RNA helicase, CrhR and polynucleotide phosphorylase PNP are cold-inducible. Hence, we had investigated the involvement of the exoribonuclease, PNP and the RNA helicase, CrhR in the regulatory mechanism of PS genes during cold acclimation. To check their potential role in regulating photosynthetic genes, we used 3xFLAG tagged-PNP and 3XFLAG tagged CrhR as a bait protein to co-immunoprecipitate the associated mRNA targets. We have generated two different Synechocystis strains to overexpress PNP and CrhR with 3X-FLAG tag. The 3X-FLAG peptide consists of 23 amino acid residues '(Met-Asp-Tyr-Lys-Asp-His-Asp-Gly-Asp-Tyr-Lys-Asp-His-Asp-Ile-Asp-Tyr-Lys-Asp-Asp-Asp-Lys)'. Both the proteins PNP and CrhR tagged with 3X-FLAG were independently used as bait proteins to co-elute the mRNA targets associated with the proteins by performing RNA co-immunoprecipitation. As described in materials and methods, we cloned 3X-FLAG PNP and 3X-FLAG CrhR downstream to the

copper repressible promoter, PpetJ. The generated plasmids were mobilized into wild-type *Synechocytsis* strain by triparental conjugation to generate the strains- PNP⁺ and CrhR⁺. In the case of CrhR⁺, its respective plasmid construct was mobilized into $\triangle CrhR$ strain; the strain was generated in our laboratory previously [7]. The induction and expression of 3X FLAG-PNP and 3X FLAG (negative control) were checked and confirmed by western blotting (Figure 20). The expressed protein was purified using the FLAG immunoprecipitation Kit- FLAGIPT1 from Sigma.

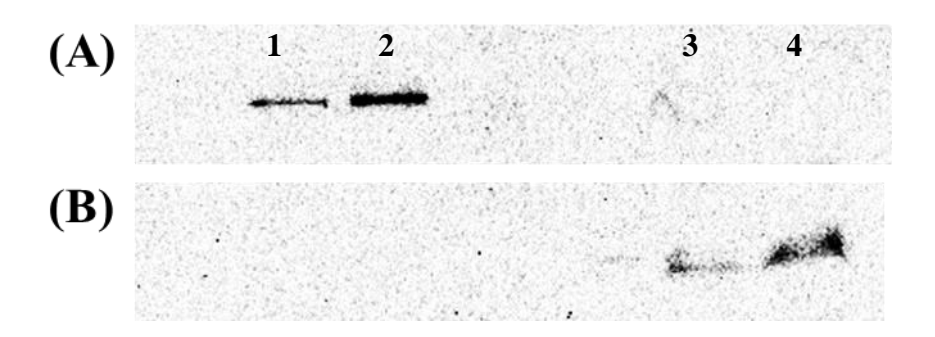


Figure 20: Induction and expression of 3X FLAG-PNP. The Western Blot image of the 3X FLAG-PNP (A) and 3X FLAG (B) protein. The soluble fractions of protein extract of the lysed cells of PNP⁺ and Flag^{neg} were used to purify the protein following the protocol manual provided with the FLAG immunoprecipitation Kit- FLAGIPT1. Elutes collected were allowed to run in 12% SDS-PAGE. The 3XFLAG- PNP (Elute 1 and Elute 2: Lane 1&2 respectively) as well as the 3X-FLAG (Elute 1 and Elute 2: Lane 3&4 respectively) on the blot were detected with Anti-FLAG antibody. The molecular weight of PNP with the 3X FLAG tag is ~80.7kD and that of 3X FLAG is ~3kD.

4.11 Co-elution and identification of the RNA targets of PNP and CrhR:

The expression of 3X-FLAG, 3X-FLAG-PNP and 3X-FLAG-CrhR were induced using the respective strains by growing them in a copper depleted YBG-11 medium. The induced cells were also subjected to low temperature treatment (15°C) for 0.5 h. The treated cultures' cell lysate was used to perform RNA-co immunoprecipitation as mentioned in the methodology.

The RNAs co-eluted with the 3XFLAG tagged proteins were identified by deep sequencing analysis on Ion-Torrent platform. The identified RNAs are listed in the Table 3. Interestingly, the most abundant RNAs that co-eluted with PNP and CrhR were *psaA* and *psaB*, the genes encode photosystem I P700 chlorophyll, an apoprotein- A1 and A2, respectively. RNAs corresponding to the genes encoding almost all the subunits of PSI, PSII and phycobilisomes were identified as target mRNAs. The heat shock genes *groEL* and *groEL2* were also identified as targets of both PNP and CrhR. It was reported that CrhR stabilizes *groEL*1 and *groEL2* during cold acclimation [7]. Thus the result indicates that PNP and CrhR are involved in the regulatory mechanism of cold stress-responsive genes during cold acclimation.

Gene Name	ORF	Function	Reads		
			3XFLAG- PNP	3XFLAG- CrhR	3X FLAG
psaA	slr1834	P700 apoprotein subunit Ia	1092	8459	279
psaB	slr1835	P700 apoprotein subunit Ib	1518	6527	210
slr0374	slr0374	hypothetical protein	678	3328	1159
sll1951	sll1951	Unknown protein	937	3181	558
rpoC2	sll1789	RNA polymerase beta prime subunit	808	3168	292
slr1841	slr1841	probable porin; major outer membrane protein	703	3016	463
dnaK_sll0170	sll0170	DnaK protein 2, heat shock protein 70, molecular chaperone	619	2742	1327
rpoB	sll1787	RNA polymerase beta subunit	527	2282	245

clpC sll0020 ATP-dependent Clp protease regulatory subunit 480 2148 886 deaD slr0083 RNA helicase Light 241 1938 76 slr5005 slr5005 hypothetical protein 946 1790 631 slr1028 slr1028 unknown protein 843 1730 673 htrA slr1204 protease 100 1635 680 sll1946 sll1946 hypothetical protein 117 1632 236 slr090 slr6090 unknown protein 294 1529 395 slr0408 slr0408 unknown protein 749 1520 582 slr1403 slr1403 unknown protein 727 1481 649 sll0821 sll0821 phytochrome-like protein 437 1428 346 slr0543 sll0543 hypothetical protein 268 1397 151 rpD_sll0306 sll0306 RNA polymerase group 2 sigma factor 234 1316 378						
slr5005 slr5005 slr5005 hypothetical protein 946 1790 631 slr1028 slr1028 unknown protein 843 1730 673 htrA slr1204 protease 100 1635 680 sll1946 sll1946 hypothetical protein 117 1632 236 slr6090 slr6090 unknown protein 294 1529 395 slr0408 slr0408 unknown protein 749 1520 582 slr1403 slr1403 unknown protein 727 1481 649 sll0821 phytochrome-like protein 437 1428 346 slr1740 slr1740 oligopeptide binding protein 122 1428 394 sll0543 slr0543 hypothetical protein 268 1397 151 rpoD_sll0306 sll0306 RNA polymerase group 2 sigma factor 234 1316 378 slr0551 slr0551 hypothetical protein 258 1296 256 <	clpC	sll0020	protease regulatory	480	2148	886
slr1028 slr1028 unknown protein 843 1730 673 htrA slr1204 protease 100 1635 680 sll1946 sll1946 hypothetical protein 117 1632 236 slr6090 slr6090 unknown protein 294 1529 395 slr0408 slr0408 unknown protein 749 1520 582 slr1403 unknown protein 727 1481 649 sll0821 phytochrome-like protein 437 1428 346 slr1740 slr1740 oligopeptide binding protein of ABC transporter 122 1428 394 sll0543 hypothetical protein 268 1397 151 151 rpoD_sll0306 sll0306 RNA polymerase group 2 sigma factor 234 1316 378 slr0551 slr0551 hypothetical protein 258 1296 256 infB slr0744 translation initiation factor IF-2 529 1196 430 <t< th=""><th>deaD</th><th>slr0083</th><th>RNA helicase Light</th><th>241</th><th>1938</th><th>76</th></t<>	deaD	slr0083	RNA helicase Light	241	1938	76
htrA slr1204 protease 100 1635 680 sll1946 sll1946 hypothetical protein 117 1632 236 slr6090 slr6090 unknown protein 294 1529 395 slr0408 slr0408 unknown protein 749 1520 582 slr1403 slr1403 unknown protein 727 1481 649 sll0821 phytochrome-like protein 437 1428 346 slr1740 slr1740 oligopeptide binding protein of ABC transporter 122 1428 394 sll0543 sll0543 hypothetical protein 268 1397 151 rpoD_sll0306 sll0306 RNA polymerase group 2 sigma factor 234 1316 378 slr0551 hypothetical protein 258 1296 256 infB slr0744 translation initiation factor IF-2 309 1225 364 rpl5 sll1808 50S ribosomal protein 285 1176 59	slr5005	slr5005	hypothetical protein	946	1790	631
sll1946 sll1946 hypothetical protein 117 1632 236 slr6090 slr6090 unknown protein 294 1529 395 slr0408 slr0408 unknown protein 749 1520 582 slr1403 slr1403 unknown protein 727 1481 649 sll0821 phytochrome-like protein 437 1428 346 slr1740 slr1740 oligopeptide binding protein of ABC transporter 122 1428 394 sll0543 hypothetical protein 268 1397 151 rpoD_sll0306 sll0306 RNA polymerase group 2 sigma factor 234 1316 378 slr0551 slr0551 hypothetical protein 258 1296 256 infB slr0744 translation initiation factor IF-2 529 1196 430 rpl5 sll1808 50S ribosomal protein 285 1176 59 groEL sll1802 50S ribosomal protein 301 1134 105	slr1028	slr1028	unknown protein	843	1730	673
slr6090 slr6090 unknown protein 294 1529 395 slr0408 slr0408 unknown protein 749 1520 582 slr1403 slr1403 unknown protein 727 1481 649 sll0821 phytochrome-like protein 437 1428 346 slr1740 slr1740 oligopeptide binding protein of ABC transporter 122 1428 394 sll0543 sll0543 hypothetical protein 268 1397 151 rpoD_sll0306 sll0306 RNA polymerase group 2 sigma factor 234 1316 378 slr0551 slr0551 hypothetical protein 258 1296 256 infB slr0744 translation initiation factor IF-2 309 1225 364 slr0364 hypothetical protein 529 1196 430 rpl5 sll1808 50S ribosomal protein 285 1176 59 groEL sll1802 50S ribosomal protein 301 1134 105	htrA	slr1204	protease	100	1635	680
slr0408 slr0408 slr0408 unknown protein 749 1520 582 slr1403 slr1403 unknown protein 727 1481 649 sll0821 sll0821 phytochrome-like protein 437 1428 346 slr1740 slr1740 oligopeptide binding protein of ABC transporter 122 1428 394 sll0543 sll0543 hypothetical protein 268 1397 151 rpoD_sll0306 sll0306 RNA polymerase group 2 sigma factor 234 1316 378 slr0551 slr0551 hypothetical protein 258 1296 256 infB slr0744 translation initiation factor IF-2 309 1225 364 slr0364 slr0364 hypothetical protein 529 1196 430 rpl5 sll1808 50S ribosomal protein 285 1176 59 groEL sll1802 50S ribosomal protein 301 1134 105	sll1946	sll1946	hypothetical protein	117	1632	236
slr1403 slr1403 unknown protein 727 1481 649 sll0821 sll0821 phytochrome-like protein 437 1428 346 slr1740 slr1740 oligopeptide binding protein of ABC transporter 122 1428 394 sll0543 sll0543 hypothetical protein 268 1397 151 rpoD_sll0306 sll0306 RNA polymerase group 2 sigma factor 234 1316 378 slr0551 slr0551 hypothetical protein 258 1296 256 infB slr0744 translation initiation factor IF-2 309 1225 364 slr0364 slr0364 hypothetical protein 529 1196 430 rpl5 sll1808 50S ribosomal protein 285 1176 59 groEL slr2076 60kD chaperonin 326 1161 415 rpl2 sll1802 50S ribosomal protein 301 1134 105	slr6090	slr6090	unknown protein	294	1529	395
sll0821 sll0821 phytochrome-like protein 437 1428 346 slr1740 slr1740 oligopeptide binding protein of ABC transporter 122 1428 394 sll0543 sll0543 hypothetical protein 268 1397 151 rpoD_sll0306 sll0306 RNA polymerase group 2 sigma factor 234 1316 378 slr0551 slr0551 hypothetical protein 258 1296 256 infB slr0744 translation initiation factor IF-2 309 1225 364 slr0364 slr0364 hypothetical protein 529 1196 430 rpl5 sll1808 50S ribosomal protein 285 1176 59 groEL slr2076 60kD chaperonin 326 1161 415 rpl2 sll1802 50S ribosomal protein 301 1134 105	slr0408	slr0408	unknown protein	749	1520	582
slr1740 slr1740 oligopeptide binding protein of ABC transporter 122 1428 394 sll0543 sll0543 hypothetical protein 268 1397 151 rpoD_sll0306 sll0306 RNA polymerase group 2 sigma factor 234 1316 378 slr0551 slr0551 hypothetical protein 258 1296 256 infB slr0744 translation initiation factor IF-2 309 1225 364 slr0364 slr0364 hypothetical protein 529 1196 430 rpl5 sll1808 50S ribosomal protein 285 1176 59 groEL slr2076 60kD chaperonin 326 1161 415 rpl2 sll1802 50S ribosomal protein 301 1134 105	slr1403	slr1403	unknown protein	727	1481	649
protein of ABC transporter sll0543 sll0543 hypothetical protein 268 1397 151 rpoD_sll0306 sll0306 RNA polymerase group 2 sigma factor 234 1316 378 slr0551 slr0551 hypothetical protein 258 1296 256 infB slr0744 translation initiation factor IF-2 309 1225 364 slr0364 slr0364 hypothetical protein 529 1196 430 rpl5 sll1808 50S ribosomal protein 285 1176 59 groEL slr2076 60kD chaperonin 326 1161 415 rpl2 sll1802 50S ribosomal protein 301 1134 105	sll0821	sll0821	- ·	437	1428	346
rpoD_sll0306 sll0306 RNA polymerase group 2 sigma factor 234 1316 378 slr0551 slr0551 hypothetical protein 258 1296 256 infB slr0744 translation initiation factor IF-2 309 1225 364 slr0364 slr0364 hypothetical protein 529 1196 430 rpl5 sll1808 50S ribosomal protein 285 1176 59 groEL slr2076 60kD chaperonin 326 1161 415 rpl2 sll1802 50S ribosomal protein 301 1134 105	slr1740	slr1740	protein of ABC	122	1428	394
str0551 str0551 hypothetical protein 258 1296 256 infB str0744 translation initiation factor IF-2 309 1225 364 str0364 str0364 hypothetical protein 529 1196 430 rpl5 stl1808 50S ribosomal protein 285 1176 59 groEL str2076 60kD chaperonin 326 1161 415 rpl2 stl1802 50S ribosomal protein 301 1134 105	sll0543	sll0543	hypothetical protein	268	1397	151
infB slr0744 translation initiation factor IF-2 309 1225 364 slr0364 slr0364 hypothetical protein 529 1196 430 rpl5 sll1808 50S ribosomal protein 285 1176 59 groEL slr2076 60kD chaperonin 326 1161 415 rpl2 sll1802 50S ribosomal protein 301 1134 105	rpoD_sll0306	sl10306		234	1316	378
factor IF-2 slr0364 slr0364 hypothetical protein 529 1196 430 rpl5 sll1808 50S ribosomal protein 285 1176 59 groEL slr2076 60kD chaperonin 326 1161 415 rpl2 sll1802 50S ribosomal protein 301 1134 105	slr0551	slr0551	hypothetical protein	258	1296	256
nypothetical protein rpl5 sll1808 50S ribosomal protein 285 1176 59 groEL slr2076 60kD chaperonin 326 1161 415 rpl2 sll1802 50S ribosomal protein 301 1134 105	infB	slr0744		309	1225	364
L5 groEL slr2076 60kD chaperonin 326 1161 415 rpl2 sll1802 50S ribosomal protein 301 1134 105	slr0364	slr0364	hypothetical protein	529	1196	430
rpl2 sll1802 50S ribosomal protein 301 1134 105	rpl5	sll1808	-	285	1176	59
- · · · · · · · · · · · · · · · · · · ·	groEL	slr2076	60kD chaperonin	326	1161	415
	rpl2	sll1802	<u>=</u>	301	1134	105

groEL-2	sll0416	60 kDa chaperonin 2, GroEL2, molecular chaperone	425	1132	461
rnpB	rnpB	RNA subunit of RNase P	318	1121	79
sl10043	sll0043	positive phototaxis protein, homologous to chemotaxis protein CheA, two-component hybrid histidine kinase	455	1113	289
apcE	slr0335	phycobilisome core- membrane linker polypeptide	320	1087	176
rps3	sll1804	30S ribosomal protein S3	193	1078	39
nucH	sl10656	unknown protein	480	1053	387
psbC	sll0851	photosystem II CP43 protein	286	1039	151
fus_sll1098	sll1098	elongation factor EF-G	261	1029	198
psbA2	slr1311	photosystem II D1 protein	312	1028	150
slr1187	slr1187	unknown protein	101	1014	211
clpB_slr1641	slr1641	ClpB protein	472	994	260
ssr2153	ssr2153	unknown protein	80	993	37
sll0041	sl10041	phytochrome-like photoreceptor protein for positive phototaxis; homologous to methyl- accepting chemotaxis protein	328	970	198
rpoA	sll1818	RNA polymerase alpha subunit	152	958	79
slr0915	slr0915	putative endonuclease	143	947	181

slr0373	slr0373	hypothetical protein	202	945	335
kdpD	slr1731	potassium-transporting P-type ATPase D chain	176	939	140
slr2046	slr2046	unknown protein	458	930	368
petC_slr1185	slr1185	cytochrome b6-f complex alternative iron-sulfur subunit (Rieske iron sulfur protein)	27	914	113
sll1879	sll1879	two-component response regulator	641	897	218
rpl24	sll1807	50S ribosomal protein L24	150	870	18
sll0163	sll0163	WD-repeat protein	363	866	269
sll0723	sll0723	unknown protein	443	865	308
topA	slr2058	DNA topoisomerase I	260	863	178
rbcL	slr0009	ribulose bisphosphate carboxylase large subunit	314	857	141
psbA3	sll1867	photosystem II D1 protein	296	857	129
ilvG	slr2088	acetohydroxy acid synthase	167	854	273
sll1515	sll1515	glutamine synthetase inactivating factor IF17	34	854	453
slr8038	slr8038	WD-repeat protein	354	849	312
gltB_sll1502	sll1502	NADH-dependent glutamate synthase large subunit	325	846	201
sll1124	sll1124	two-component sensor histidine kinase,	379	838	259

		phytochrome-like protein			
sl10798	sl10798	Ni(II)-sensor and/or redox sensor, two- component sensor histidine kinase	133	819	205
slr0794	slr0794	cation efflux system protein involved in nickel and cobalt tolerance	222	805	217
frpC	sll1009	unknown protein	220	803	320
sll1945	sll1945	1-deoxyxylulose-5- phosphate synthase	118	800	195
rpl14	sll1806	50S ribosomal protein L14	137	797	24
rpl6	sll1810	50S ribosomal protein L6	155	785	28
slr0366	slr0366	unknown protein	393	783	282
secA	sll0616	preprotein translocase SecA subunit	303	782	244
rpl16	sll1805	50S ribosomal protein L16	161	770	21
rpl3	sll1799	50S ribosomal protein L3	184	768	121
slr1704	slr1704	hypothetical protein	93	763	173
slr0930	slr0930	hypothetical protein	187	759	102
slr1753	slr1753	hypothetical protein	458	758	280
gltB_sll1499	sll1499	ferredoxin-dependent glutamate synthase	319	756	286
sll0169	sll0169	cell division protein Ftn2 homolog	303	756	165
tktA	sll1070	transketolase	240	755	139

•					
ponA	sll0002	penicillin-binding protein 1A	195	755	262
slr6047	slr6047	hypothetical protein	449	754	242
epsB	sll0923	unknown protein	261	744	297
sll1265	sll1265	unknown protein	286	743	259
hsp17	sll1514	16.6 kDa small heat shock protein, molecular chaperone	124	741	473
тсрА	slr1044	methyl-accepting chemotaxis protein, required for the biogenesis of thick pilli	233	735	214
sll1864	sll1864	probable chloride channel protein	162	724	312
ilvB	sll1981	acetolactate synthase	117	723	183
amiA	slr1744	N-acetylmuramoyl-L- alanine amidase, periplasmic protein	117	722	204
slr0322	slr0322	two-component hybrid sensor and regulator	306	701	231
sll0844	sll0844	tRNA (5- methylaminomethyl-2- thiouridylate)- methyltransferase	120	689	107
ssl3364	ssl3364	CP12 polypeptide	86	687	258
sll0639	sll0639	hypothetical protein	335	684	162
Ppc	sll0920	phosphoenolpyruvate carboxylase	271	683	212
pmgA	sll1968	photomixotrophic growth related protein, PmgA	169	676	92
Pnp	sll1043	polyribonucleotide nucleotidyltransferase	208	675	206

sll0038	sl10038	positive phototaxis protein, two- component response regulator PatA subfamily	107	675	115
nifJ	sll0741	pyruvate flavodoxin oxidoreductase	255	674	134
rps8	sll1809	30S ribosomal protein S8	232	674	38
sll5080	sl15080	non-heme chloroperoxidase	244	666	83
slr0306	slr0306	unknown protein	270	665	80
slr6102	slr6102	type I restriction- modification system, R subunit	268	658	253
tufa	sll1099	elongation factor Tu	231	656	95
slr0453	slr0453	hypothetical protein	207	656	168
gyrA_slr0417	slr0417	DNA gyrase subunit A	274	654	216
sll1060	sll1060	hypothetical protein	240	652	134
nlpD	slr0993	putative peptidase	187	651	156

Table 4. List of the RNA targets co-eluted with the 3XFLAG tagged protein and identified by RNA sequencing. The cells were grown to an O.D₇₃₀ of 0.8 in Y-BG11 and then induced to express 3XFLAG tagged protein for 45h and then shifted to 15°C for 0.5h. The RNA associated with the 3XFLAG tagged protein was co-eluted with it by RNA co-immunoprecipitation. After digestion with proteinase K, the RNA contents in the sample was was extracted by phase separation using phenol-chloroform-isoamylalcohol (PCI). The extracted RNA were then subjected to RNA sequencing analysis and identified.

4.12 Interaction between RNaseII, PNP and CrhR

The homologs of RNaseII and PNP are the components of RNA exosome in Archeal, Yeast and higher Eukaryotes [80, 81]. Mitochondrial RNA comprises of two components- Dss1 3'-5' exoribonuclease and Suv3 helicase [66]. A possible exosome-like complex involved in cysteine biosynthesis was reported in E. coli [65]. Since the PNP and CrhR of Synechocystis are cold-inducible proteins, we anticipated that they might interact with each other to form an exosome-like complex. The proposed exosome-like complex might be involved in rapid mRNA degradation; in our case mRNA of photosystem genes. Hence, we performed bacterial twohybrid assay to explore the possibility of interaction between or among RNaseII, PNP and CrhR [82]. We had cloned the open reading frames of PNP (sll1043), RNaseII (sll1290) and CrhR (slr0083) to generate the plasmid DNA constructs- pT25-RNaseII, pT25-PNP, pPNP-T18 and pCrhR-T18. These generated plasmids were co-transformed into the adenylate cyclase mutant strain of E. coli, DHP1 in the following pairs- i) pT25-RNaseII- pPNP-T18, ii)pT25-RNaseII pCrhR-T18, and iii) pT25-PNP-pCrhR-T18. For the positive control, DHP1 cells harboring the plasmid pair- pT25-sll1130 and pssl2245-T18 were used and the cells upon plating onto MacConkey agar appeared as dark pink coloured colonies [77] (Figure 21). The DHP1 cells harboring the empty plasmid DNA constructs with no cloned inserts, pT25 and pT18 (as a negative control) on the MacConkey agar did not exhibit pink colour when plates containing the cells were incubated for 48 h at 30°C (Figure 21). The cells that were co-transformed with pT25-RNaseII and pPNP-T18 on the MacConkey agar changed into dark pink colour, suggesting a strong interaction between RNaseII and PNP (Figure 21A). Similarly, the DHP1 E. coli cells harbouring pT25-PNP and pCrhR-T18 turned pink upon incubation of plates for 48 h at 30°C, indicating a possible physical association between PNP and CrhR (Figure 21B). The intensity of the colour change was less in the plates with the cells harboring pT25-RNaseII and pCrhR-T18, indicating weak interaction between RNaseII and CrhR (Figure 21C). Thus

the result of the bacterial two-hybrid assays evidently shows that PNP interacts strongly with RNaseII and CrhR. However, CrhR and RNaseII interaction is not so strong to contemplate their physical association.

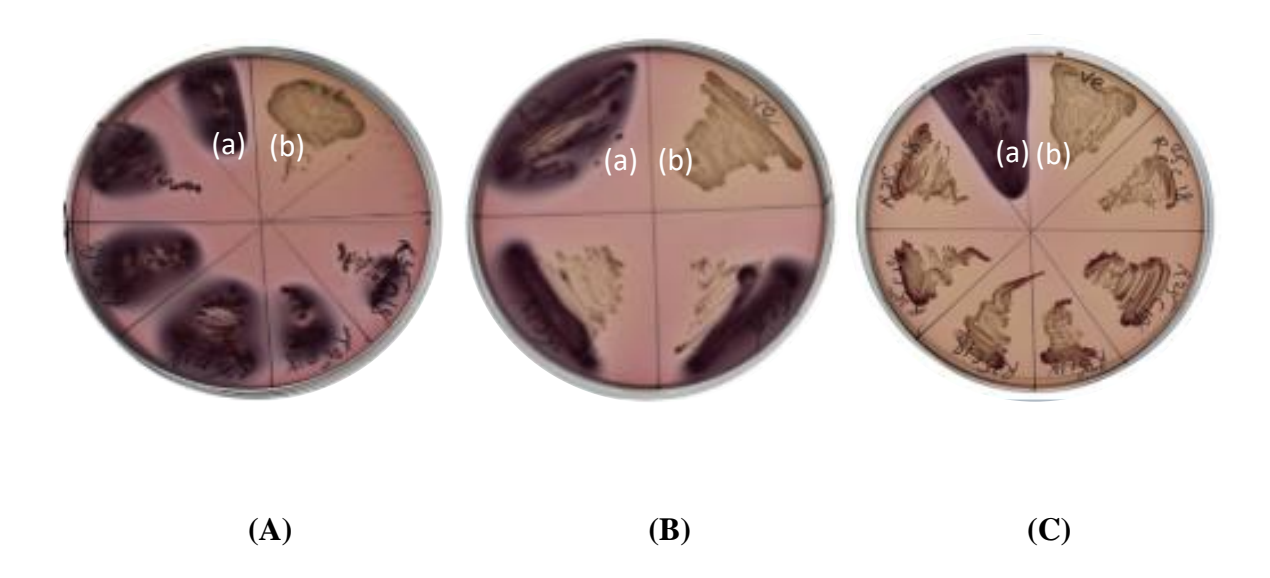
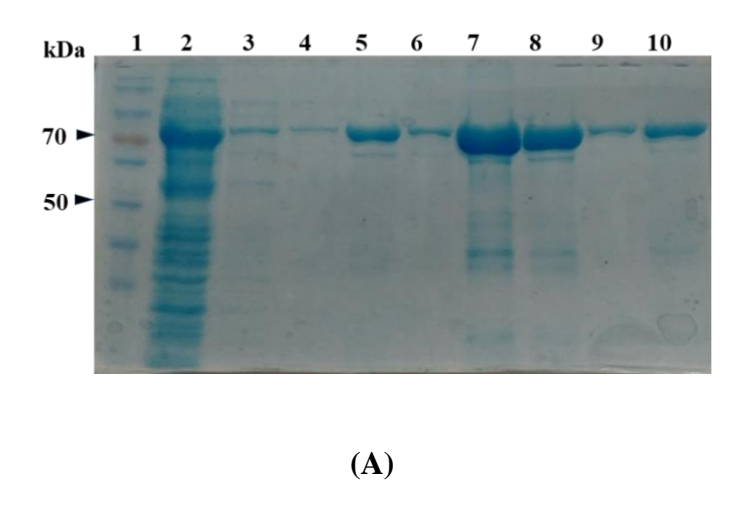


Figure 21. Bacterial two hybrid analysis of PNP, RNaseII and CrhR. The *E. coli* DHP1 cells possessing the plasmids pair that encodes the different proteins were inoculated on a maltose supplemented MacConkey plate as indicated to assess the protein-protein interactions. For the interaction assay, the cells that carry the plasmid pair, pT25-Sll1130 and pSsl2245-T18 were positive controls (a). The cells harboring pT25 and pT18 were negative controls (b). (A) Demonstration of interaction between PNP and RNaseII. The DHP1 cells harboring pT25-RNaseII along with pPNP-T18 has a dark pink colored colonies; (B) Demonstration of interaction between PNP and CrhR. The cells harbour pT25-PNP and pCrhR-T18 exhibited dark pinkish colonies; (C) Demonstration of interaction between RNaseII and CrhR. The cells harboring pT25-RNaseII and pCrhR-T18 exhibited very less pink coloration.

4. 13 Overexpression of PNP, RNaseII and CrhR with 6XHis tag using the bacterial expression system.

We prepared the *E. coli* strains to overexpress proteins used in interaction studies. We have cloned RNaseII, PNP and CrhR respective ORFs into the *E.coli* bacterial expression system-

pCold-I and pET28a+ plasmid vectors. The ORF encoding PNP- sll1043 and CrhR- slr0083 were cloned into pCold-I plasmid vector, and RNaseII-sll1290 was cloned into pET28⁺ plasmid vector. The three proteins were induced, expressed and purified using the Ni-NTA affinity method (Figure 22).



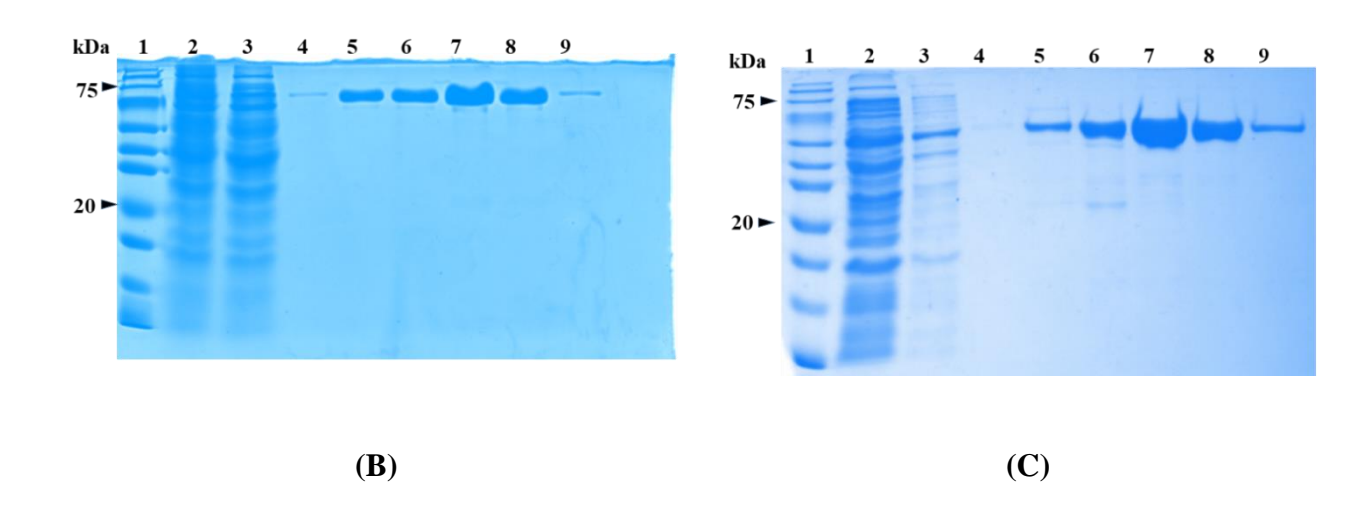


Figure 22. SDS-PAGE analysis of the overexpressed and purified (A) 6XHis-tag RNaseII in *E. coli* BL21 (DE3), (B) 6X His-PNP and (C) 6X His-CrhR proteins in *E. coli* Rosetta (DE3). Lane 1, protein molecular weight standards; lane 2, whole cell lysate of the induced *E. coli* possessing the plasmid pET-*RNaseII*, pCold I-*PNP* and pColdI-*CrhR* in (A), (B) and (C) respectively; lane 3, flow through collected from Ni-NTA column; lane 4, protein washes of Ni-NTA column with 40mM imidazole; lane 5-9, protein elutes with increasing concentrations of imidazole (100, 100, 200, 300 and 400 mM).

4.14 Study of the interaction of PNP, CrhR and RNaseII using Surface Plasmon Resonance (SPR).

The purified PNP, RNaseII and CrhR proteins were used further confirmation of the interaction among these proteins by Surface Plasmon Resonance. Since two of these proteins are strongly upregulated during low temperature stress, and bacterial two-hybrid assays indicated their possible interactions, we anticipated that these proteins might possibly forms an exosome-like complex consisting of PNP, RNaseII and CrhR. The experiments were performed at two temperatures- 25°C (low temperature) and 34°C (optimum growth temperature). 6XHis- PNP protein (ligand) was immobilized on the CM5 sensor chip, whereas the other two proteins, 6X-His-RNaseII and 6X-His-CrhR, were injected as the analyte. The interaction tested were in 1: 1 mode (PNP: RNaseII and PNP: CrhR). The sensogram of the interaction of PNP and RNaseII; and between PNP and CrhR (Figure 23) suggested positive interaction between the proteins. The dissociation constant (K_D) of the interacting proteins are tabulated in Table 4. The smaller the value of K_D, the stronger is the interaction between the protein partners, or higher affinity between the proteins. The K_D value of the interaction between PNP and RNaseII at 34°C and 25°C were 3.36x10⁻⁷ M and 3.54x10⁻⁷, respectively which indicated a strong interaction between the interacting protein partners. Moreover, the similar K_D value at both the temperatures indicated a temperature-independent interaction between PNP and RNAseII. The K_D value of the interaction between PNP and CrhR at 34°C and 25°C were 5.57x10⁻⁷ M and 1.43x10⁻⁵ M, respectively suggesting strong interaction between them. However, it was observed that the K_D value of the interaction at 25°C is smaller by 2 magnitudes compared to that at 34°C, suggesting temperature-dependent interaction. The smaller K_D value at lower temperature indicated that the interaction between PNP and CrhR is favoured at low temperature.

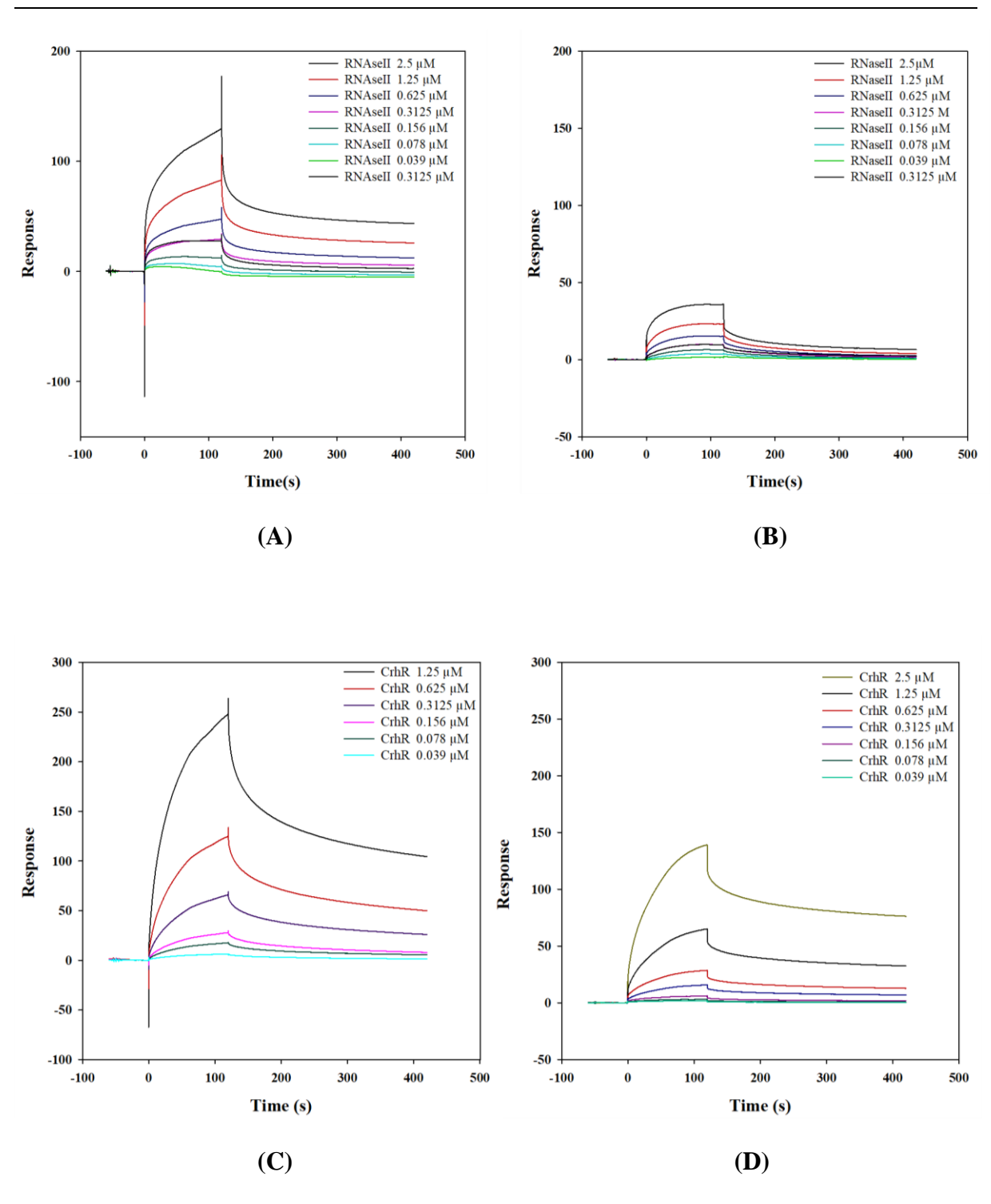
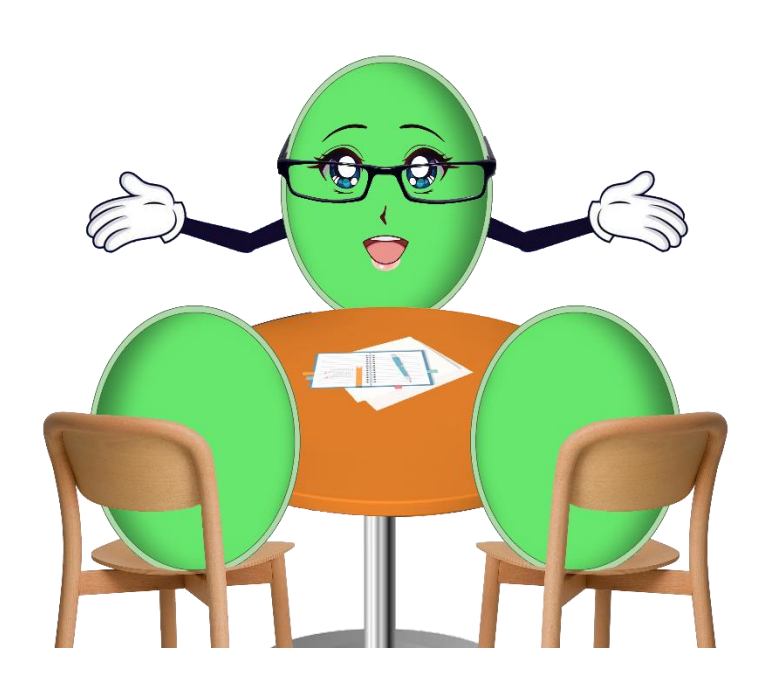


Figure 23. Kinetic analysis of the interaction between PNP – RNaseII and PNP- CrhR. A) Kinetic data analysis if the interaction between PNP and RNaseII set at 25°C; B) between PNP and RNaseII at 34°C; C) Kinetic data analysis between PNP and CrhR at 25°C and D) between PNP and CrhR at 34°C.

Kinetic analysis of different protein pairs										
Protein pairs Temperature ka (1/Ms) kd (1/s) K _D (M)										
PNP-RNaseII	25°C	1.32 *10 ⁴	0.004682	3.54 *10 ⁻⁰⁷						
PNP-RNaseII	34°C	1.40 *104	0.004696	3.36 *10 ⁻⁰⁷						
PNP-CrhR	25°C	4.41 *10 ³	0.002453	5.57 *10 ⁻⁰⁷						
PNP-CrhR	34°C	8.08 *101	0.001153	1.43 *10-05						

Table 5. The calculated dissociation constant at equilibrium (K_D) from the kinetic analysis of the interaction between PNP –RNaseII and between PNP and CrhR. The kinetic analysis between the interacting proteins were carried out at two temperatures- 25°C and 34°C. The K_D value of interaction between PNP and RNaseII at both the temperature was similar. The value K_D between PNP and CrhR is comparatively less at 25°C than at 34°C, indicating the interaction being favorable at low temperature.

5.DISCUSSION



Cyanobacteria are the group of prokaryotes that have survived throughout the ages owing to being highly adaptable. They are found almost in all types of environment and are exposed to the harmful effects of environmental changes. Abiotic stress affects the overall cellular functional events of an organism. All kinds of stress, like change in light intensity, temperature fluctuations, salt, heavy metals etc. can affect the physiological and biochemical processes in microorganisms [29]. Photosynthesis carried out by cyanobacteria and other photosynthetic organisms is immensely affected by abiotic stress. It is a very complex biochemical process that involves multimeric-protein complexes, enzymes and co-factors. The coordination between the major components, PSI and PSII as well as the other co-factors is very crucial to maintain the balance and rate of flow of electrons in the ETC. Temperature is one of the many abiotic factors that is known to have an effect on photosynthesis. Cyanobacteria have a wide range of niches, and are often exposed to temperature fluctuations. Temperatures below the optimum growth temperature range of an organism in the environment is perceived as cold stress. Low temperature creates imbalance in the functional co-ordination between the components of the photosynthetic machinery. In order to evade the detrimental consequences of low temperature on photosynthesis, cyanobacteria employs various defensive strategies which includes downregulation of many PS genes to optimize photosynthesis for their better survival [25]. Besides the genes that encodes different subunits of PS I and the phycobilisomes genes, the genes involved in the photosynthetic pigment synthesis were also reported to be downregulated [9, 25, 27]. Such downregulation of photosynthetic genes also occur during high light acclimation [24]. The small regulatory RNA, PsrR1 and the response regulator, RpaB were identified as the regulators of photosystem-I genes during high-light acclimation [14, 23]. However, the gene regulatory mechanism of the photosynthetic genes during low temperature acclimation is not known. The present study was attempted to elucidate the regulatory mechanism of the expression of photosynthetic genes during cold acclimation. We have found that the sRNA PsrR1, the regulator of PS I genes during HL acclimation, is transiently upregulated during low temperature in *Synechocystis* (Figure 12). This led us to investigate the effect of mutation of psrR1 in the photosynthetic genes during cold stress. The whole transcriptome analysis (NGS) data implies that during cold stress, mutation of PsrR1 in $\Delta psrRI$ led to decrease in the fold of downregulation of the photosynthetic genes relatively to that in the WT. However, the total number of reads obtained in the analysis was very less. The qRT-PCR analysis further confirmed the data generated in the NGS analysis (Figure 14). The decrease in the fold of downregulation of the photosynthetic genes- psaL, cpcB, apcA in the \(\Delta psrR1\) clearly indicated importance of PsrR1 in the regulation of PS I and PBS genes during cold acclimation. Moreover, overexpression of PsrR1 in psrR1+ had relatively led to increase in the fold of downregulation compared to WT (Figure 15). Thus, we can conclude from the data generated that, PsrR1 is essential in the regulation of the photosystem I and the phycobilisome genes during cold acclimation. The growth of $\Delta psrR1$ was relatively faster whereas the overexpression strain, psrR1⁺ exhibited slow growth than the WT (Figure 16A). photosynthetic pigments (phycocyanin, allophycocyanin and chlorophyll a) in $\Delta psrR1$ were always high than the WT cells irrespective of temperature (Figure 17). The image of the culture growing at 20°C for 60h also confirmed the same (Figure 16B). However, decrease in the pigment content during low temperature is relatively less in $\Delta psrR1$.

As per our discussion, optimization of photosynthesis is very essential for the organism to adapt and thrive the cold stress. During such optimization, the rate of flow of the excited electrons between the photosystems and the other electron carriers during photosynthesis has to be maintained. At low temperature, the PSI and PSII re-balance the excitation of electrons in its reaction centres which is known as state-transition. One of the method of state-transition is by changing the ratio of PSII to PSI in the organism. Low temperature altered the ratio of PSI to PSII as seen in the 77K emission spectrum of the WT (Figure 18). The peak at ~720nm declined

drastically when the WT was exposed to low temperature. The decline in the peak implies decrease in the PSI content, thus altering the ratio of PSI to PSII. However, in $\Delta psrR1$ irrespective of the cold-treatment, the intensity of the peak at 720nm did not change. Absence of PsrR1 in the mutant led to nullify the effect of cold stress and thus $\Delta psrR1$ had failed to undergo state transition. Thus, we can conclude that PsrR1 is crucial in the optimization of photosynthesis during cold stress.

RpaB, the response regulator is an essential gene which was confirmed from the fact that $\triangle RpaB$, the mutant strain generated was partially segregated (Figure 19B). This transcription factor transduces the signal of low temperature as well as high light stress in *Synechocystis*. RpaB binds to the HLR1 sequence located in the PSI promoter region and activates the expression of PSI genes during low-light [53]. However, whole genome transcriptome analysis indicated that reduction in the copy number of RpaB in the mutant, $\Delta rpaB$ led to upregulation of the genes associated to photosystem I, phycobilisomes and ATP synthase (Table 2). Being the transcriptional activator for PSI genes, disruption of RpaB in the mutant $\Delta rpaB$, the PS genes were expected to undergo downregulation. Instead, the upregulation of PS genes was observed in the $\triangle rpaB$, very clearly indicating the presence of an alternative regulatory mechanism to regulate the photosynthetic genes in *Synechocystis*. It is highly possible that in $\Delta rpaB$, reduced copy number of slr0947 led to decrease in the levels of RpaB in the cell, and thus was unavailable to activate the expression of the PS genes. This condition might have triggered Synechocystis to activate the alternate regulatory pathway to compensate the decreased level of RpaB. The activated alternative pathway possibly had led the upregulation of the gene expression of photosystem I, phycobilisomes and ATP synthase. Thus it can be concluded that the sRNA, PsrR1 and the response regulator, RpaB is involved in the regulation of the photosynthetic genes. Besides these two elements, there are also alternative regulatory mechanism involved in the regulation of the photosynthetic genes.

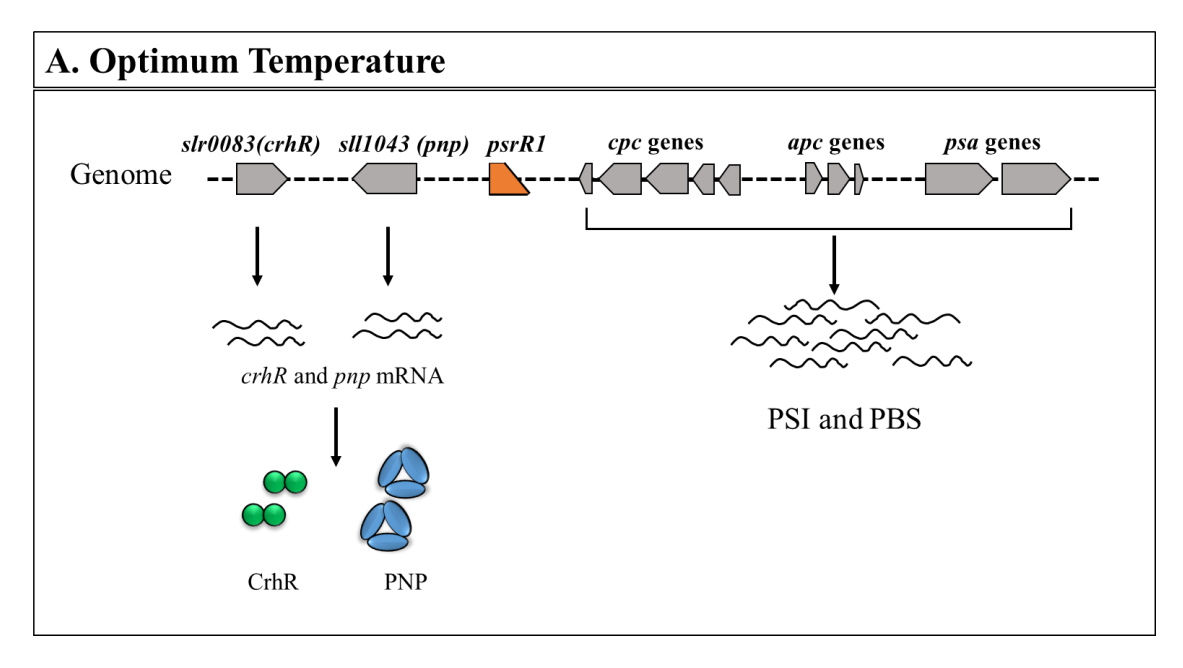
The small regulatory RNA, PsrR1 regulates the expression of photosynthetic genes during high-light acclimation [23]. We had concluded in the present study, that the PsrR1 is also an important participant in the regulatory mechanism of photosynthetic genes at low temperature. Such post-transcriptional regulation by small regulatory RNAs are assisted by different ribonucleases. Interestingly, the RNA helicase, CrhR and the exoribonuclease, PNP are reported to be cold-inducible in Synechocystis [9, 19, 25, 83]. Since PNP and CrhR are cold inducible, we assumed that they might be involved in the gene regulatory mechanism which are crucial during cold acclimation. The RNA co-immunoprecipitation confirms our assumption. We have identified the RNA targets that co-eluted with 3X FLAG -PNP and 3X FLAG- CrhR. The top RNA targets of 3XFLAG-PNP and 3XFLAG-CrhR were the photosystem I genes, psaA and psaB (Table 3). Other RNAs related to the subunits of photosystem II (psb) and phycobilisomes (apc and cpc) were also identified as the targets of PNP and CrhR. The number of reads of the RNA targets were high in case of CrhR⁺ compared to PNP⁺. Since the PNP⁺ strain was generated using the WT Synechocystis, PNP⁺ had the wildtype PNP, which might have acted as the competitor of 3XFLAG- PNP and thus, we had lost number of reads. However, this indicates the involvement of the exoribonuclease, PNP and the RNA helicase, CrhR in the regulation of photosynthetic genes during cold acclimation. Interestingly, it was observed that most of the RNA targets which co-eluted with 3XFLAG -PNP coincides with that of 3XFLAG-CrhR. This observation further led us to investigate the possibility of the formation of a cold inducible RNA exosome-like complex consisting of PNP and CrhR participates in the regulation of PS genes during cold stress.

RNA exosome complex are found in archaea, yeast, higher eukaryotes as well as in the cell organelle, mitochondria. Though the complexity of the structure of RNA exosome increases with complexity of the organism, but the core subunits of the complex remains similar and have structure similarity with the bacterial PNPase. The catalytic activity of the yeast RNA

exosome is contributed by Rrp44/Dis3, an RNase II-like 3'-5' exoribonuclease [80]. The mitochondrial RNA exosome is composed of Dss1 (3'-to-5' exoribonuclease) and Suv3 (RNA helicase) [66]. In cyanobacteria, no RNA degrading protein complex have been identified yet. But, since we had identified similar set of RNA as targets for both- PNP and CrhR during cold acclimation, it implies the possibility of the existence of a cold inducible RNA exosome-like complex in Synechocystis (Table 4). Thus, this observation led us to examine the interaction between PNP and CrhR by bacterial two hybrid analysis. Since RNaseII like proteins is a component of RNA exosome complex, we have also included it in the interaction studies. Indeed bacterial two hybrid study indicated very strong interaction between the pair PNP and CrhR; and the pair PNP and RNaseII (Figure 21). The interaction of PNP, CrhR and RNaseII was further confirmed by Surface Plasmon Resonance (SPR) (Figure 23). The kinetic analysis study by SPR between PNP and CrhR exhibits a very strong interaction between the two. However, the lower K_D value at 25°C than that at 34°C implies that low temperature favours the interaction between PNP and CrhR. In case of PNP and RNaseII, decrease in temperature did not alter the K_D value of the interaction, thus indicating that the interaction between the two is temperature independent (Table 5). It confirms the interaction between PNP interacts with both CrhR and RNaseII. It also implies the possibility of the existence of a cold-inducible RNA exosome-like complex composed of PNP and CrhR. Also, this cold inducible RNAexosome complex might be assisted by RNaseII.

From the evidences in the study, we can conclude the following; 1) the sRNA, PsrR1 regulates the photosystems and phycobilisomes genes during cold stress in *Synechocystis*, 2) the exoribonuclease PNP and the cold inducible-CrhR helicase participates during the post-transcriptional regulation of the photosynthetic genes during cold stress and 3) PNP interacts with CrhR and also with RNaseII. This interaction might be triggered during cold acclimation, thus leading to the formation of RNA exosome-like complex consisting of PNP, CrhR and

RNaseII. This complex possibly is involved in the gene regulatory system of the photosynthetic
genes at low temperature.



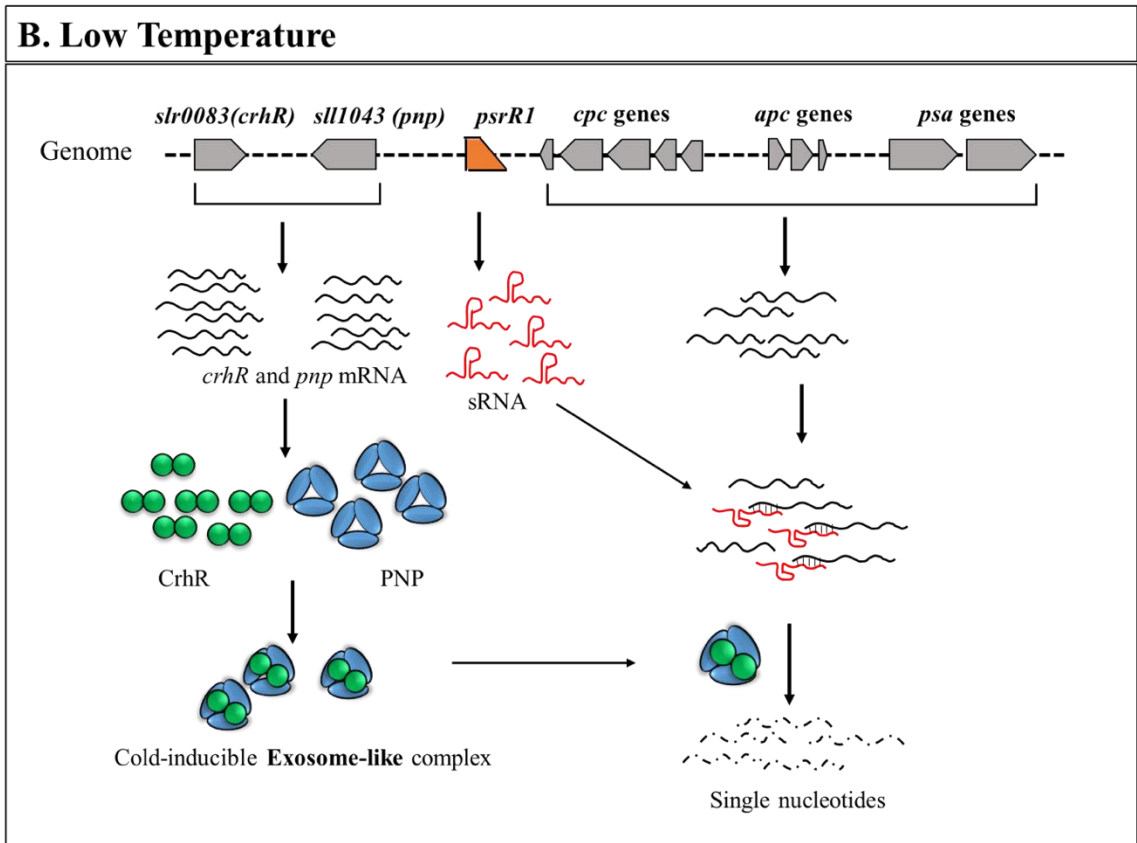
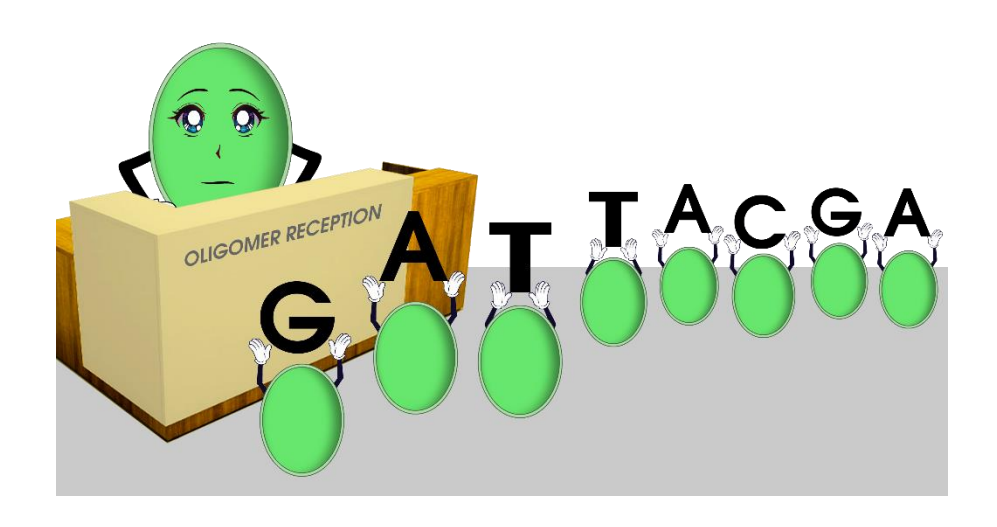


Figure 24: Schematic representation of the regulation of photosystem I and phycobilisomes genes at low temperature. (A) The transcription of PNP, CrhR and the photosystem-I (*psa*) and phycobilisomes genes (*cpc* and *apc*). (B) At low temperature, the expression of PNP and CrhR is upregulated and might form the cold-inducible RNA exosomelike complex. Low temperature (cold stress) led to the downregulation in the expression of PSI genes but upregulates the expression of the sRNA, PsrR1. PsrR1 leads to the post-transcriptional regulation of the PSI transcripts. The transcripts are finally degraded by the cold-inducible RNA exosome complex.

6.OLIGOMERS



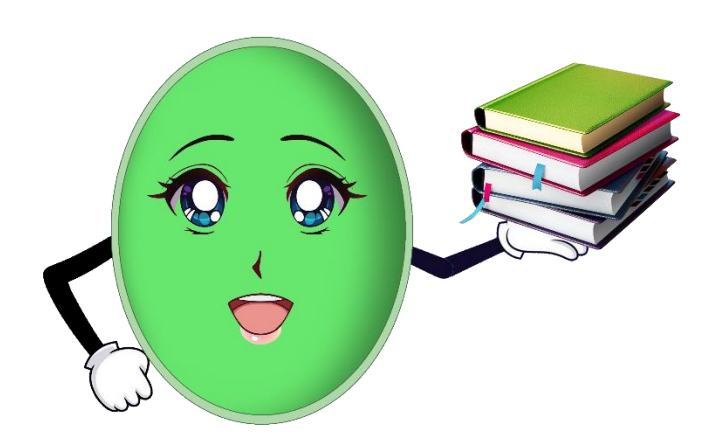
Sl	Name	Sequence (5'-3')		
No.				
1.	PsrR1 RT-PCR FP	GCA TGA ACT ATT AAG GGC ACG GGT TCT		
2.	PsrR1 RT-PCR RP	CCC CGG CAT CAC CGA GGG CAT ATC		
3.	sll1577 RT FP	CAG TTA GAT GCT TTG AGC GCT ACC G		
4	sll1577 RT RP	GCA AAC AAG CAG CCA TAC GAC GGC		
5	slr2067 RT FP	CCG GCG AAC TGG ATC GTA TTA AAG C		
6	slr2067 RT RP GGT CAT TTC TTC ACC GTA GGC ATT GC			
7	sll1322 RT FP	GAA GTG GGT CAG CAG TGG TAT TGG G		
8	sll1322 RT RP	CCA GCA CGT ATT CCA TGA GGT TTT GG		
9	smr0008 RT FP	ATG TTC GCA GAA GGC AGA ATC CC		
10	smr0008 RT RP	ATG GAA GAA CCT AAA CCA GCA TAG GC		
11	PsaA-RT-F	GCATCTTGAACGGGGATGTGG		
12	PsaA-RT-R	GGAGCTTTGACGTGGTAGTGG		
13	PsaL-RT-F	CATTTCCGACTCCGCTTTCACC		
14	PsaL-RT-R	CGATCAGACCACCAATGTACTGG		
15	psrR1–FP	ATC GAG CTC CCA CAG TGC CCA GCA AGC CG		
16	psrR1-RP	ATA CCC GGG GCT GGA GGT GTG GCC ACG TCC		
17	psrR1-INV-FP	ATG CCC TCG GTG ATG CCG		
18	psrR1-INV-RP	CTG TCG GGT TTC CAT AGC C		
19	Cm-FP	AAT GAG ACG TTG ATC GGC ACG TAA G		
20	Cm-RP	GTC CAA AGG TTG TCT TTA CGC CCC GCC CTG		
		CCA C		
21	PpetJ-PsrR1-INV-FP	TGC CTG GCG GCA GTA GCG C		
22	PpetJ-PsrR1-INV-RP	AAT GAG ACG TTG ATC GGC ACG TAA GAG GTT CCA ACT TTC ACC		
23	PpetJ-pSyn-INF-FP	GAT CAA CGT CTC ATT GGA ATT GCT CTG GCA ACT GAT TAA TCC A		
24	PpetJ-PsrR1-INF-R1	CCA TAG CCT TAT GAA GGT ATT ATG GGA GG		
25	PpetJ-psrR1-INF-FP	CAT AAT ACC TTC ATA AGG CTA TGG AAA CCC GAC		

PpetJ-psrR1-INF-RP	TAC TGC CGC CAG GCA GGA ACT AAT TAA GTC
	CAT CCA GCG
slr0947-FP	CTT TGC CAA AAC TTT AGG GGC CGG C
slr0947-RP	GTT TGC ATT ACC CGT TCT ACA ATC GG
mut-inv-947 FP	CTA GAG GAA GAC CCC AGC AAT CCC G
mut-inv- 947 RP	CAG CGG TCA CCA CTT CAT AGC CAA TC
Spec-FP	AAG TGG TGA CCG CTG TTA TTT GCC GAC TAC CTT GGT GAT CTC G
Spec-RP	GGG GTC TTC CTC TAG AGC CAG CCA GGA CAG AAA TGC CTC G
PpetJ-prom-F	GGG AAT TCA GGT TGA CCA CAT CGG
PpetJ prom-R	AAC ATA TGT TCT CCT TTC AAG G
3X-FL-PNP-2015-F1	GAT TAC AAG GAT GAC GAT GAC AAG CAA GAG TTT GAC AAG TCC ATA TCC
3XFL-PNP-2015-F2	GAT TAT AAA GAT CAT GAT ATC GAT TAC AAG GAT GAC GAT GAC AAG C
3XFL-PNP-2015-F3	GCC ATA TGG ACT ACA AAG ACC ATG ACG GTG ATT ATA AAG ATC ATG ATA TC
3XFLAG-PNP-R	CCG TCT AGA CC A GAG CTC ATT AAC CCC GGC TAG CGT TAC GAC GGG
3xFL-CrhR-2015-F1	GAT TAC AAG GAT GAC GAT GAC AAG ACT AAT ACT TTG ACT AGT ACC TTC G
3xFL-CrhR-2015-F2	5'GATTATAAAGATCATGATATCGATTACAAGGAT GACGATGACAAGAC
3xFL-CrhR-2015-F3	GCCATATGGACTACAAAGACCATGACGGTGATTA TAAAGATCATGATATC
3xFL-CrhR-2015-R	CCGTCTAGACCAGAGCTCATTACTGTTGGCGATC ACTATAGGCAGGAC G
rrnBT-TT-F	GGC GAG CTC GCC TGG CGG CAG TAG CGC GG
rrnBT-TT-R	CCG TCT AGA GGA ATT CAA AAA GGC CAT CCG TCA GGA TG
PNPase-T25-F	GGG CTG CAG GGA TGC AAG AGT TTG ACA AGT CC
PNPase-T25-R	GGA CCC GGG CTT AAC CCC GGC TAG CGT TAC
RNaseII-t25-F	GGG CTG CAG GGA TGG AAA AAG GAC AAC TAA TTG AAT TCC
RNaseII-t25-R	GGA CCC GGG CTT AGG CTT CAT TGG CCA ACA ATT CC
PNPase-T18-F	CCC TCG AGG ATG CAA GAG TTT GAC AAG TCC
PNPase-T18-R	CGG AAG CTT AT A CCC CGG CTA GCG TTA CG
	slr0947-RP mut-inv-947 FP mut-inv- 947 RP Spec-FP Spec-RP PpetJ-prom-F PpetJ prom-R 3X-FL-PNP-2015-F1 3XFL-PNP-2015-F2 3XFL-PNP-2015-F3 3XFL-CrhR-2015-F3 3XFL-CrhR-2015-F1 3xFL-CrhR-2015-F2 7xFL-CrhR-2015-F3 RFL-CrhR-2015-F3 RFL-Cr

51	CrhR-T18-F	CCC TCG AGG ATG ACT AAT ACT TTG ACT AG
52	CrhR-T-18-R	CGG AAG CTT ATC TGT TGG CGA TCA CTA TAG G
53	pet-RNaseII-INF-RP	ACG GAG CTC GAA TTC TTA GGC TTC ATT GGC
		CAA CAA TTC CC
54	pet-RNaseII-INF-FP	CCG CGC GGC AGC CAT ATG GAA AAA GGA CAA
		CTA ATT GAA TTC C
55	pet28-synPNP FP	CCG CGC GGC AGC CAT ATG CAA GAG TTT GAC
		AAG TCC
56	pet28-synPNP-RP	ACG GAG CTC GAA TTC TTA ACC CCG GCT AGC
		GTT ACG
57	crhR-pet28a-FP	CGG CAT ATG ACT AAT ACT TTG ACT AGT ACC
		TTC GCT GAC C
58	crhR-pet28a-RP	GGC AAG CTT TTA CTG TTG GGA TCA CTA TAG
		GCA GG
59	pVZ3XFL-inv-neg	GCA GGG ATC CGT TTT GGT CAC TTG TCA TCG
	cont F	TCA TCC TTG
60	pVZ3XFL-inv-neg	GCG GAT CCG TAG TGA GCT CGC CTG GCG GCA
	cont R	GTA G

Table 6: List of oligomers and their sequences used for the study. The primers from Sl. No. 1-14 were used to perform the qRT-PCR analysis. Primers from Sl. No. 15-60 were used for PCR reaction involved in the various cloning to generate the mutants and overexpression strains in the study.

7.REFERENCES



- Kaneko, T., & Tabata, S. (1997). Complete genome structure of the unicellular cyanobacterium Synechocystis sp. PCC6803. Plant and Cell Physiology, 38(11), 1171-1176.ya
- 2. Gupta, V., Ratha, S. K., Sood, A., Chaudhary, V., & Prasanna, R. (2013). New insights into the biodiversity and applications of cyanobacteria (blue-green algae)—prospects and challenges. Algal research, 2(2), 79-97.
- 3. Zahra, Z., Choo, D. H., Lee, H., & Parveen, A. (2020). Cyanobacteria: Review of current potentials and applications. Environments, 7(2), 13.
- 4. Rachedi, R., Foglino, M., & Latifi, A. (2020). Stress Signalling in Cyanobacteria: A Mechanistic Overview. Life, 10(12), 312.
- 5. Nixon, P. J., Michoux, F., Yu, J., Boehm, M., & Komenda, J. (2010). Recent advances in understanding the assembly and repair of photosystem II. Annals of botany, 106(1), 1-16.
- 6. Los, D. A. (2004). The effect of low-temperature-induced DNA supercoiling on the expression of the desaturase genes in *Synechocystis*. Cellular And Molecular Biology-Paris-Wegmann-, 50(5), 605-612.
- Prakash, J. S., Krishna, P. S., Sirisha, K., Kanesaki, Y., Suzuki, I., Shivaji, S., & Murata, N. (2010). An RNA helicase, CrhR, regulates the low-temperature-inducible expression of heat-shock genes groES, groEL1 and groEL2 in *Synechocystis* sp. PCC 6803. Microbiology, 156(2), 442-451.
- 8. Sinetova, M. A., & Los, D. A. (2016). New insights in cyanobacterial cold stress responses: Genes, sensors, and molecular triggers. Biochimica et Biophysica Acta (BBA)-General Subjects, 1860(11), 2391-2403.

- 9. Suzuki, I., Kanesaki, Y., Mikami, K., Kanehisa, M., & Murata, N. (2001). Cold regulated genes under control of the cold sensor Hik33 in *Synechocystis*. Molecular microbiology, 40(1), 235-244.
- 10. Srivastava, A., Summers, M. L., & Sobotka, R. (2020). Cyanobacterial sigma factors: Current and future applications for biotechnological advances. Biotechnology advances, 40, 107517.
- 11. Huckauf, J., Nomura, C., Forchhammer, K., & Hagemann, M. (2000). Stress responses of Synechocystis sp. strain PCC 6803 mutants impaired in genes encoding putative alternative sigma factors. Microbiology, 146(11), 2877-2889.
- 12. Singh, A. K., Summerfield, T. C., Li, H., & Sherman, L. A. (2006). The heat shock response in the cyanobacterium Synechocystis sp. strain PCC 6803 and regulation of gene expression by HrcA and SigB. Archives of microbiology, 186(4), 273-286.
- 13. Burnap, R. L., Hagemann, M., & Kaplan, A. (2015). Regulation of CO2 concentrating mechanism in cyanobacteria. Life, 5(1), 348-371.
- Georg, J., Dienst, D., Schürgers, N., Wallner, T., Kopp, D., Stazic, D., ... & Wilde, A.
 (2014). The small regulatory RNA SyR1/PsrR1 controls photosynthetic functions in cyanobacteria. The Plant Cell, 26(9), 3661-3679.
- 15. Murata, N., & Los, D. A. (2006). Histidine kinase Hik33 is an important participant in cold-signal transduction in cyanobacteria. Physiologia plantarum, 126(1), 17-27.
- 16. Brauer, V. S., Stomp, M., Rosso, C., van Beusekom, S. A., Emmerich, B., Stal, L. J., & Huisman, J. (2013). Low temperature delays timing and enhances the cost of nitrogen fixation in the unicellular cyanobacterium Cyanothece. The ISME journal, 7(11), 2105-2115.

- 17. Staehr, P. A., & Birkeland, M. J. (2006). Temperature acclimation of growth, photosynthesis and respiration in two mesophilic phytoplankton species. Phycologia, 45(6), 648-656.
- 18. Suzuki, I., Los, D. A., Kanesaki, Y., Mikami, K., & Murata, N. (2000). The pathway for perception and transduction of low-temperature signals in Synechocystis. The EMBO journal, 19(6), 1327-1334.
- 19. Prakash, J., Krishna, P., & Shivaji, S. (2013). Sensing and molecular responses to low temperature in cyanobacteria. Stress Biology of Cyanobacteria; CRC Press: Boca Raton, FL, USA, 155-170.
- 20. Sakayori, T., Shiraiwa, Y., & Suzuki, I. (2009). A *Synechocystis* homolog of SipA protein, Sslμ51, enhances the activity of the histidine kinase Hik33. Plant and cell physiology, 50(8), 1439-1448.
- 21. Riediger, M., Kadowaki, T., Nagayama, R., Georg, J., Hihara, Y., & Hess, W. R. (2018). Global analysis of the RpaB regulon based on the positional distribution of HLR1 sequences and comparative differential RNA-Seq data. bioRxiv, 443713.
- 22. Kappell, A. D., & van Waasbergen, L. G. (2007). The response regulator RpaB binds the high light regulatory 1 sequence upstream of the high-light-inducible hliB gene from the cyanobacterium Synechocystis PCC 6803. Archives of microbiology, 187(4), 337-342.
- 23. Kadowaki, T., Nagayama, R., Georg, J., Nishiyama, Y., Wilde, A., Hess, W. R., & Hihara, Y. (2016). A feed-forward loop consisting of the response regulator RpaB and the small RNA PsrR1 controls light acclimation of photosystem I gene expression in the cyanobacterium Synechocystis sp. PCC 6803. Plant and Cell Physiology, 57(4), 813-823.

- 24. Hihara, Y., Kamei, A., Kanehisa, M., Kaplan, A., & Ikeuchi, M. (2001). DNA microarray analysis of cyanobacterial gene expression during acclimation to high light. The Plant Cell, 13(4), 793-806.
- 25. Sireesha, K., Radharani, B., Krishna, P. S., Sreedhar, N., Subramanyam, R., Mohanty, P., & Prakash, J. S. (2012). RNA helicase, CrhR is indispensable for the energy redistribution and the regulation of photosystem stoichiometry at low temperature in *Synechocystis* sp. PCC6803. Biochimica et Biophysica Acta (BBA)-Bioenergetics, 1817(9), 1525-1536.
- 26. Migur, A., Heyl, F., Fuss, J., Srikumar, A., Huettel, B., Steglich, C., ... & Hess, W. R. (2021). The temperature-regulated DEAD-box RNA helicase CrhR interactome: autoregulation and photosynthesis-related transcripts. Journal of Experimental Botany, 72(21), 7564-7579.
- 27. Los, D. A., & Murata, N. (2002). Sensing and response to low temperature in cyanobacteria (Vol. 3, pp. 139-153). Amsterdam: Elsevier Science BV.
- Prakash, J. S., Sinetova, M., Zorina, A., Kupriyanova, E., Suzuki, I., Murata, N., & Los,
 D. A. (2009). DNA supercoiling regulates the stress-inducible expression of genes in
 the cyanobacterium Synechocystis. Molecular Biosystems, 5(12), 1904-1912.
- 29. Shevela, D., Pishchalnikov, R. Y., & Eichacker, L. A. (2013). Oxygenic photosynthesis in cyanobacteria (pp. 3-40). Boca Raton: CRC Press.
- 30. Gisriel, C. J., Zhou, K., Huang, H. L., Debus, R. J., Xiong, Y., & Brudvig, G. W. (2020).
 Cryo-EM structure of monomeric photosystem II from Synechocystis sp. PCC 6803
 lacking the water-oxidation complex. Joule, 4(10), 2131-2148.
- 31. Stadnichuk, I. N., Krasilnikov, P. M., & Zlenko, D. V. (2015). Cyanobacterial phycobilisomes and phycobiliproteins. Microbiology, 84(2), 101-111.

- 32. Rillema, R., MacCready, J. S., & Vecchiarelli, A. G. (2020). Cyanobacterial growth and morphology are influenced by carboxysome positioning and temperature. bioRxiv.
- 33. Huner, N. P. A., Maxwell, D. P., Gray, G. R., Savitch, L. V., Krol, M., Ivanov, A. G., & Falk, S. (1996). Sensing environmental temperature change through imbalances between energy supply and energy consumption: redox state of photosystem II. Physiologia Plantarum, 98(2), 358-364.
- 34. Shimoni, Y., Friedlander, G., Hetzroni, G., Niv, G., Altuvia, S., Biham, O., & Margalit, H. (2007). Regulation of gene expression by small non-coding RNAs: a quantitative view. Molecular systems biology, 3, 138.
- 35. Regulatory RNAs in photosynthetic cyanobacteria. FEMS microbiology reviews, 39(3), 301-315.
- 36. Jørgensen, M. G., Pettersen, J. S., & Kallipolitis, B. H. (2020). sRNA-mediated control in bacteria: An increasing diversity of regulatory mechanisms. Biochimica et Biophysica Acta (BBA)-Gene Regulatory Mechanisms, 1863(5), 194504.
- 37. Saramago, M., Bárria, C., Dos Santos, R. F., Silva, I. J., Pobre, V., Domingues, S., ... & Arraiano, C. M. (2014). The role of RNases in the regulation of small RNAs. Current opinion in microbiology, 18, 105-115.
- 38. Storz, G., Vogel, J., & Wassarman, K. M. (2011). Regulation by small RNAs in bacteria: expanding frontiers. Molecular cell, 43(6), 880-891.
- 39. Hu, J., & Wang, Q. (2018). Regulatory sRNAs in Cyanobacteria. Frontiers in microbiology, 9, 2399.
- 40. Georg, J., Voss, B., Scholz, I., Mitschke, J., Wilde, A., & Hess, W. R. (2009). Evidence for a major role of antisense RNAs in cyanobacterial gene regulation. Molecular systems biology, 5, 305.

- 41. Gottesman, S. (2005). Micros for microbes: non-coding regulatory RNAs in bacteria. TRENDS in Genetics, 21(7), 399-404.
- 42. Waters, L. S., & Storz, G. (2009). Regulatory RNAs in bacteria. Cell, 136(4), 615-628.
- 43. Mitschke, J., Georg, J., Scholz, I., Sharma, C. M., Dienst, D., Bantscheff, J., ... & Hess, W. R. (2011). An experimentally anchored map of transcriptional start sites in the model cyanobacterium *Synechocystis* sp. PCC6803. Proceedings of the National Academy of Sciences, 108(5), 2124-2129
- 44. Kopf, M., Klähn, S., Scholz, I., Hess, W. R., & Voß, B. (2015). Variations in the non-coding transcriptome as a driver of inter-strain divergence and physiological adaptation in bacteria. Scientific reports, 5(1), 1-12.
- 45. Wright, P. R., Georg, J., Mann, M., Sorescu, D. A., Richter, A. S., Lott, S., ... & Backofen, R. (2014). CopraRNA and IntaRNA: predicting small RNA targets, networks and interaction domains. Nucleic acids research, 42(W1), W119-W123.
- 46. Xu, W., Chen, H., He, C. L., & Wang, Q. (2014). Deep sequencing-based identification of small regulatory RNAs in Synechocystis sp. PCC 6803. PloS one, 9(3), e92711.
- 47. Hu, J., Li, T., Xu, W., Zhan, J., Chen, H., He, C., & Wang, Q. (2017). Small antisense RNA RblR positively regulates RuBisCo in Synechocystis sp. PCC 6803. Frontiers in microbiology, 8, 231.
- 48. Duhring, U., Axmann, I. M., Hess, W. R., & Wilde, A. (2006). An internal antisense RNA regulates expression of the photosynthesis gene isiA. Proceedings of the National Academy of Sciences, 103(18), 7054-7058.
- Sakurai, I., Stazic, D., Eisenhut, M., Vuorio, E., Steglich, C., Hess, W. R., & Aro, E.
 M. (2012). Positive regulation of psbA gene expression by cis-encoded antisense RNAs in Synechocystis sp. PCC 6803. Plant Physiology, 160(2), 1000-1010.

- 50. Eisenhut, M., Georg, J., Klähn, S., Sakurai, I., Mustila, H., Zhang, P., ... & Aro, E. M. (2012). The antisense RNA As1_flv4 in the cyanobacterium Synechocystis sp. PCC 6803 prevents premature expression of the flv4-2 operon upon shift in inorganic carbon supply. Journal of Biological Chemistry, 287(40), 33153-33162.
- 51. Klähn, S., Schaal, C., Georg, J., Baumgartner, D., Knippen, G., Hagemann, M., ... & Hess, W. R. (2015). The sRNA NsiR4 is involved in nitrogen assimilation control in cyanobacteria by targeting glutamine synthetase inactivating factor IF7. Proceedings of the National Academy of Sciences, 112(45), E6243-E6252.
- 52. Pei, G., Sun, T., Chen, S., Chen, L., & Zhang, W. (2017). Systematic and functional identification of small non-coding RNAs associated with exogenous biofuel stress in cyanobacterium *Synechocystis* sp. PCC 6803. Biotechnology for biofuels, 10(1), 1-17.
- 53. Seino, Y., Takahashi, T., & Hihara, Y. (2009). The response regulator RpaB binds to the upstream element of photosystem I genes to work for positive regulation under low-light conditions in *Synechocystis* sp. strain PCC 6803. Journal of bacteriology, 191(5), 1581-1586.
- 54. Wilde, A., & Hihara, Y. (2016). Transcriptional and posttranscriptional regulation of cyanobacterial photosynthesis. Biochimica et Biophysica Acta (BBA)-Bioenergetics, 1857(3), 296-308.
- 55. Vargas-Blanco, D. A., & Shell, S. S. (2020). Regulation of mRNA stability during bacterial stress responses. Frontiers in Microbiology, 11.
- 56. Arraiano, C. M., & Maquat, L. E. (2003). Post transcriptional control of gene expression: effectors of mRNA decay. Molecular microbiology, 49(1), 267-276.
- 57. Viegas, S. C., & Arraiano, C. M. (2008). Regulating the regulators: how ribonucleases dictate the rules in the control of small non-coding RNAs. RNA biology, 5(4), 230-243.

- 58. Bechhofer, D. H., & Deutscher, M. P. (2019). Bacterial ribonucleases and their roles in RNA metabolism. Critical reviews in biochemistry and molecular biology, 54(3), 242-300.
- 59. Lin-Chao, S., Chiou, N.-T., and Schuster, G. (2007) The PNPase, exosome and RNA helicases as the building components of evolutionarily-conserved RNA degradation machines. J Biomed Sci. 14, 523-532.
- 60. Januszyk, K., & Lima, C. D. (2010). Structural components and architectures of RNA exosomes. RNA exosome, 9-28.
- 61. Miczak, A., Kaberdin, V. R., Wei, C. L., & Lin-Chao, S. (1996). Proteins associated with RNase E in a multicomponent ribonucleolytic complex. Proceedings of the National Academy of Sciences, 93(9), 3865-3869.
- 62. Kaberdin, V. R., Singh, D., & Lin-Chao, S. (2011). Composition and conservation of the mRNA-degrading machinery in bacteria. Journal of biomedical science, 18(1), 1-12.
- 63. Cho, K. H. (2017). The structure and function of the gram-positive bacterial RNA degradosome. Frontiers in microbiology, 8, 154.
- 64. Evguenieva-Hackenberg, E., Hou, L., Glaeser, S., & Klug, G. (2014). Structure and function of the archaeal exosome. Wiley Interdisciplinary Reviews: RNA, 5(5), 623-635.
- 65. Tseng, Y. T., Chiou, N. T., Gogiraju, R., & Lin-Chao, S. (2015). The protein interaction of RNA helicase B (RhlB) and polynucleotide phosphorylase (PNPase) contributes to the homeostatic control of cysteine in *Escherichia coli*. Journal of Biological Chemistry, 290(50), 29953-29963.
- 66. Razew, M., Warkocki, Z., Taube, M., Kolondra, A., Czarnocki-Cieciura, M., Nowak, E., ... & Nowotny, M. (2018). Structural analysis of mtEXO mitochondrial RNA

- degradosome reveals tight coupling of nuclease and helicase components. Nature communications, 9(1), 1-12.
- 67. Rott, R., Zipor, G., Portnoy, V., Liveanu, V., & Schuster, G. (2003). RNA polyadenylation and degradation in cyanobacteria are similar to the chloroplast but different from Escherichia coli. Journal of Biological Chemistry, 278(18), 15771-15777.
- 68. Cameron, J. C., Gordon, G. C., & Pfleger, B. F. (2015). Genetic and genomic analysis of RNases in model cyanobacteria. Photosynthesis research, 126(1), 171-183.
- 69. Matos, R. G., Fialho, A. M., Giloh, M., Schuster, G., & Arraiano, C. M. (2012). The rnb gene of Synechocystis PCC6803 encodes a RNA hydrolase displaying RNase II and not RNase R enzymatic properties. PLoS One, 7(3), e32690.
- 70. Horie, Y., Ito, Y., Ono, M., Moriwaki, N., Kato, H., Hamakubo, Y., ... & Asayama, M. (2007). Dark-induced mRNA instability involves RNase E/G-type endoribonuclease cleavage at the AU-box and SD sequences in cyanobacteria. Molecular Genetics and Genomics, 278(3), 331-346.
- 71. Phadtare S. (2011). Unwinding activity of cold shock proteins and RNA metabolism. RNA biology, 8(3), 394–397. https://doi.org/10.4161/rna.8.3.14823
- 72. Phadtare, S., & Severinov, K. (2010). RNA remodeling and gene regulation by cold shock proteins. RNA biology, 7(6), 788-795.
- 73. Wada, H., & Murata, N. (1989). Synechocystis PCC6803 mutants defective in desaturation of fatty acids. Plant and cell physiology, 30(7), 971-978.
- 74. Sambrook, J. (1989). Molecular cloning: a laboratory manual. Synthetic oligonucleotides.

- 75. Zinchenko, V. V., Piven, I. V., Melnik, V. A., & Shestakov, S. V. (1999). Vectors for the complementation analysis of cyanobacterial mutants. RUSSIAN JOURNAL OF GENETICS C/C OF GENETIKA, 35, 228-232.
- 76. Karimova, G., Pidoux, J., Ullmann, A., & Ladant, D. (1998). A bacterial two-hybrid system based on a reconstituted signal transduction pathway. Proceedings of the National Academy of Sciences, 95(10), 5752-5756.
- 77. Srikumar, A., Krishna, P. S., Sivaramakrishna, D., Kopfmann, S., Hess, W. R., Swamy, M. J., ... & Prakash, J. S. (2017). The Ssl2245-Sll1130 toxin-antitoxin system mediates heat-induced programmed cell death in Synechocystis sp. PCC6803. Journal of Biological Chemistry, 292(10), 4222-4234.
- 78. De Marsac, N. T., & Houmard, J. (1988). [34] Complementary chromatic adaptation: physiological conditions and action spectra. Methods in enzymology, 167, 318-328.
- 79. Cassier-Chauvat, C., Blanc-Garin, V., & Chauvat, F. (2021). Genetic, Genomics, and Responses to Stresses in Cyanobacteria: Biotechnological Implications. Genes, 12(4), 500.
- 80. Dziembowski, A., Lorentzen, E., Conti, E., & Séraphin, B. (2007). A single subunit, Dis3, is essentially responsible for yeast exosome core activity. Nature structural & molecular biology, 14(1), 15-22.
- 81. Lubas, M., Chlebowski, A., Dziembowski, A., & Jensen, T. H. (2012). Biochemistry and function of RNA exosomes. In The Enzymes (Vol. 31, pp. 1-30). Academic Press.
- 82. Battesti, A., & Bouveret, E. (2012). The bacterial two-hybrid system based on adenylate cyclase reconstitution in Escherichia coli. Methods, 58(4), 325-334.
- 83. Mikami, K., Kanesaki, Y., Suzuki, I., & Murata, N. (2002). The histidine kinase Hik33 perceives osmotic stress and cold stress in *Synechocystis* sp. PCC 6803. Molecular microbiology, 46(4), 905-915.

List of Publication

1. Konduri Ranjith, Jahnabi Ramchiary, Jogadhenu S. S. Prakash, Kotakonda Arunasri, Savitri Sharma and Sisinthy Shivaji. Gene targets in ocular pathogenic Escherichia coli for mitigation of biofilm formation to overcome antibiotic resistance. Frontiers in Microbiology, Volume 10, 2019, p 1308.

Gene Targets in Ocular Pathogenic Escherichia coli for Mitigation of **Biofilm Formation to Overcome** Antibiotic Resistance

Konduri Ranjith^{1,2}, Jahnabi Ramchiary³, Jogadhenu S. S. Prakash³, Kotakonda Arunasri¹, Savitri Sharma¹ and Sisinthy Shivaii¹

licrobiology Centre – Prof. Brien Holden Eye Research Centre, LV Prasad Eye Institute, Hyderabad, India, Research Scholar, Manipal Academy of Higher Education, Manipal, India, 3 Department of Bioter and Bioinformatics, School of Life Sciences, University of Hyderabad, Hyderabad, India

The present work is an attempt to establish the functionality of genes involved in biofilm formation and antibiotic resistance in an ocular strain of Escherichia coli (L-1216/2010) which was isolated and characterized from the Vitreous fluid of a patient with Endophthalmitis. For this purpose, seven separate gene-specific knockout mutants were generated by homologous recombination in ocular E. coli. The genes that were mutated included three transmembrane genes ytfR (ABC transporter ATP-binding protein), mdtO (multidrug efflux system) and toIA (inner membrane protein), ryfA coding for non-coding RNA and three metabolic genes mhpA (3-3-hydroxyphenylpropionate 1,2-dioxygenase), mhpB (2,3-di hydroxyphenylpropionate 1,2-dioxygenase), and bdcR (regulatory gene of bdcA). Mutants were validated by sequencing and Reverse transcription-PCR and monitored for biofilm formation by XTT method and confocal microscopy. The antibiotic susceptibility of the mutants was also ascertained. The results indicated that biofilm formation was inhibited in five mutants (\(\Delta bdcR, \Delta mhpA, \Delta mhpB, \) $\Delta ryfA$, and $\Delta tolA$) and the thickness of biofilm reduced from 17.2 μm in the wildtype to 1.5 to 4.8 μm in the mutants. Mutants $\Delta ytfR$ and $\Delta mdtO$ retained the potential to form biofilm. Complementation of the mutants with the wild type gene restored biofilm formation potential in all mutants except in $\Delta mhpB$. The 5 mutants which lost their ability to form biofilm ($\Delta bdcR$, $\Delta mhpA$, $\Delta mhpB$, $\Delta tolA$, and $\Delta ryfA$) did not exhibit any change in their susceptibility to Ceftazidime, Cefuroxime, Ciprofloxacin, Gentamicin, Cefotaxime, Sulfamethoxazole, Imipenem, Erythromycin, and Streptomycin in the planktonic phase compared to wild type ocular E. coli. But AmdtO was the only mutant with altered MIC to Sulfamethoxazole, Imipenem, Erythromycin, and Streptomycin both in the planktonic and biofilm phase. This is the first report demonstrating the involvement of the metabolic genes mhpA and mhpB and bdcR (regulatory gene of bdcA) in biofilm formation in ocular E. coli. In addition we provide evidence that tolA and ryfA are required for biofilm formation while ytfR and mdtO are not required. Mitigation of biofilm formation to overcome antibiotic resistance could be achieved by targeting the genes bdcR, mhpA, mhpB, ryfA, and tolA.

Keywords: antimicrobial resistance, biofilm, ocular, E. coli, endophthalmitis, mutation

OPEN ACCESS

Edited by:

Paris Diderot University, France

Yosuke Tashiro Shizuoka University, Japan The University of Tokyo, Japan

> *Correspondence: Sisinthy Shiyaii shivas@lvpei.org

Specialty section:

This article was submitted to Antimicrobials, Resistance and Chemotherapy. Frontiers in Microbiology

Received: 24 December 2018 Accepted: 27 May 2019 Published: 21 June 2019

Citation:

Ranjith K, Ramchiary J. Prakash JSS, Arunasri K, Sharma S and Shivaji S (2019) Gene Targets in Ocular Pathogenic Escherichia coli for Mitigation of Biofilm Formation to Overcome Antibiotic Resistance. Front, Microbiol. 10:1308 doi: 10.3389/fmicb.2019.01308

Frontiers in Microbiology | www.frontiersin.org

June 2019 | Volume 10 | Article 1308

List of Poster Presentations

- 1. Presented poster virtually at International Symposium "Advances In Plant Biotechnology And Genome Editing"- (APBGE 2021) (Virtual conference), April 2021.
- 2. Presented oral at the conference of 59th Annual Conference of Association of Microbiologists of India (AMI-2018) held at University of Hyderabad, India, November, 2018.
- 3. Presented poster at the conference of 59th Annual Conference of Association of Microbiologists of India (AMI-2018) held at University of Hyderabad, India, November, 2018.

Elucidation of a small regulatory RNA PsrR1 mediated photosynthetic gene regulatory mechanism during cold acclimation in Synechocystis sp. PCC 6803

by Jahnabi Ramchiary

Submission date: 09-Jun-2022 07:03PM (UTC+0530)

Submission ID: 1853621827

File name: Jahnabi-PhD_Thesis_Final.pdf (3.07M)

Word count: 23872 Character count: 126843

Prof. J.S.S. PRAKASH

Prof. J.S.S. PRAKASH

Dept. of Biotechnology & Bioinformatics
School of Life Sciences
University of Hyderabad

HYDERABAD-500 046. INDIA.

Elucidation of a small regulatory RNA PsrR1 mediated photosynthetic gene regulatory mechanism during cold acclimation in Synechocystis sp. PCC 6803

ORIGINA	ALITY REPORT				
SIMILA	% RITY INDEX	5% INTERNET SOURCES	5% PUBLICATIONS	2% STUDENT	PAPERS
PRIMARY	Y SOURCES				
1	Submitted to University of Hyderabad, Hyderabad Student Paper 1				
2	genome Internet Source	,	1%		
3	www.accentbrokerage.com Internet Source				<1%
4	www.ncbi.nlm.nih.gov Internet Source				<1%
5	Prakash, Jogadhenu, Pilla Krishna, and Sisinthy Shivaji. "Sensing and Molecular Responses to Low Temperature in Cyanobacteria", Stress Biology of Cyanobacteria Molecular Mechanisms to Cellular Responses, 2013.				<1%
6			aj Chauhan, Afs akawa, Iwane Su		<1%

Prof. J.S.S. PRAKASH

National Sciences

Prof. J.S.S. PRAKASH

Prof. J.S. PRAKASH

P